UNIVERSITEIT VAN PRETORIA
UNIVERSITY OF PRETORIA
YUNIBESITHI YA PRETORIA
Denkleiers • Leading Minds • Dikgopolo tša Dihlalefi

Correlation of cloacal gland histomorphology, ultrastructure and androgen receptor expression with testosterone levels during sexual maturation in the Japanese quail (*Coturnix coturnix japonica*).

by:

Siyamamkela Zikhona Gunuza

A dissertation submitted to the:

FACULTY OF VETERINARY SCIENCE

DEPARTMENT OF ANATOMY AND PHYSIOLOGY

In fulfilment of the requirements for the degree of:

Masters in Veterinary Science

2020

Supervisor: Professor M.N. Madekurozwa

Co-supervisor: Professor L. Neves

TABLE OF CONTENTS

Acknowledgements

My sincere gratitude goes to my supervisor Professor M-C. Madekurozwa, for designing and hands-on supervision of this research. Her guidance, constructive criticism and keen scrutiny of my write-up contributed greatly in the production of this dissertation.

My co-supervisor Professor L. Neves

Dr. Mohamed Mahdy for his input and constructive criticism of my protocol.

My fellow colleagues, for their constant encouragement and motivation.

My family and friends for their unwavering support, love and patience in the entire duration of my studies.

The National Research Foundation (NRF) for awarding me a scholarship through Professor Madekurozwa's grant (Competitive Programme for Rated Researchers, #N01521). In addition, the NRF funded my research project.

The University of Pretoria for awarding me an opportunity to further my studies, as well as for the postgraduate bursary I received.

And lastly, God Almighty who is the author and finisher of all things.

List of figures

List of graphs

List of tables

Table 2.10: Percentage of androgen receptor immunopositive and immunonegative epithelial secretory cells in pre-pubertal, pubertal and adult Japanese quails.

Summary

The cloacal gland of the Japanese quail is an enlarged glandular protuberance, found on the dorsal wall of the cloaca. The gland is unique to the genus *Coturnix* and is present in both male and female quails, but only sexually active males demonstrate functional development. There is a positive correlation between the size of the gland and circulating testosterone levels. Furthermore, it is known that testicular activity and cloacal gland size are influenced by photoperiod. However, it is unknown whether sexual maturation during a period of decreasing daylength affects the morphology of the cloacal gland. Thus, the aim of the current study was to investigate the correlation of cloacal gland histomorphology and ultrastructure with testosterone levels in the Japanese quail during sexual maturation through a period of decreasing daylength.

A total of 7 pre-pubertal, 7 pubertal and 7 adult male Japanese quails were used in this study. The cloacal glands of the birds were investigated using: haematoxylin and eosin staining; periodic acid Schiff and alcian blue histochemistry; terminal deoxynucleotidyl transferase-mediated deoxyuridine 5'-triphosphate nick-end labelling (TUNEL); androgen receptor immunohistochemistry and transmission electron microscopy. In addition, testosterone levels were measured in blood samples collected during euthanasia.

Histological examinations revealed that the glandular units of the cloacal glands in pre-pubertal, pubertal and adult birds were lined by columnar secretory cells. The secretory cells showed positive staining for periodic acid Schiff and alcian blue, indicating the presence of both acidic and neutral mucopolysaccharides. The cloacal gland cells in pre-pubertal birds were TUNEL negative, while positive TUNEL staining was observed in nuclei of the secretory cells in pubertal and adult birds.

These results suggest that decreasing daylengths caused a decrease in testicular activity which led to a reduction in circulating testosterone levels in the pubertal and adult birds. Due to the fact that the cloacal gland is an androgen-dependent organ, the reduction in testosterone resulted in glandular regression. At an ultrastructural level apoptotic cells were observed in the glandular units of pubertal and adult birds. These ultrastructural findings corroborate the TUNEL results.

This study has shown that changes in plasma testosterone concentrations, during sexual maturation, are positively correlated with histomorphological and ultrastructural alterations in the cloacal glands of Japanese quails.

1.0 Chapter one

1.1 General introduction

The Japanese quail (*Coturnix coturnix japonica*) is a *gallinaceous* bird. *Gallinaceous* is a term used for heavy-bodied birds that are largely ground-feeding (Howard, 2004). Other gallinaceous birds include the partridge, pheasant, domestic fowl and turkey (Howard, 2004). The wild-type adult female quail has pale breast feathers which are speckled with dark coloured spots (Figure 1.1), whereas the adult male has dark, rust-red breast feathers (Figure 1.2). The first record of the Japanese quail, as a wild bird, dates back to the 8th century in Japan (Vali, 2008). Records indicate that the species was originally domesticated in the 11th century (Vali, 2008).

Figure 1.1: Female Japanese quail with a black speckled breast.

Figure 1.2: Male Japanese quail with rust coloured breast feathers.

Currently the Japanese quail is bred for meat and eggs (Kayang *et al.*, 2004). The Japanese quail has also increasingly been used as a laboratory animal model because of its low maintenance cost, small body size, resistance to disease, high egg production, and short generation interval (Vali, 2008). Importantly, newly-hatched quail chicks are well-developed, independent of their parents, and require minimal care after hatching (Quinn, 2012). In addition, Japanese quails are characterized by their early attainment of puberty (six weeks of age), which makes them the ideal avian species in experiments involving reproductive endpoints (Quinn, 2012). A further advantage of this species, in terms of research, is that its reproductive activities can be controlled photoperiodically (Vali, 2008). As a result, the Japanese quail is commonly used as an experimental animal in a variety of

scientific fields including developmental biology (Le Douarin and Kalcheim, 1999; Lalloue and Ayer-Le Lievre, 2003), reproductive biology (Ottinger *et al.*, 2004), as well as reproductive toxicology (Ottinger *et al.*, 2005).

The cloacal region of the sexually active male Japanese quail contains a well-developed gland, termed the cloacal or proctodeal gland (Figure 1.3) The cloacal gland is an enlarged, red glandular protuberance, which is located on the dorsal wall of the cloaca (Klemm *et al.*, 1973). The cloacal gland is an aggregate gland made up of several separate and distinct glandular units (Biswas *et al.*, 2007). The cloacal gland of sexually active male Japanese quails produces a large quantity of meringue-like white foam, termed cloacal foam (Seiwert and Adkins-Regan, 1998). Cloacal foam and ejaculated semen are deposited into the female cloaca during copulation (Seiwert and Adkins-Regan, 1998). The cloacal foam is also present in the quail's excrement during defecation (Seiwert and Adkins-Regan, 1998).

The cloacal gland occurs in other galliform species, such as the chicken and turkey (Bakst and Cecil, 1985). The morphology of the gland in the mature male turkey is similar to that of the Japanese quail (Bakst and Cecil, 1985). However, the secretion and function of the cloacal gland in the turkey are different from the gland of the Japanese quail (Fujihara, 1992). The cloacal gland of the turkey secretes muco-substances and is thought to have immunogenic capabilities (Bakst and Cecil, 1985).

The cloacal gland is present in both sexes of quail, but is functionally developed only in sexually active males (Biswas *et al.*, 2007). The size of the cloacal gland is directly correlated with the degree of testicular development and the amount of testosterone produced by the testis (Coil and Wetherbee, 1959; Biswas *et al.*, 2007). In addition, the development and foam production of the cloacal gland is affected by the

photoperiodic regime (Sachs, 1967). Rudimentary cloacal glands, with little secretory activity and no foam production, are present in intact male quails subjected to short days (Adkins and Alder, 1972). Recrudescence of the cloacal gland occurs when the birds are exposed to long daylengths (Seiwert and Adkins-Regan, 1998). Long daylengths result in an increase in circulating androgens which stimulate cloacal gland development (Sachs, 1967).

Figure 1.3: Cloacal gland of a male Japanese quail. Note the meringue-like cloacal foam.

Due to the fact that cloacal gland size is correlated with testicular activity (Sachs, 1967), cloacal gland area is commonly used as an endpoint in toxicological studies

(Quinn, 2012). However, several studies have shown that cloacal gland area, which is a gross parameter, does not reflect subtle changes in testosterone levels (Halldin, 2005). Thus, in order to render the cloacal gland a more sensitive endpoint there is a need to establish a correlation between circulating testosterone levels and histomorphological, as well as ultrastructural observations. Several studies have been conducted to investigate the microscopic morphology of the cloacal gland in the Japanese quail (Coil and Wetherbee, 1959; McFarland *et al.*, 1968; Klemm *et al.*, 1973). The only available information on the ultrastructure of the cloacal gland is a dissertation by Ochs (1979) which has been uploaded onto the internet. Ochs (1979) studied the ultrastructure of the cloacal gland in adult male and female quails exposed to long daylengths.

There is currently a lack of published information on histomorphological and ultrastructural changes occurring in the cloacal gland during sexual maturation– a period of development critical in reproductive toxicology. In addition, the effect on cloacal gland morphology of a decreasing photoperiod during sexual maturation is unknown. Thus, in light of the paucity of information on the cloacal gland, the current study aimed to correlate circulating testosterone levels with histomorphological, and ultrastructural changes occurring in this glandular organ during sexual maturation in a period of decreasing daylength.

1.2 General literature review

1.2.1 Gross morphology

The cloacal gland of the Japanese quail is situated on the dorsal wall of the proctodeum (Klemm *et al.*, 1973). The gland extends from the opening of the cloacal bursa to the distal end of the cloaca's dorsal lip and laterally down the walls of the cloaca (Klemm *et al.*, 1973). In sexually active males, the cloacal gland appears

ovoid in shape and measures approximately 10.0 mm in length, 11.0 mm in width and 2.0 mm in thickness (Coil and Wetherbee, 1959). In sexually active females, the gland measures approximately 8.0 mm in length and its thickness ranges from 0.9 mm to 1.6 mm (Klemm *et al.*, 1973).

1.2.2 The cloacal gland as an androgen-dependent structure

A positive correlation exists between testicular weight, plasma testosterone concentration, and cloacal gland size (Ottinger and Brinkley, 1979). Exposure of Japanese quails to short days (8 hours light:16 hours dark) instead of long days (16 hours light:8 hours dark), decreases circulating testosterone levels resulting in testicular regression (Sachs, 1967). The cells forming the cloacal gland subsequently regress resulting in a reduction in cloacal gland size (Sachs, 1967).

The development of the cloacal gland and the maintenance of its secretory activity are regulated by androgens via the activation of androgen receptors (Kaku *et al.*, 1993). Kaku *et al.* (1993) further noted that the expression of androgen receptors in the cloacal gland was positively correlated with circulating androgen levels. Therefore, mature birds that had higher levels of circulating testosterone had a greater concentration of androgen receptors compared to younger birds with lower testosterone levels (Kaku *et al.*, 1993). These findings have led to the conclusion that testosterone stimulates the development and activity of the cloacal gland (Biswas *et al.*, 2007).

1.2.3 Biochemical composition of cloacal gland foam

In sexually mature males the cloacal gland produces a clear to opalescent, mucoid secretion which is known as cloacal foam (McFarland *et al.*, 1968). The secretion becomes foamy when it interacts with carbon dioxide and hydrogen produced by the

metabolism of glucose by the bacteria *Escherichia coli* and *Proteus mirabilis* (Singh *et al.*, 2011).

Cloacal foam is composed of substances that are almost similar to those found in blood serum (Singh *et al.*, 2011). Protein, lactate, and various enzymes commonly found in blood have been identified in cloacal foam using biochemical analysis techniques (Singh *et al.*, 2011). Biswas *et al.* (2013) further established that the foam contained transaminase and phosphatase, which were thought to enhance sperm motility. The increased duration of motility of sperm mixed with cloacal foam suggests the presence of a non-sugar component, which may serve as an energy source for spermatozoa (Biswas *et al.*, 2013).

1.2.4 Functions of cloacal foam

There are conflicting reports on the physiological functions of cloacal foam in the Japanese quail (Singh *et al.*, 2011). Cheng *et al.* (1989a) suggested that cloacal foam deposited in the female proctodeum trapped sperm, and subsequently prevented the voiding of spermatozoa during egg-laying (Cheng *et al*., 1989a).

It has been shown that the activity and motility of spermatozoa greatly increase when semen is combined with cloacal foam (Singh *et al.*, 2012). Hence the foam appears to be vital for the migration of sperm through the oviduct, as well as for subsequent fertilization success (Singh *et al.*, 2012). When cloacal foam is present, the effectiveness of fertilization is increased and the fertility period after a single insemination is extended (Adkins-Regan, 1999; Cheng *et al.*, 1989a; Singh *et al.*, 2012). Under *in vitro* conditions, quail sperm aggregates in the absence of cloacal foam, whereas when supplemented with cloacal foam, spermatozoa are: well distributed within the medium; retain normal morphology; become motile for

prolonged periods of time and show increased metabolic activity (Cheng *et al.*, 1989b; Chelmonska *et al.*, 2006; Biswas *et al.*, 2010). These findings suggest that cloacal foam contains components that provide energy to sustain motility for extended periods and also aids in the disaggregation of spermatozoa (Singh *et al.*, 2011; Farooq *et al.*, 2015).

1.3 Aim of the study

To correlate gross anatomical, histomorphological, and ultrastructural changes occurring in the cloacal gland to plasma testosterone levels during the sexual maturation of the male Japanese quail (*Coturnix coturnix japonica*) in a period of decreasing daylength.

1.3.1 Specific Objectives

- To investigate the correlation between biometric data and testosterone levels in the pre-pubertal, pubertal and adult male Japanese quail.
- To determine the changes in the cloacal gland morphology of male Japanese quails during the pre-pubertal, pubertal, and adult stages using light and transmission electron microscopy.
- To determine the correlation between testosterone levels and the heights of secretory cells in the cloacal glands of pre-pubertal, pubertal, and adult quails.
- To determine the incidence of apoptosis in the secretory cells of cloacal glands from pre-pubertal, pubertal, and adult quails using the terminal deoxynucleotidyl transferase-mediated deoxyuridine 5'-triphosphate nick-end labelling (TUNEL) technique.

- To determine the correlation between testosterone levels and the number of apoptotic cells in the cloacal glands of pre-pubertal, pubertal, and adult quails.
- To investigate the distribution of androgen receptors in the cloacal glands of pre-pubertal, pubertal, and adult quails using immunohistochemistry.

2.0 Chapter two

2.1 Introduction and literature review

The cloacal gland is present in the *lamina propria* between the *M. sphincter cloacae* and the stratified squamous epithelium of the cloacal skin (Klemm *et al.*, 1973). Klemm and co-workers (1973) described the cloacal gland as a collection of separate glandular lobes composed of glandular units. Enclosing the glandular mass is a connective tissue capsule from which extend intraglandular trabeculae (Coil and Wetherbee, 1959). Each glandular lobe has a terminal papilla through which the secretory product (cloacal foam) is released into the cloaca (Klemm *et al.*, 1973).

2.1.1 Connective tissue of the cloacal gland

The connective tissue capsule of the cloacal gland is composed of collagen, reticular, as well as elastic fibres (Klemm *et al.*, 1973). Intraglandular trabeculae, which are extensions of the connective tissue capsule, form the walls of the glandular units. These trabeculae contain reticular fibres which extend into the primary and secondary folds of the glandular units (Klemm *et al.*, 1973). The regions of the connective tissue capsule separating the cloacal gland mass from the overlying *M. sphincter cloacae* and the underlying cloacal epithelium are termed the supraglandular and subglandular sub-divisions respectively (Klemm *et al.*, 1973). The supraglandular connective tissue is consistently thick throughout the length of the gland, while that of the subglandular region is relatively thin (Klemm *et al.*, 1973).

2.1.2 Histology of cloacal gland secretory cells

The secretory epithelium of the glandular units forms a series of primary and secondary folds which extend into the lumina of the units (Klemm *et al.*, 1973). The secretory cells lining the glandular units of the cloacal gland contain basally-located

oval nuclei (Klemm *et al.*, 1973). Klemm and co-workers (1973) described the apical cytoplasm as being granular in appearance.

2.1.3 Morphometry of secretory cells in the cloacal gland

Ochs (1979) reported that the secretory cells of the cloacal gland in male quails were taller than those in female quails. Klemm and co-workers (1973) determined that the secretory cells in sexually active males were 22.14 ± 0.46 µm in height, while the cells in female quails were 16.24 ± 0.24 µm ($p < 0.05$).

2.1.4 Ultrastructure of secretory cells in the cloacal gland

Due to marked differences in the appearance and organization of organelles, such as the rough endoplasmic reticulum (RER) and the Golgi complex within the cellular cytoplasm of adult quails, Ochs (1979) described the ultrastructure of secretory cells in the cloacal gland in terms of three progressive stages which constituted the "secretory process" (Ochs, 1979). The three stages of the secretory process were described as follows:

Stage 1: The secretory cells rest on a basal lamina and are attached to adjacent cells via junctional complexes. The cells contain basally-located, oval nuclei with distinct nucleoli. Heterochromatin is dispersed throughout the nucleoplasm. The perinuclear region is occupied by RER profiles and elongated mitochondria. Golgi complexes have closely-packed membranous saccules and a few associated vesicles. Secretory vacuoles with limiting membranes are rarely observed in close association with the Golgi complexes. The apical cell cytoplasm is characterized by the presence of tonofilaments, small membrane-bound vesicles, free ribosomes, as well as a few mature secretory vesicles. The apical cell membrane exhibits microvilli, which extend into the lumen of the glandular unit.

Stage 2: In stage 2, cells demonstrate increased secretory activity. The RER has distended cisternae, which contain electron-dense material. The Golgi complexes have dilated cisternae and are associated with numerous vesicles. Mature secretory droplets occupy most of the apical cytoplasm.

Stage 3: This stage marks the discharge phase of the secretory process. The RER cisternae are greatly distended and disorganized. A granular electron-dense material is present within the RER cisternae. The Golgi complexes have irregular profiles due to the presence of swollen membranous saccules. Few vesicles are associated with the Golgi complexes. The apical cytoplasm has abundant mature secretory droplets which fuse with the apical cell membrane and displace the apical microvilli. The secretory droplets and some cell organelles are expelled into the lumen of the glandular units.

2.1.5 Androgens

The androgens, testosterone and 5α-dihydrotestosterone, are steroidogenic hormones that are formed within the Leydig cells of the testes (Hiort, 2002). Testosterone is converted to its most active and potent metabolite- 5α-dihydrotestosterone, through catalysis by 5α-reductase (Dohle *et al.*, 2003; Davey and Grossmann, 2016). Testosterone and 5α-dihydrotestosterone are crucial for the development and differentiation of androgen-dependent structures (Hiort, 2002). These hormones also play an important role in puberty, fertility, sexual functions and muscle formation (Dohle *et al.*, 2003). Androgen activity is mediated via activation of the androgen receptor (Dohle *et al.*, 2003).

2.1.6 The androgen receptor

The steroid hormone nuclear receptor family is composed of receptors for androgen, oestrogen, progesterone, glucocorticoid and mineralocorticoids (Evans, 1988). The androgen receptor is a 110 kDa nuclear protein that is composed of 918 amino acids (Heinlein and Chang, 2002; Lee and Chang, 2003). The androgen receptor was one of the later steroid receptors to be isolated and characterised (Evans, 1988). This was due to difficulties encountered in the acquisition of sufficient amounts of purified protein required for the synthesis of antibodies (Chang *et al.*, 1988a). Due to the fact that the DNA binding domain is the most conserved in steroid receptors, probes that were previously produced in the cloning of other steroid receptors were used for the screening of cDNA libraries resulting in the first ever cloning of the androgen receptor cDNA (Chang *et al.*, 1988a; Chang *et al.*, 1988b).

The androgen receptor has been localized within the cytoplasm and nucleus (Dohle *et al.*, 2003). Androgen receptors have been identified in several tissues including the prostate, seminal vesicle, vas deferens, testis, vagina, sebaceous glands, liver, kidneys, muscle and brain (Takeda *et al.*, 1990; Ruizeveld de Winter *et al.*, 1991). The level of androgen receptor expression is tissue specific (Ruizeveld de Winter *et al.*, 1991).

2.1.7 The structure of the androgen receptor

The androgen receptor gene is located on the X-chromosome and is composed of eight exons that encode the four different functional domains of the receptor (Lubahn *et al.*, 1989). The amino (NH_2)-terminal transcriptional domain is encoded by exon 1 and the DNA binding domain is encoded by exons 2 and 3. The hinge region is encoded by exon 4, while exons 5-8 encode the ligand binding domain (Evans, 1988; Lubahn *et al.*, 1989). The NH_2-terminal domain of nuclear receptors differs in

size and amino acid composition (Heinlein and Chang, 2002). The NH_2-terminal domain contains two regions, AF-1 and AF-2, which are responsible for regulating transcription. The AF-1 function lies between amino acids 360-494 and acts independently of ligand binding and hence creates a continuously active receptor (Chang *et al.*, 1988b; Jenster *et al.*, 1991; Heinlein and Chang, 2002). The AF-2 function is ligand dependent and occurs between amino acids 141-338 within the ligand binding domain (Chang *et al.*, 1988b; Jenster *et al.*, 1991; Heinlein and Chang, 2002). Any deletions or mutations of the AF-2 function result in a reduced activation of transcription (Chang *et al.*, 1988b; Jenster *et al.*, 1991; Heinlein and Chang, 2002).

The DNA binding domain is unchanged in the steroid hormone nuclear receptor family (Evans, 1988). It is composed of two zinc fingers that allow the androgen receptor to bind directly to the regions within the genes mediated by the androgen receptor, where transcription is activated (Davey and Grossmann, 2016). This binding will then result in either the enhancement or repression of the transcription of these genes (Davey and Grossmann, 2016). The hinge region attaches the DNA binding domain to the ligand binding domain (Heinlein and Chang, 2002; Davey and Grossmann, 2016). Nuclear receptors also share a common structure of the ligand binding domain (Davey and Grossmann, 2016). This domain forms ligand attachment sites and functions in regulating the association of the androgen receptor with heatshock proteins (Heinlein and Chang, 2002; Davey and Grossmann, 2016). It also stabilizes the bound androgen at the NH_2-terminal (Davey and Grossmann, 2016).

2.1.8 Molecular mechanisms of androgen action

Upon secretion by the testes, testosterone binds to sex hormone binding globulins and is then transported to the target cells (Hiort, 2002). When testosterone reaches a target cell, it diffuses into the cytoplasm as an unbound molecule and either induces certain changes within the cell or is further metabolized into 5α-dihydrotestosterone by 5α-reductase (Hiort, 2002). The androgens then bind to cytoplasmic androgen receptors and induce structural changes, including separation from chaperone proteins. This interaction exposes nuclear localisation signals (Hiort, 2002; Davey and Grossmann, 2016). The hormone/receptor complex then migrates to the nucleus where it associates with androgen responsive elements that regulate gene transcription through either synergistic or antagonistic mechanisms (Davey and Grossmann, 2016). Gene expression followed by protein translation then occur with resultant changes in the functioning of the cell (Lee and Chang, 2003).

2.1.9 Regulation of androgen receptor expression

Androgen receptor expression varies during foetal development, sexual maturation, aging, as well as in malignant transformation (Keller *et al.*, 1996). Androgen receptor levels can be regulated at the transcription, translation, post-translational modification, or at the protein level (Keller *et al.*, 1996). The androgen receptor protein and mRNA expression are regulated by various elements, such as growth factors as well as by various hormones, including androgens (Keller *et al.*, 1996). There have been conflicting reports on the role of androgens in androgen receptor expression (Keller *et al.*, 1996). Androgens were found to decrease the mRNA expression of the androgen receptor in: the ventral prostate of the rat (Quarmby *et al.*, 1990; Shan *et al.*, 1990); human androgen-responsive prostate carcinoma cell line (Quarmby *et al.*, 1990; Wolf *et al.*, 1993), as well as in a hepatoma cell line

(Shan *et al.*, 1990). However, increased androgen receptor mRNA expression was reported in the dorsal prostate glands of rats and mice (Takeda *et al.*, 1991), genital fibroblasts (Keller *et al.*, 1996) and in fat-pad adipose precursor cells of male rats (De Pergola *et al.*, 1990). These differences, may be attributed to the different methods used in the studies or may be as a result of tissue specific transcription factors (Keller *et al.*, 1996).

2.2 Materials and methods

2.2.1 Animals and management

This study was conducted during the autumnal decrease in daylength. The precise daylengths for Pretoria, South Africa, on the sampling dates were obtained from www.timeanddate.com. The birds were maintained in a poultry house exposed to natural day light. The room temperature was maintained at 25^0C.

A total of 7 pre-pubertal (4 weeks old), 7 pubertal (6-7 weeks old) and 7 adult (12 weeks old) male Japanese quails were used in the present study. The birds were maintained in individual cages. The pre-pubertal birds were sampled when the daylength was 12 hours, 28 minutes. Collections from pubertal birds occurred when daylengths were 12 hours, 19 minutes (2 birds), 12 hours, 8 minutes (3 birds) and 11 hours, 57 minutes (2 birds). Puberty was determined as the first day of release of cloacal foam. Samples from adult birds were collected when the daylength was 11 hours, 6 minutes.

The bodyweights of the birds were measured prior to decapitation. In addition, the maximum length and maximum width (Figure 2.1) of the cloacal gland of each bird was measured using a digital calliper.

The cloacal gland area was determined using the formula:

Cloacal gland area = maximum cloacal gland height x maximum cloacal gland width.

A blood sample was taken from each bird at decapitation. The birds were killed at between 08:00 and 09:00 hours.

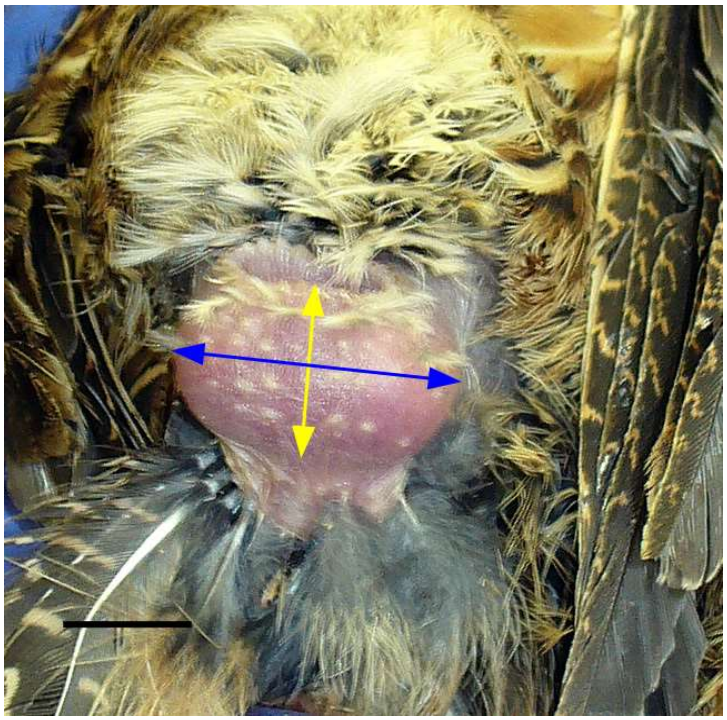

Figure 2.1: Cloacal gland of a pubertal quail held in dorsal recumbency. Yellow arrow: maximum cloacal gland height. Blue arrow: maximum cloacal gland width. Bar = 2cm.

2.2.2 Hormone analysis

Blood samples were collected during decapitation. The blood was collected into heparinized tubes and kept on ice. The blood samples were subsequently centrifuged at 3000 rpm for 15 minutes at 4^0C. The plasma fraction was then aspirated and stored in microcentrifuge tubes at -86^0C. Testosterone concentrations were measured using a commercially available radioimmunoassay (RIA)

Testosterone, direct kit (Beckman Instruments Pty Ltd., Johannesburg, South Africa) following the manufacturer's instructions.

2.2.3 Tissue processing for light microscopy

Cloacal gland tissue was fixed in a solution of 10% neutral buffered formalin (pH 7.0). The tissue samples were processed using an automated tissue processor (Shandon Excelsior; Thermo Scientific, Germany). In brief, the tissues were dehydrated in a series of alcohol concentrations (50%, 70%, 80%, 95%, and 100%), cleared in xylene, infiltrated with molten paraffin wax, and then embedded in paraffin wax. Tissue sections (5 µm thick) were mounted on glass slides and stained with haematoxylin and eosin. In addition, the tissues were stained using periodic acid Schiff (Abcam, ab150680) and alcian blue (Abcam, ab150662) staining kits. The periodic acid Schiff and alcian blue kits were used following the manufacturer's instructions.

2.2.4 Morphometry of secretory epithelial cells

The heights of 15 random cells per haematoxylin and eosin-stained section in five different sections were measured. The heights of the cells were measured by drawing a vertical line from the bases to the luminal ends of the cells. All measurements were made using an image analyser (AnalySIS®; Olympus BX63; Optical Company LTD, Japan) at a magnification of x40.

2.2.5 Quantification of apoptosis using the terminal deoxynucleotidyl transferase-mediated deoxyuridine 5'-triphosphate nick-end labelling (TUNEL) technique.

An *in situ* TUNEL Assay- Apoptag$^{(R)}$-peroxidase kit (Millipore, Temecula, USA) was used to quantitatively assess the incidence of apoptotic cells in the cloacal gland

tissue sections. TUNEL was performed on 5µm thick sections. TUNEL staining was performed according to the manufacturer's instructions. In brief, the tissue sections were deparaffinized, rehydrated through a graded series of ethanol and washed in 0.01M phosphate buffered saline solution (PBS, pH 7.4). The sections were then pretreated with proteinase-K (20 µg/ml) for 15 minutes at room temperature. The slides were then rinsed in two changes of distilled water for 2 minutes each. Endogenous peroxidase activity was blocked using a 3% (v/v) hydrogen peroxide solution in PBS for 5 minutes. The slides were then rinsed in PBS for 5 minutes. Thereafter, the sections were incubated with an equilibration buffer (ApopTag plus peroxidase kit, Millipore, Temecula, USA) at room temperature for 10 minutes. Excess buffer was tapped off the sections before the application of working strength terminal deoxynucleotidyl transferase enzyme (77µl reaction buffer and 33µl TdT enzyme). The sections were then incubated in a humidified chamber at 37°C for 1 hour. The reaction was stopped by rinsing the sections in stop/wash buffer (ApopTag plus peroxidase kit, Millipore, Temecula, USA) for 10 minutes at room temperature. The sections were then rinsed in three changes of PBS for 1 minute each. The excess buffer was tapped off before the application of anti-digoxigenin conjugate (ApopTag plus peroxidase kit, Millipore, Temecula, USA). The sections were then incubated in a humidified chamber for 30 minutes at room temperature. The sections were then rinsed in four changes of PBS for 2 minutes each. Excess buffer was then tapped off the slides. Apoptotic nuclei were visualized after the addition of a diaminobenzidine solution (ApopTag plus peroxidase kit, Millipore, Temecula, USA). The sections were then rinsed in distilled water and counterstained with 0.5% (w/v) methyl green for 10 minutes at room temperature. The slides were then rinsed in distilled water and then dehydrated in 100% N-butanol and cleared in xylene.

In the negative controls the TdT enzyme reagent was replaced with distilled water. Rat mammary gland (supplied with the ApopTag plus peroxidase kit) was used as a positive control.

The number of apoptotic cells were counted with the aid of an image analyser system (CellSens dimension software) connected to an Olympus BX-63 microscope.

2.2.6 Immunohistochemistry

Tissue samples from the cloacal gland were fixed in 10% buffered formalin (pH 7.0) for 5 days and processed routinely for light microscopy. The immunostaining technique was performed on 5 µm thick sections using a Biogenex super sensitive one-step polymer-HRP detection system kit (Emergo Europe, The Hague, The Netherlands). The sections were deparaffinized and endogenous peroxidase activity was blocked, using a 3% (v/v) hydrogen peroxide solution in water for 5 minutes. The slides were then rinsed in a 0.01 M phosphate buffered saline solution (PBS, pH 7.4) for 5 minutes. Thereafter, the sections were microwaved in citrate buffer (pH 6.0) for 3 cycles of 7 minutes each.

The sections were then incubated for 1 hour at 37^0C with a rabbit polyclonal anti-androgen receptor antibody (Abcam, ab3509) at a dilution of 1:10. This antibody localizes the androgen receptor in both the nucleus and cytoplasm. The slides were then rinsed with PBS and subsequently incubated for 15 minutes with the one-step polymer-HRP reagent (Emergo Europe, The Hague, The Netherlands). Slides were then rinsed in PBS. Bound antibody was visualized after the addition of a 3,3'-diaminobenzidine tetrachloride solution (Emergo Europe, The Hague, The Netherlands). The sections were counter-stained with Mayer's haematoxylin. In the

negative control sections, the primary antibody was replaced with rabbit IgG1 (Dakocytomation, Glostrup, Denmark).

The number of androgen receptor immunopositive secretory cells was determined in ten randomly selected glandular units per section. The number of immunopositive cells was then expressed as a percentage of the total number of epithelial cells forming the glandular units. Statistical analysis of values obtained was performed using the statistical software package IBM SPSS (version 25.0, IBM SPSS Inc., Chicago, USA). Significant differences between developmental stages were determined using one-way Analysis of Variance (ANOVA) after testing for normality and homogeneity.

2.2.7 Transmission Electron Microscopy

Tissue samples from the cloacal gland were immersion-fixed in 2.5% glutaraldehyde in 0.075M phosphate buffer (pH 7.4) for 24 hours. Thereafter, the tissue samples were rinsed with phosphate buffer (pH 7.4) and post-fixed in 0.5% osmium tetroxide for 2 hours. The tissue samples were then washed with double distilled water, dehydrated in a graded series of ethanol concentrations, followed by a propylene oxide rinse. The samples were then infiltrated with a propylene oxide:epoxy resin mixture at a ratio of 1:2 for 1 hour, 1:1 for 2 hours and 100% resin overnight. The samples were then polymerized in fresh 100% resin for 24 hours at 60°C. Semi-thin (350nm) sections were cut and stained with toluidine blue.

Ultra-thin sections of selected areas were cut using a diamond knife, placed on copper grids, and stained with uranyl acetate and lead citrate. The sections were then examined using a Phillips CM10 transmission electron microscope (Phillips Electron Optical Division, Eindhoven, The Netherlands), operated at 80kV. A

megaview III side-mounted digital camera (Olympus Soft Imaging Solutions GmbH, Munster, Germany) was used to capture the images and iTEM software (Olympus Soft Imaging Solutions GmbH, Munster, Germany) was used to adjust the brightness and contrast.

2.2.8 Statistical analysis

Statistical analysis was performed using the statistical software package IBM SPSS (version 25.0, IBM SPSS Inc., Chicago, USA). Significant differences between the different age groups were determined using one-way analysis of variance (ANOVA) or the Kruskal-Wallis test, after testing for variance homogeneity and normality. Correlations between parameters were determined using the Pearson's correlation coefficient. The level of statistical significance was set at $p< 0.05$

2.3 Results

2.3.1 Hormone analysis

The data on plasma testosterone levels was tested for homogeneity and normality. The Shapiro Wilks test revealed that the data was not normally distributed ($p<0.05$). Therefore, the data was analysed using the Kruskal-Wallis test. The data on plasma testosterone levels in pre-pubertal, pubertal and adult birds is presented in Table 2.1 and Graph 2.1. Analysis of plasma testosterone concentrations with the Kruskal-Wallis test showed significant differences ($p<0.05$) in the mean values between pre-pubertal and pubertal birds, as well as between pre-pubertal and adult birds.

Table 2.1: Plasma testosterone concentrations in pre-pubertal, pubertal and adult Japanese quails.

Age group	Testosterone concentration (nmol/L)
Pre-pubertal	0.04 ± 0.04^{ab}
Pubertal	1.05 ± 0.34^{a}
Adult	2.73 ± 0.78^{b}

All data is expressed as mean ± standard error with $p<0.05$ considered to be statistically significant. There are statistically significant differences between means sharing the same superscript.

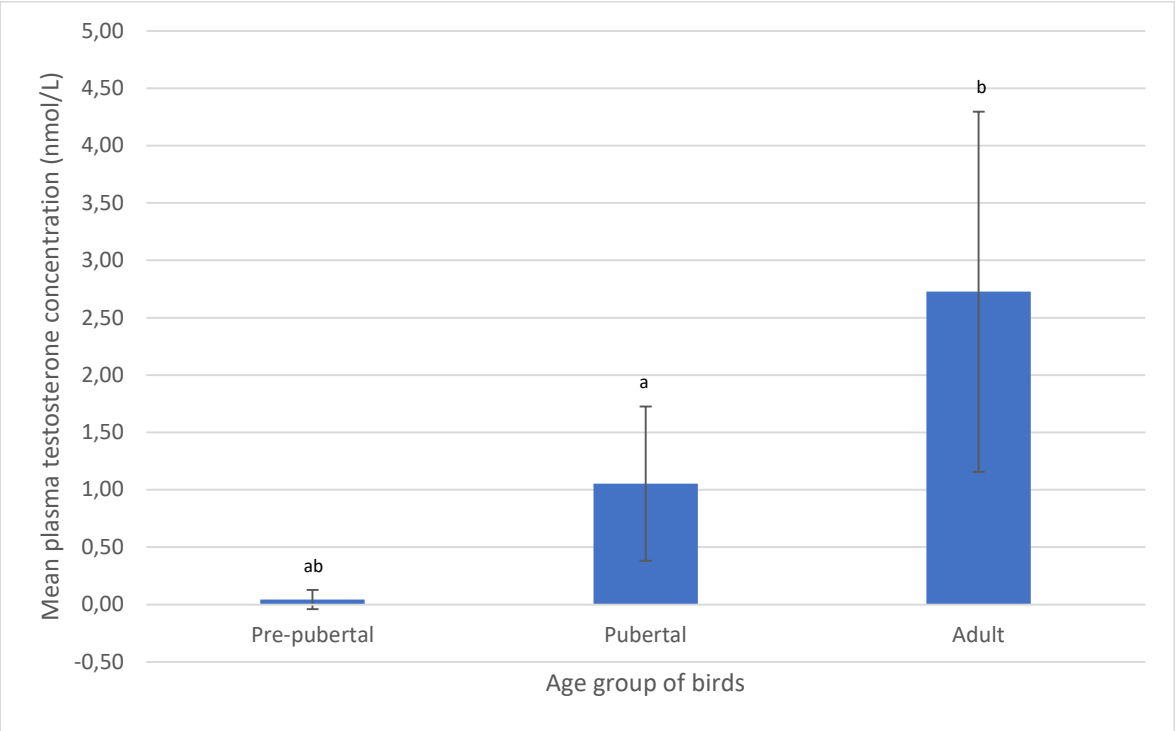

Graph 2.1: Plasma testosterone levels in pre-pubertal, pubertal and adult birds. Data is expressed as mean ± standard error. There are statistically significant differences between means sharing the same lettering. The data was analyzed using the Kruskal-Wallis test.

2.3.2 Biometric data

The data on biometric parameters (bodyweights, cloacal gland height, width and area) was tested for homogeneity and normality. The Shapiro Wilks test showed that the data for bodyweight, cloacal gland height, as well as the cloacal gland area was normally distributed ($p>0.05$). Therefore, the data was analyzed using one way-ANOVA. However, the data for cloacal gland width did not show a normal distribution ($p<0.05$). Therefore, the Kruskal-Wallis test was used to analyze this data.

The data for changes in biometric parameters (bodyweight, cloacal gland height, width and area) for the various age groups is presented in Table 2.2 and Graphs 2.2-2.5. Analysis of bodyweight and cloacal gland area data using one-way ANOVA showed statistically significant differences ($p<0.05$) in the mean values of pre-pubertal, pubertal and adult birds (Table 2.2, Graphs 2.2 & 2.3). However, significant differences ($p<0.05$) in the mean values for cloacal gland height were only observed between pre-pubertal and pubertal birds, as well as between pre-pubertal and adult birds (Table 2.2, Graph 2.4). The Kruskal-Wallis test showed statistically significant differences ($p<0.05$) in cloacal gland width only between pre-pubertal and adult birds (Table 2.2, Graph 2.5)**.**

Correlations between the biometric parameters and testosterone concentrations were determined using Pearson's correlation test. Data on the correlations between plasma testosterone concentrations and biometric parameters is presented in Tables 2.3-2.6. Analysis of data revealed moderate positive correlations that were statistically significant between plasma testosterone concentrations and biometric parameters of the birds.

Table 2.2: Biometric parameters of pre-pubertal, pubertal and adult male Japanese quails.

Age group	Bodyweight (g)	Cloacal gland		
		Height (mm)	Width (mm)	Area (mm^2)
Pre-pubertal	88.20 ± 5.70^{ab}	7.86 ± 0.84^{ab}	8.18 ± 0.74^{a}	67.34 ± 12.34^{ab}
Pubertal	131.90 ± 4.05^{ac}	12.94 ± 0.55^{a}	15.68 ± 0.37	203.93 ± 13.63^{ac}
Adult	161.36 ± 8.12^{bc}	13.99 ± 0.49^{b}	19.17 ± 0.37^{a}	268.30 ± 10.96^{bc}

All data is expressed as mean ± standard error with $p<0.05$ considered to be statistically significant. There are statistically significant differences between means sharing the same superscript within each column.

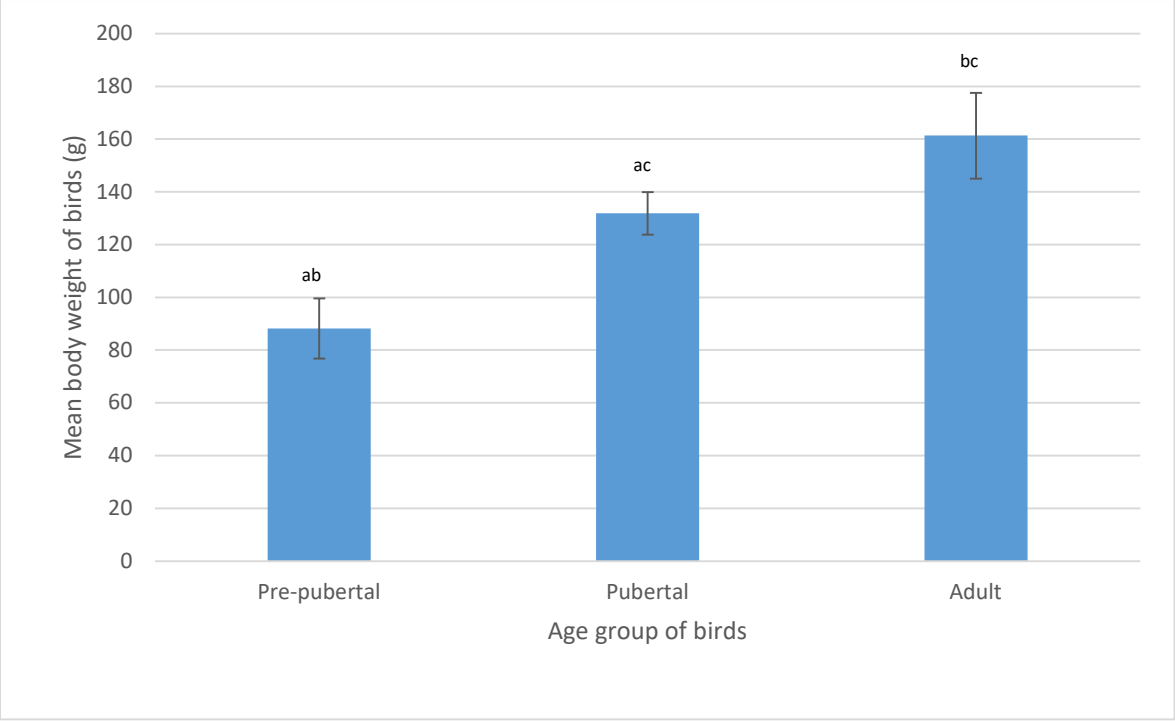

Graph 2.2: Bodyweights of pre-pubertal, pubertal and adult birds. Data is expressed as mean ± standard error. There are statistically significant differences between means sharing the same lettering. The data was analyzed using one-way ANOVA.

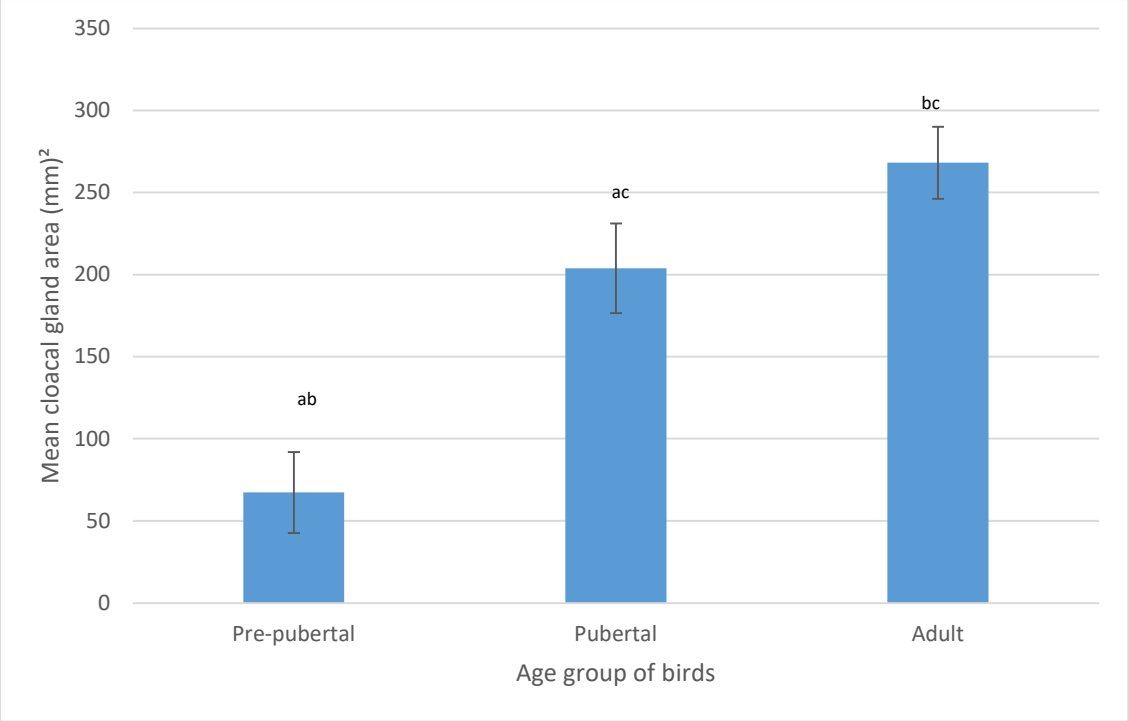

Graph 2.3: Cloacal gland areas of pre-pubertal, pubertal and adult birds. Data is expressed as mean ± standard error. There are statistically significant differences between means sharing the same lettering. The data was analyzed using one-way ANOVA.

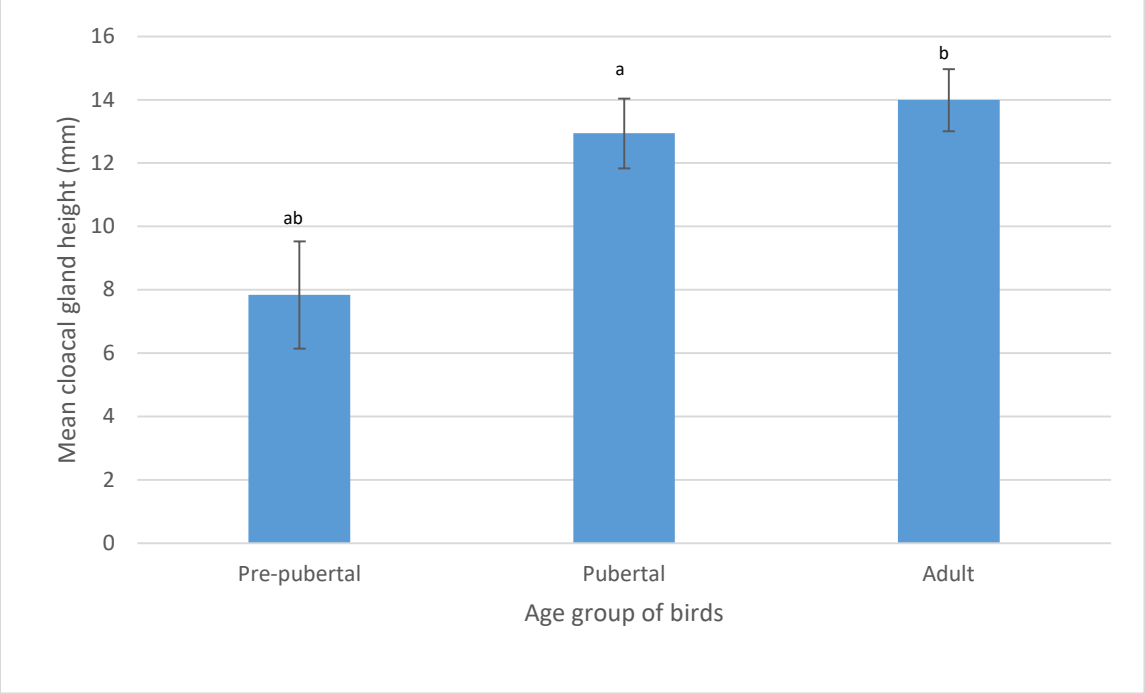

Graph 2.4: Cloacal gland heights in pre-pubertal, pubertal and adult birds. Data is expressed as mean ± standard error. There are statistically significant differences between means sharing the same lettering. The data was analyzed using one-way ANOVA.

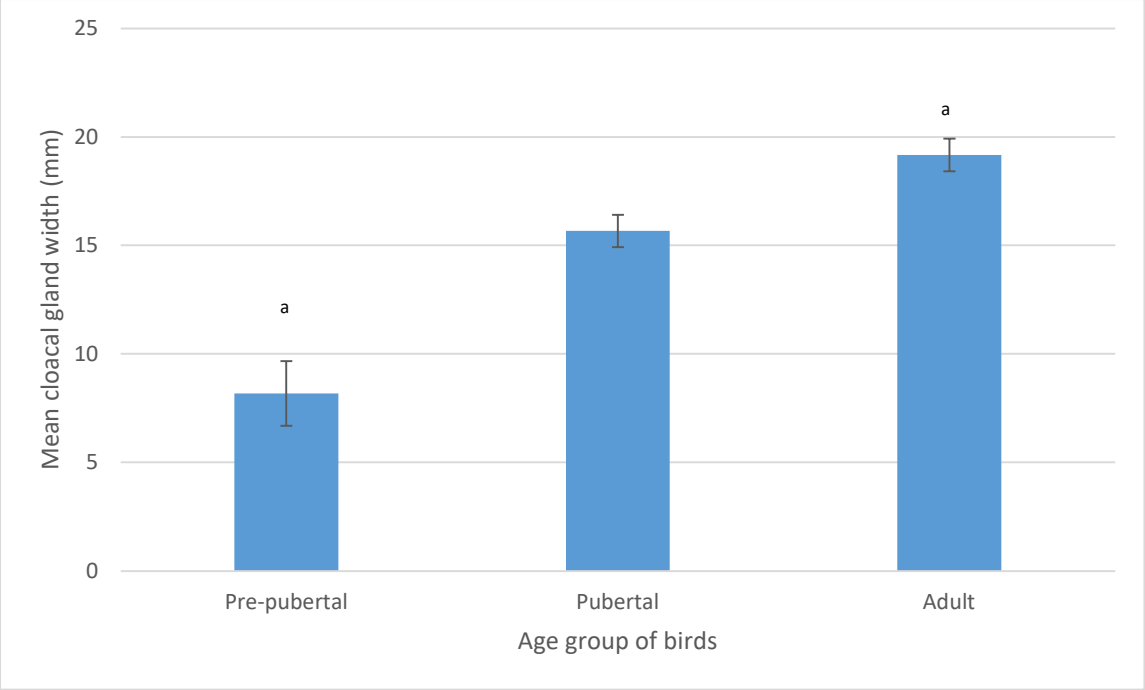

Graph 2.5: Cloacal gland widths in pre-pubertal, pubertal and adult birds. Data is expressed as mean ± standard error. There are statistically significant differences between means sharing the same lettering. The data was analyzed using the Kruskal-Wallis test.

Table 2.3: Correlation between the plasma testosterone concentrations and body weights of quails.

		Plasma testosterone concentrations	Body weight of birds
Plasma testosterone concentrations	Pearson Correlation	1	.519*
	Sig. (2-tailed)		.016
	N	21	21
Body weight of birds	Pearson Correlation	.519*	1
	Sig. (2-tailed)	.016	
	N	21	21

*. Correlation is significant at the 0.05 level (2-tailed).

Table 2.4: Correlation between plasma testosterone concentration and cloacal gland height.

		Plasma testosterone concentrations	Cloacal gland height
Plasma testosterone concentrations	Pearson Correlation	1	.444*
	Sig. (2-tailed)		.044
	N	21	21
Cloacal gland height	Pearson Correlation	.444*	1
	Sig. (2-tailed)	.044	
	N	21	21

*. Correlation is significant at the 0.05 level (2-tailed).

Table 2.5: Correlation between plasma testosterone concentration and cloacal gland width.

Correlations

		Plasma testosterone concentrations	Cloacal gland width
Plasma testosterone concentrations	Pearson Correlation	1	.624**
	Sig. (2-tailed)		.003
	N	21	21
Cloacal gland width	Pearson Correlation	.624**	1
	Sig. (2-tailed)	.003	
	N	21	21

**. Correlation is significant at the 0.01 level (2-tailed).

Table 2.6: Correlation between plasma testosterone concentration and cloacal gland area.

		Plasma testosterone concentrations	Cloacal gland area
Plasma testosterone concentrations	Pearson Correlation	1	.562**
	Sig. (2-tailed)		.008
	N	21	21
Cloacal gland area	Pearson Correlation	.562**	1
	Sig. (2-tailed)	.008	
	N	21	21

**. Correlation is significant at the 0.01 level (2-tailed).

2.3.3 Haematoxylin and eosin-stained sections

Pre-pubertal birds

In pre-pubertal birds, the developing cloacal gland was located between the stratified squamous epithelium of the cloaca and muscle bundles of the *M. sphincter cloacae* (Figure 2.2). Dorsal to the *M. sphincter cloacae* was connective tissue with numerous adipocytes and feather follicles (Figure 2.3).

The cloacal gland in pre-pubertal quails was poorly-developed. The gland was composed of glandular lobes, each connected via individual ducts to the non-keratinized squamous epithelium lining of the cloaca (Figure 2.3). Each glandular lobe contained several glandular units. The majority of glandular units contained well-defined lumina. A few glandular units were composed of clusters of differentiating cells with no apparent lumina (Figure 2.3).

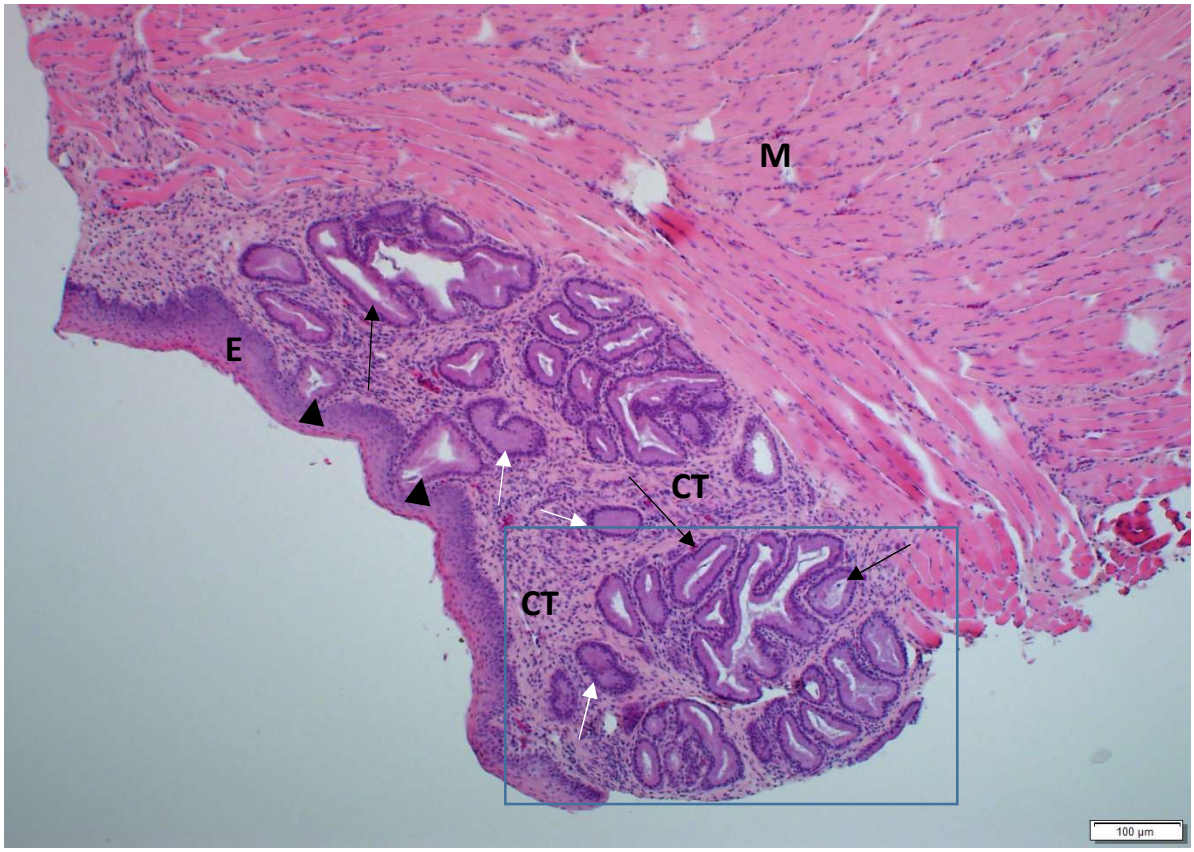

Figure 2.2: Light photomicrograph showing the cloacal gland in a pre-pubertal bird. E: non-keratinized stratified squamous epithelium. M: muscle fibres of the *M. sphincter cloacae*. Arrowheads: glandular ducts. Rectangular outline: glandular lobe. Black arrows: glandular units with well-defined lumina. White arrows: glandular units lacking apparent lumina. CT: connective tissue. Haematoxylin and eosin stain.

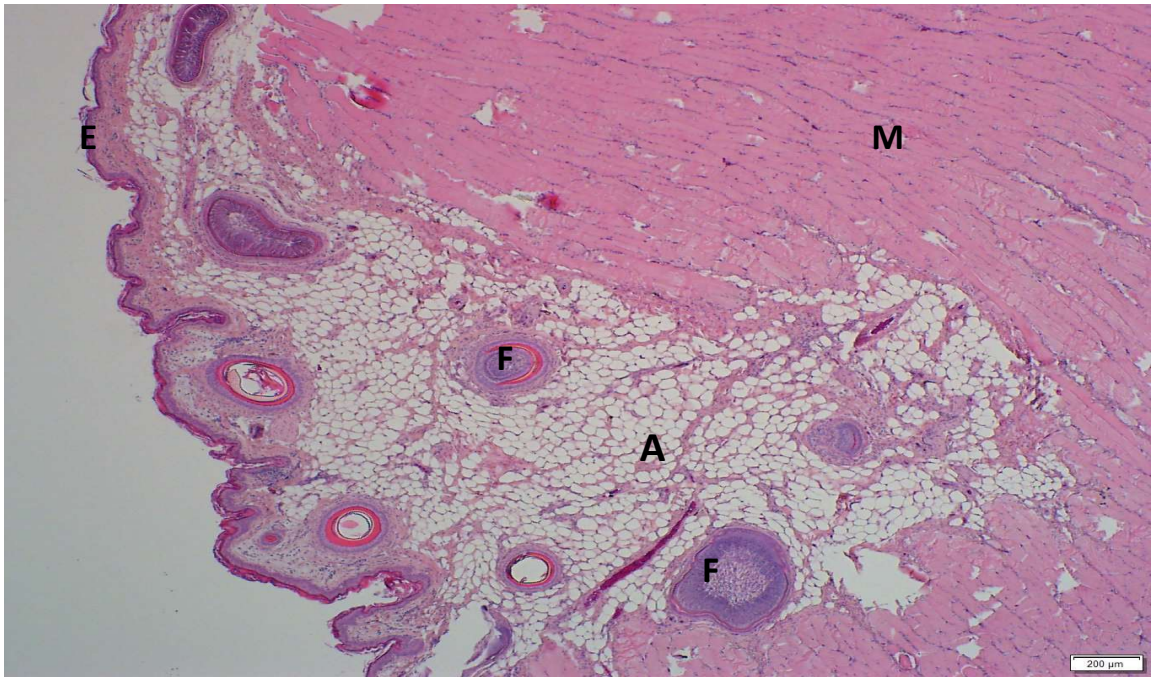

Figure 2.3: Light photomicrograph of the keratinized stratified squamous epithelium (E), subcutaneous connective tissue and *M. sphincter cloacae* (M) overlying the cloacal gland in a pre-pubertal bird. A: adipose tissue. F: feather follicles. Haematoxylin and eosin stain.

In pre-pubertal quails, adjacent glandular units were separated by wide areas of dense irregular connective tissue (Figure 2.4). Numerous dark-stained leukocytes, as well as blood vessels were observed within the connective tissue (Figure 2.5).

As the developing glandular units extended into the connective tissue, they became convoluted in form (Figure 2.6). Extending from the glandular units were several branched epithelial buds (Figure 2.6). The buds were initially formed by a solid mass of cells, with a lumen forming in the later stages of development. The resultant glandular units were lined by simple columnar epithelium containing basally-located nuclei and foamy, eosinophilic cytoplasm (Figures 2.5 & 2.6). Eosinophilic secretory material was observed in some of the lumina of the glandular units (Figure 2.5). As

stated previously a collection of glandular units formed a glandular lobe. The secretory material from the glandular lobes was excreted into the cloaca through individual ducts. These ducts were lined with non-keratinized stratified squamous epithelium (Figure 2.5).

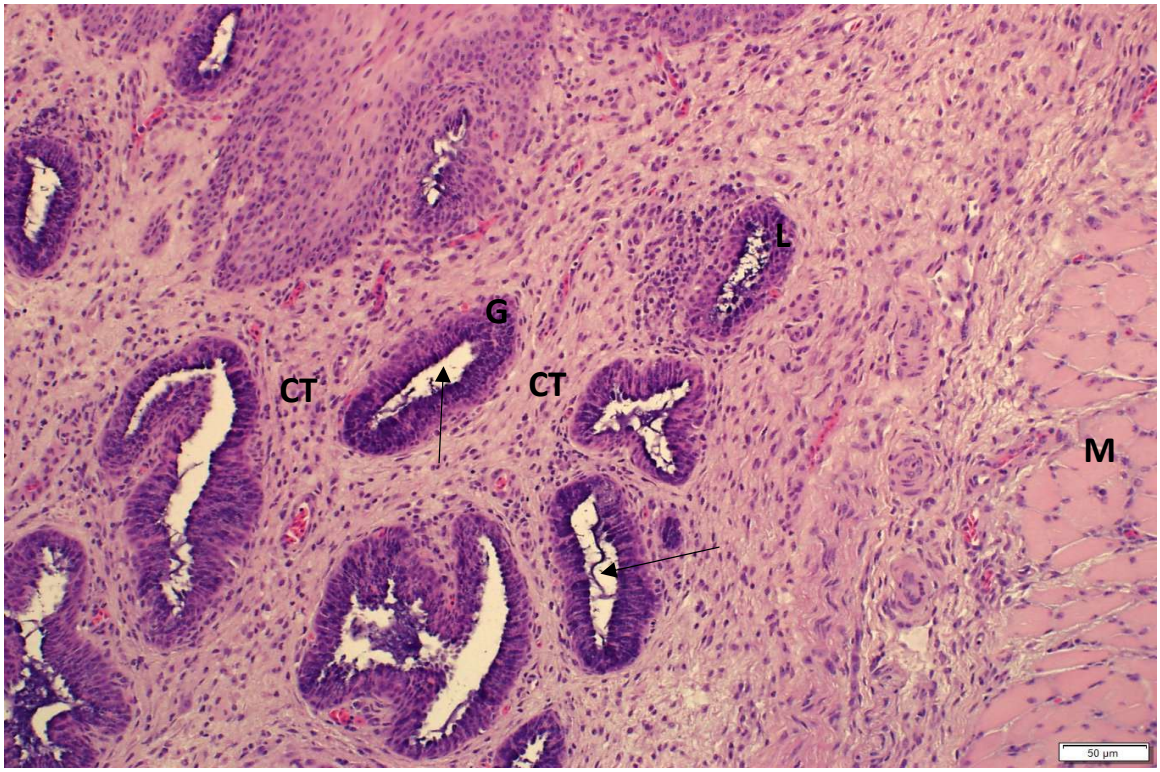

Figure 2.4: Light photomicrograph showing cloacal glandular units (G) in a pre-pubertal bird. CT: dense irregular connective tissue. Arrows: lumina. M: muscle fibres of the *M. sphincter cloacae*. Haematoxylin and eosin stain.

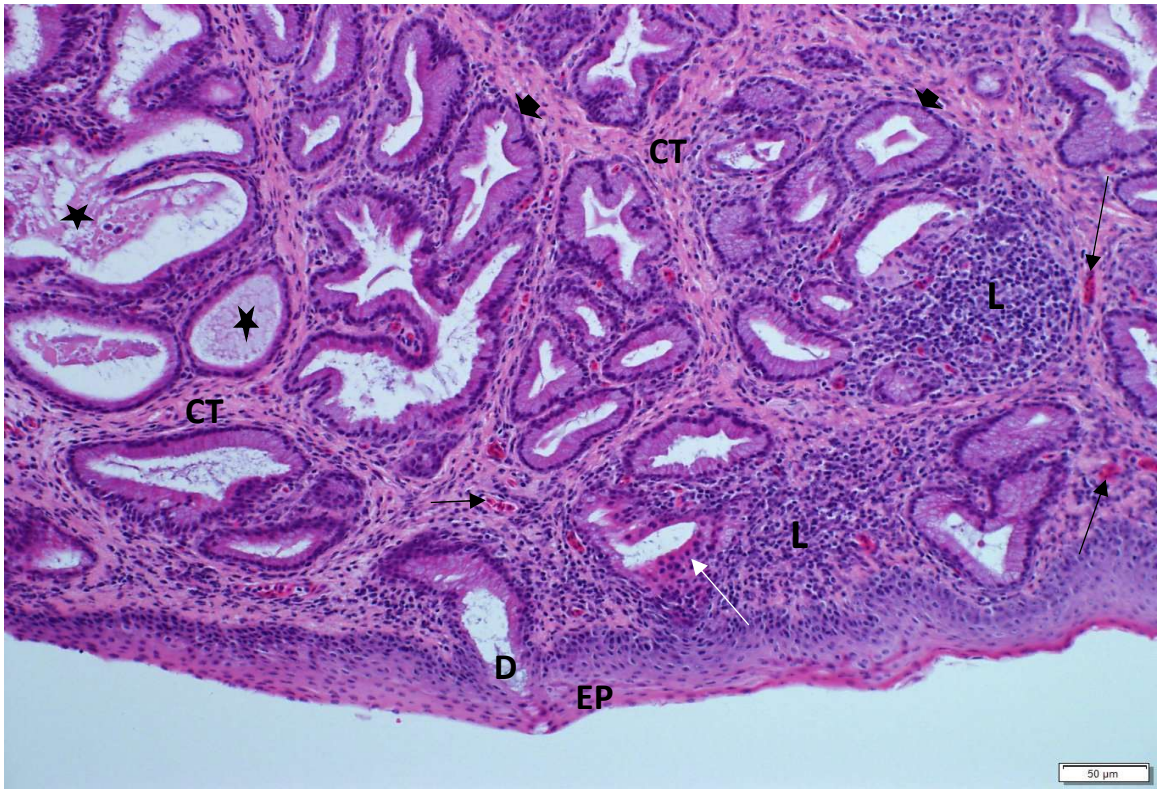

Figure 2.5: Light photomicrograph of the cloacal gland from a pre-pubertal bird. L: leukocytic infiltrations. Black arrows: blood vessels containing nucleated red blood cells. Arrowheads: simple columnar epithelium lining glandular units. Asterisks: secretory material. D: duct leading to the epithelial surface. EP: non-keratinized stratified squamous epithelium. White arrow: developing glandular unit. CT: connective tissue. Haematoxylin and eosin stain.

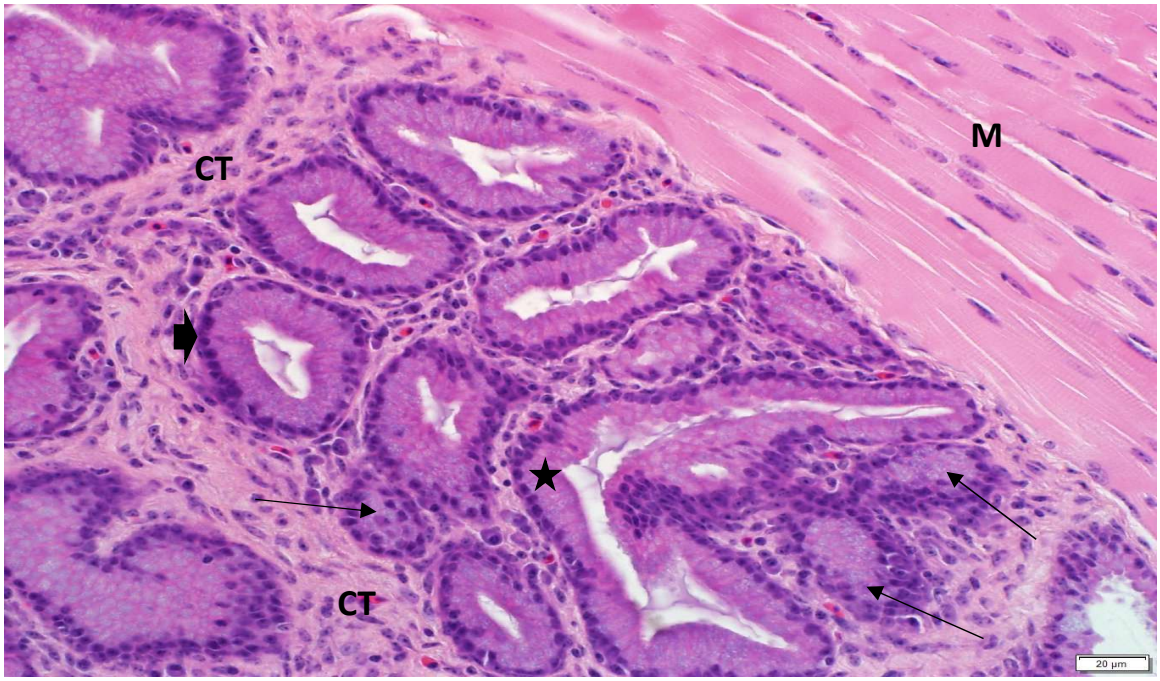

Figure 2.6: Light photomicrograph of a cloacal gland from a pre-pubertal quail showing developing glandular units within a lobe. Asterisk: convoluted glandular unit. Arrows: epithelial buds. Arrowhead: simple columnar epithelium. CT: connective tissue. M: muscle fibres of the *M. sphincter cloacae*. Haematoxylin and eosin stain.

Pubertal birds

The cloacal gland in pubertal birds was composed of well-developed glandular units, which were separated by connective tissue trabeculae (Figure 2.7). Due to the size and extensive distribution of the glandular units it was not possible to define individual glandular lobes.

The epithelial lining and *lamina propria* of glandular units formed primary and occasional secondary folds, which projected into the lumina of the units (Figure 2.7). Glandular units lacking folds were also observed (Figure 2.8).

Glandular units of the cloacal gland in pubertal quails were lined by secretory, columnar epithelial cells. The nuclei of the cells were darkly-stained and basally-located. The supranuclear cytoplasm was vacuolated.

In some glandular units, primary folds were lined by degenerating cells (Figure 2.9). In addition, cellular debris was observed in the lumina of several glandular units (Figure 2.10). The degenerative process culminated in the presence of regressed glandular units within the connective tissue areas between units exhibiting a normal histological appearance (Figure 2.11).

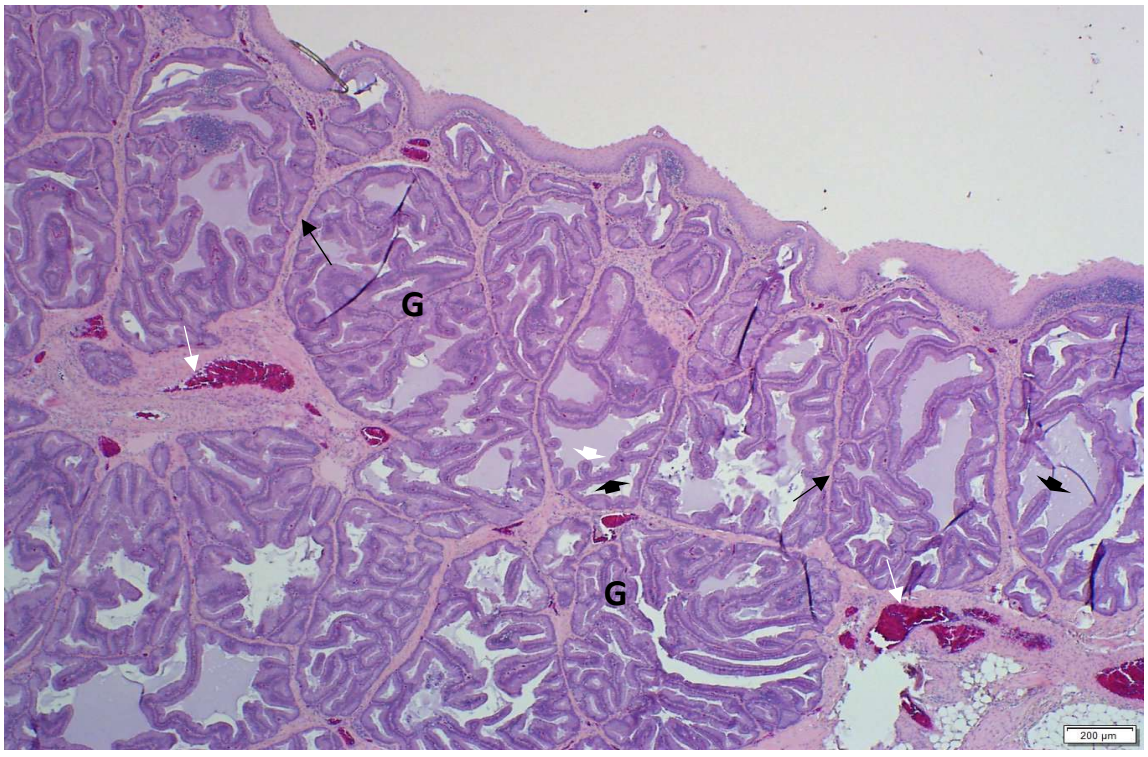

Figure 2.7: Light photomicrograph of a cloacal gland from a pubertal bird. G: glandular units. Black arrows: connective tissue trabeculae. Black arrowheads: primary folds. White arrowhead: secondary fold. White arrows: blood vessels containing red blood cells. Haematoxylin and eosin stain.

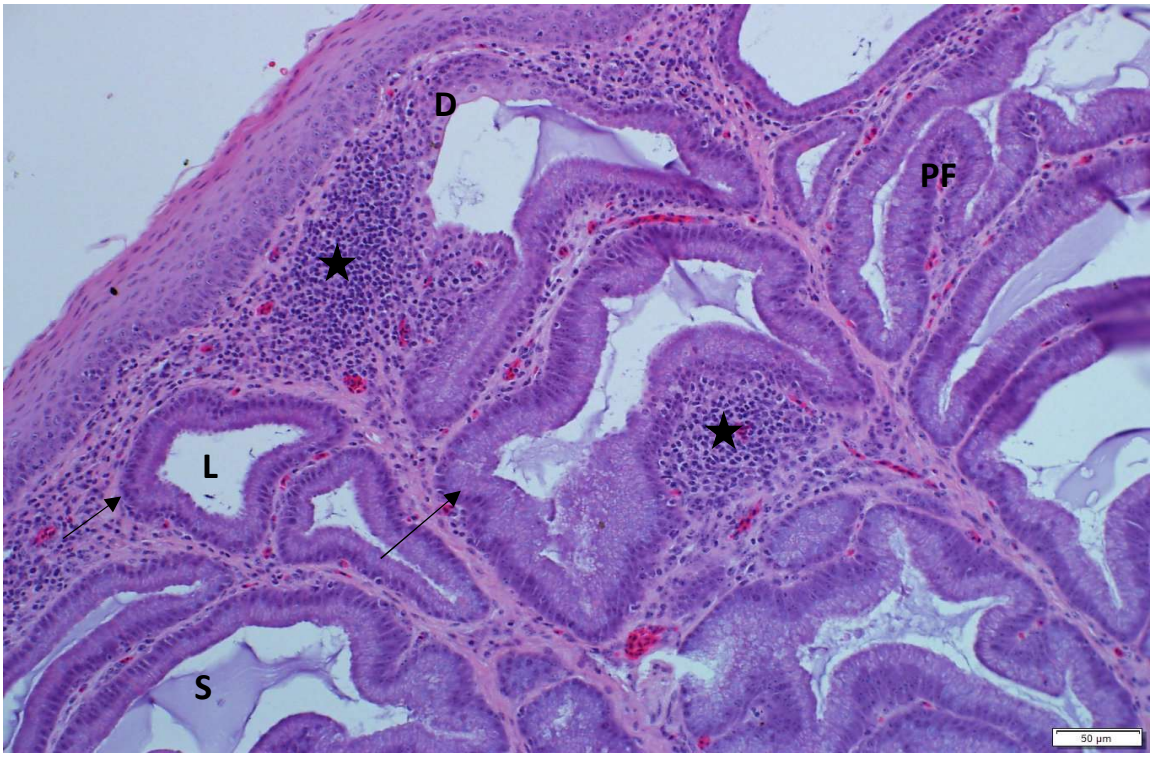

Figure 2.8: Light photomicrograph of a cloacal gland from a pubertal bird. Note the presence of glandular units lacking mucosal folds (arrows). Asterisks: leukocytic infiltrations. D: initial segment of a duct. L: lumen. PF: primary fold. S: secretion. Haematoxylin and eosin stain.

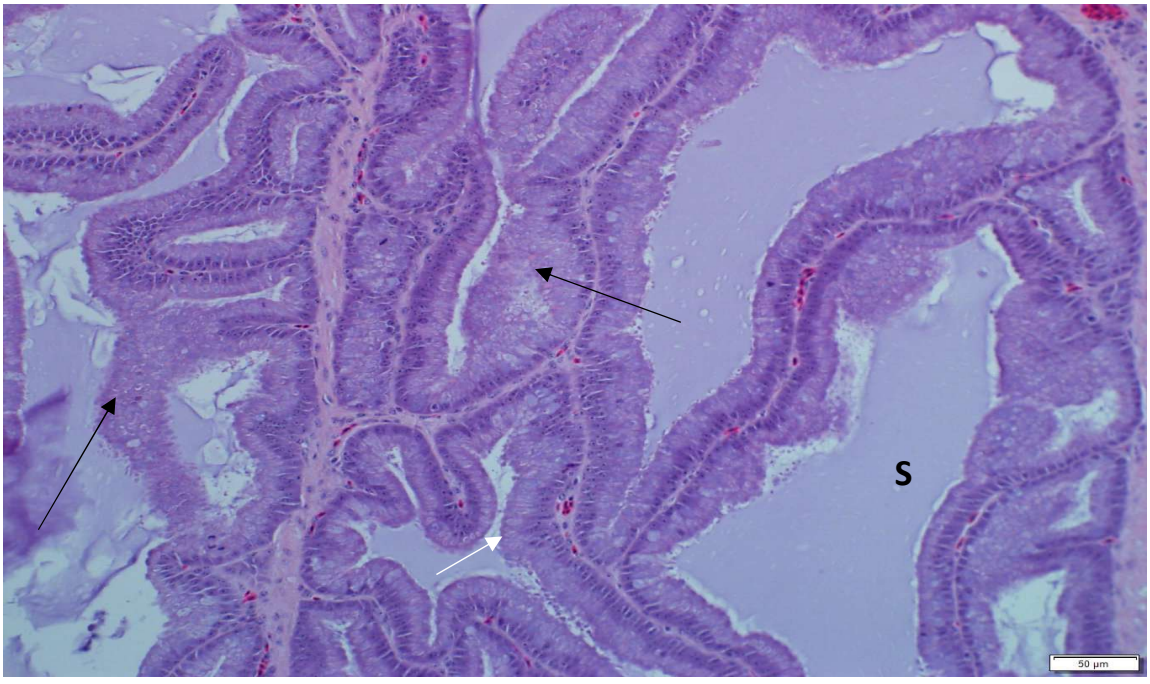

Figure 2.9: Light photomicrograph showing groups of degenerating secretory cells (arrows) within the lining epithelium of glandular units in a pubertal bird. S: secretory material. Haematoxylin and eosin stain.

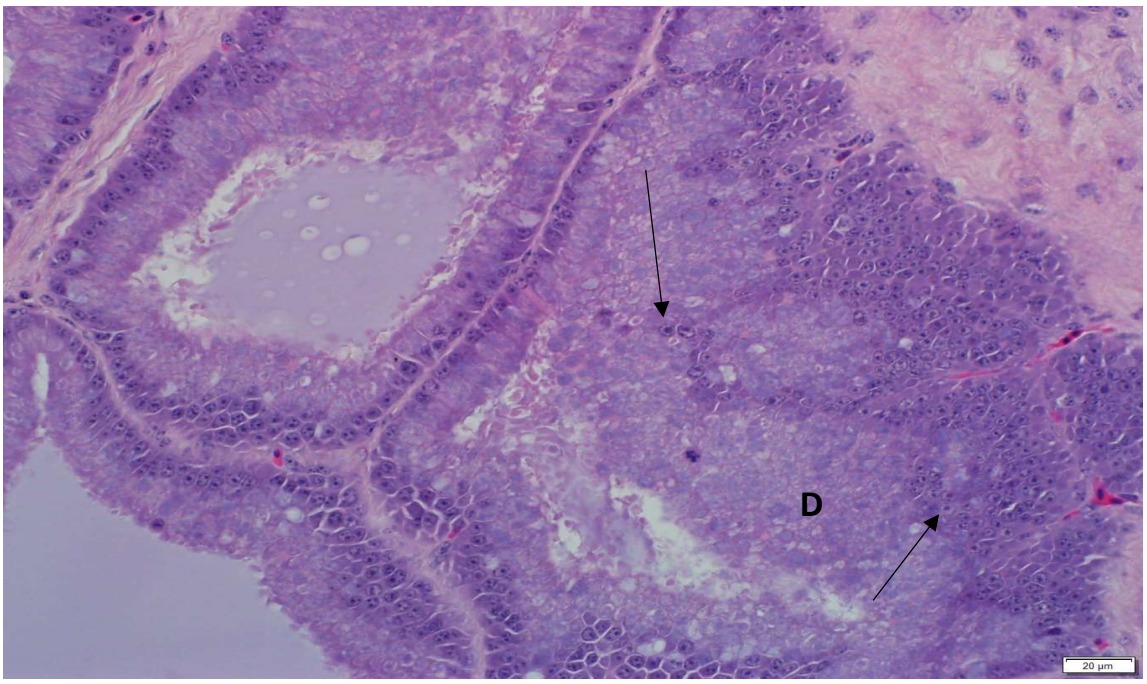

Figure 2.10: Light photomicrograph of a cloacal gland in a pubertal quail showing glandular units filled with cellular debris (D). Arrows: apparently normal nuclei. Haematoxylin and eosin stain.

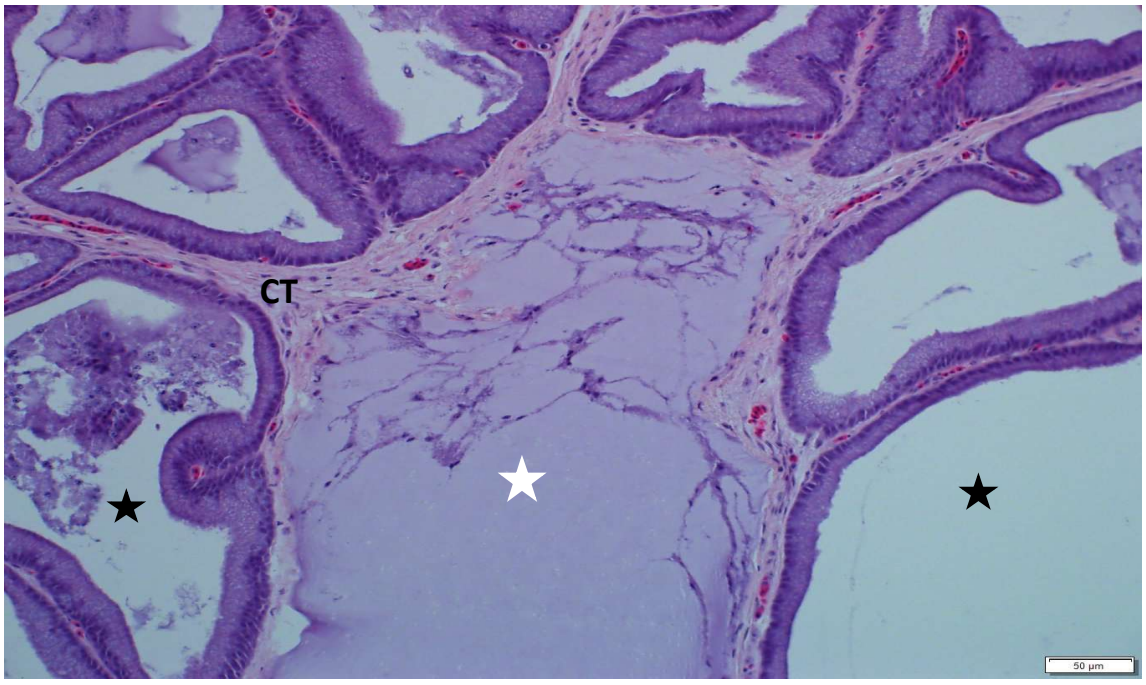

Figure 2.11: Light photomicrograph of a cloacal gland in a pubertal quail showing a degenerated glandular unit (white asterisk) between apparently normal units (black asterisks). Haematoxylin and eosin stain.

Adult birds

The cloacal gland in adult birds was formed by poorly-defined glandular lobes composed of large glandular units. The majority of glandular units were situated in the connective tissue between the stratified squamous epithelium of the cloaca and the muscle fibres of the *M. sphincter cloacae*. A few glandular units were also observed between the muscle fibres of the *M. sphincter cloacae* (Figure 2.12). Glandular units of the cloacal gland were separated by well-vascularized connective tissue trabeculae (Figure 2.13)**.** Several leukocytic aggregations were observed in the connective tissue between glandular units (Figure 2.14).

Glandular units in adult quails were composed of glandular epithelium and connective tissue, which enclosed wide lumina. The glandular epithelium and underlying connective tissue were arranged in primary and secondary folds which extended into the lumina of the glandular units. In some instances, anastomosing folds were formed by the merger of primary folds (Figure 2.15). Primary, secondary and anastomosing folds were lined by tall columnar secretory cells with foamy cytoplasm (Figures 2.14 & 2.15). The lumina of the glandular units contained secretory material. Secretory material from the glandular units forming a glandular lobe emptied into the cloaca via a single duct (Figure 2.14). The ducts connecting the glandular lobes to the cloacal surface were lined by a low columnar or cuboidal

epithelium, which imperceptibly merged with the non-keratinized squamous epithelium of the cloaca (Figure 2.14).

Degenerating glandular units were observed in the cloacal glands of adult quails (Figure 2.16). The lumina of these regressing glandular units contained desquamated glandular cells (Figure 2.16).

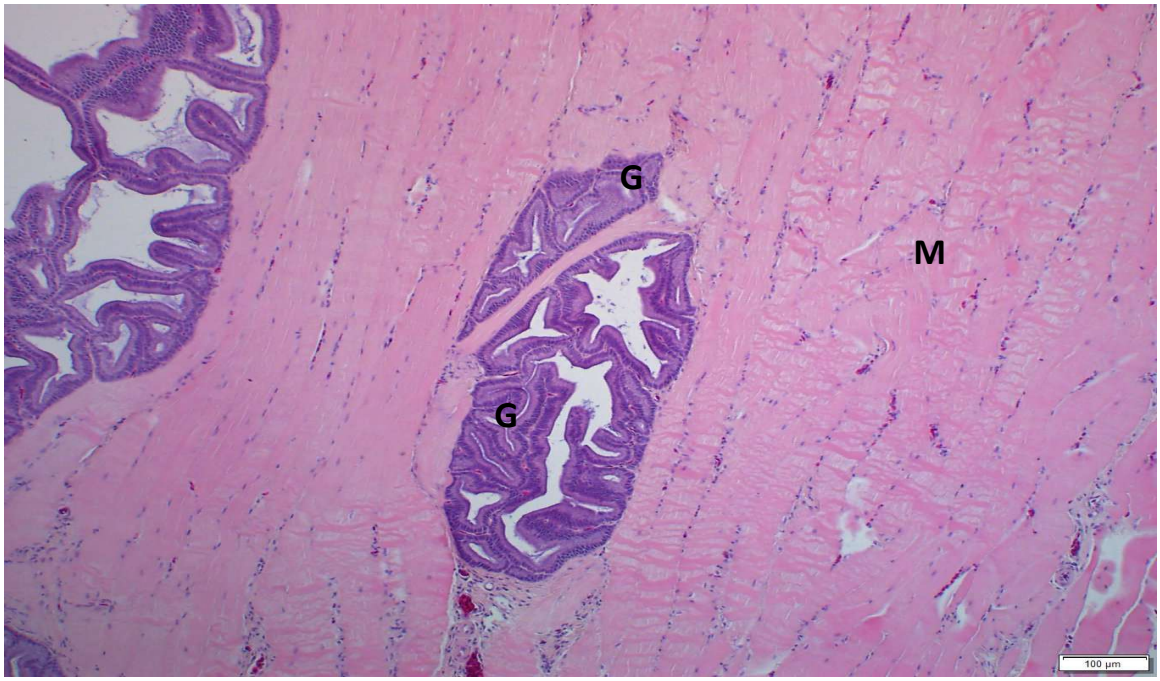

Figure 2.12: Light photomicrograph of a cloacal gland in an adult quail. G: glandular units between the muscle fibres of the *M. sphincter cloacae* (M). Haematoxylin and eosin stain.

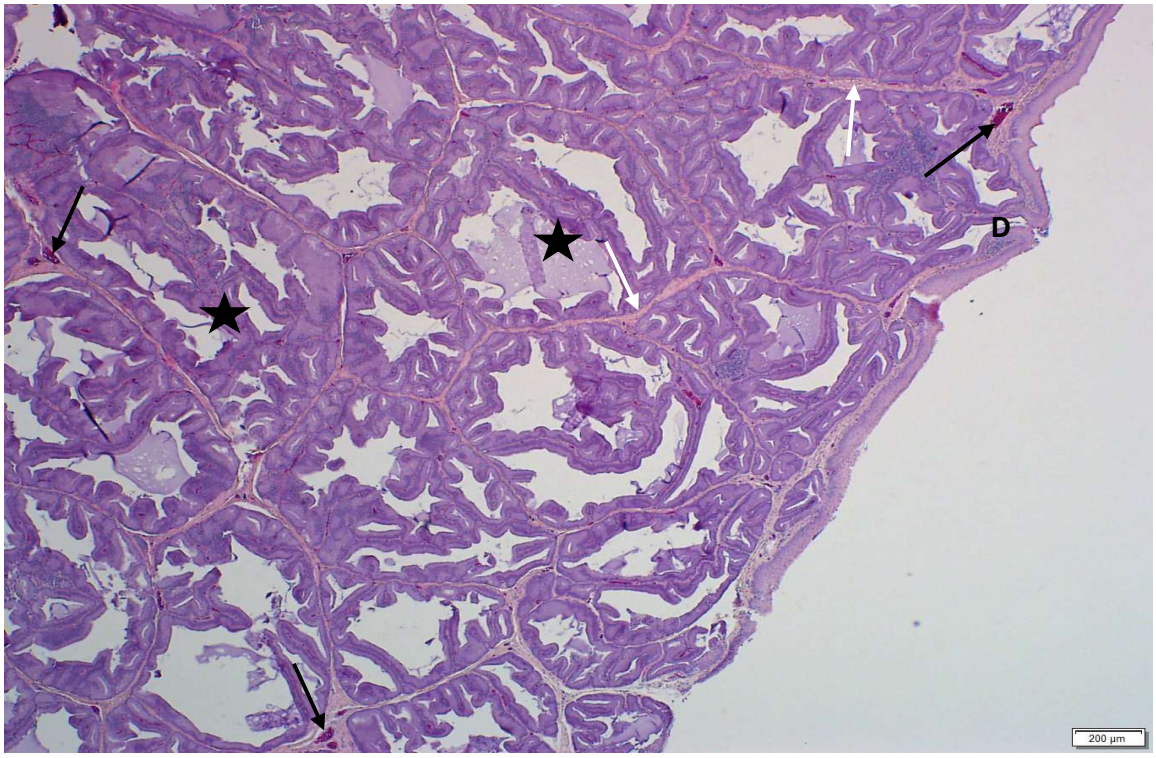

Figure 2.13: Light photomicrograph of a cloacal gland from an adult quail showing well-developed glandular units (asterisks) separated by connective tissue trabeculae (white arrows). Black arrows: blood vessels. D: duct. Haematoxylin and eosin stain.

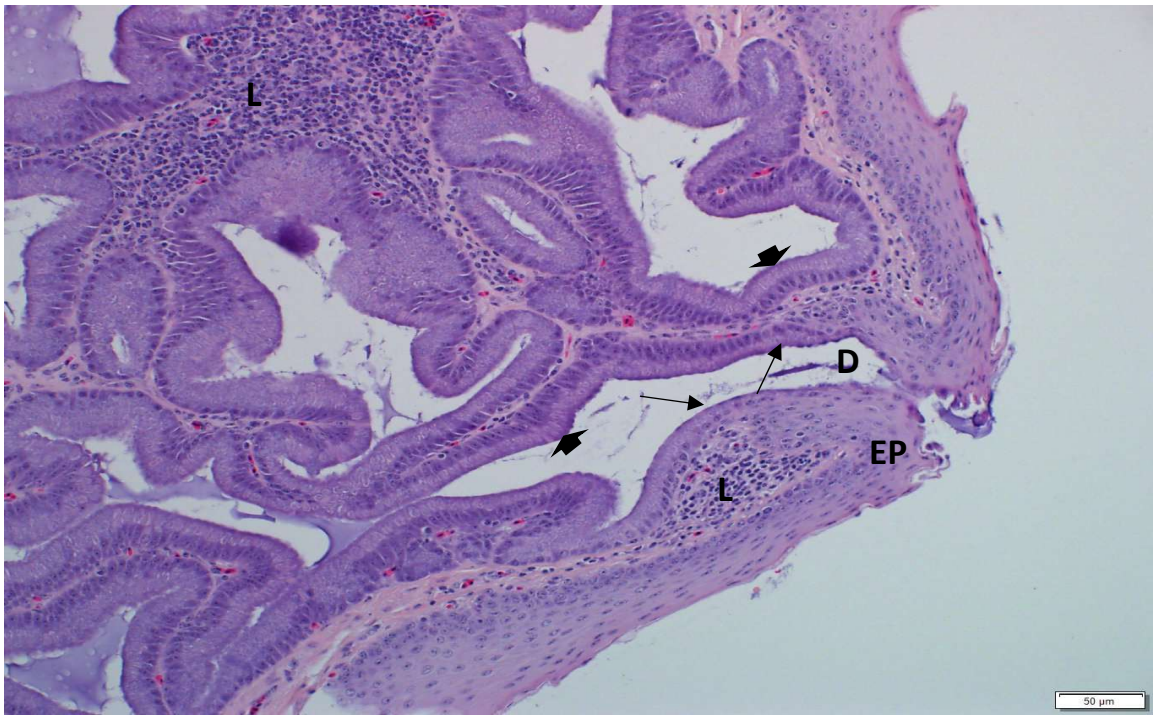

Figure 2.14: Light photomicrograph of a cloacal gland from an adult quail. L: areas of leukocytic aggregations. Arrowheads: simple columnar epithelium. Note the presence of a duct (D) lined by low columnar and cuboidal epithelium (arrows). EP: non-keratinized stratified squamous epithelium. Haematoxylin and eosin stain.

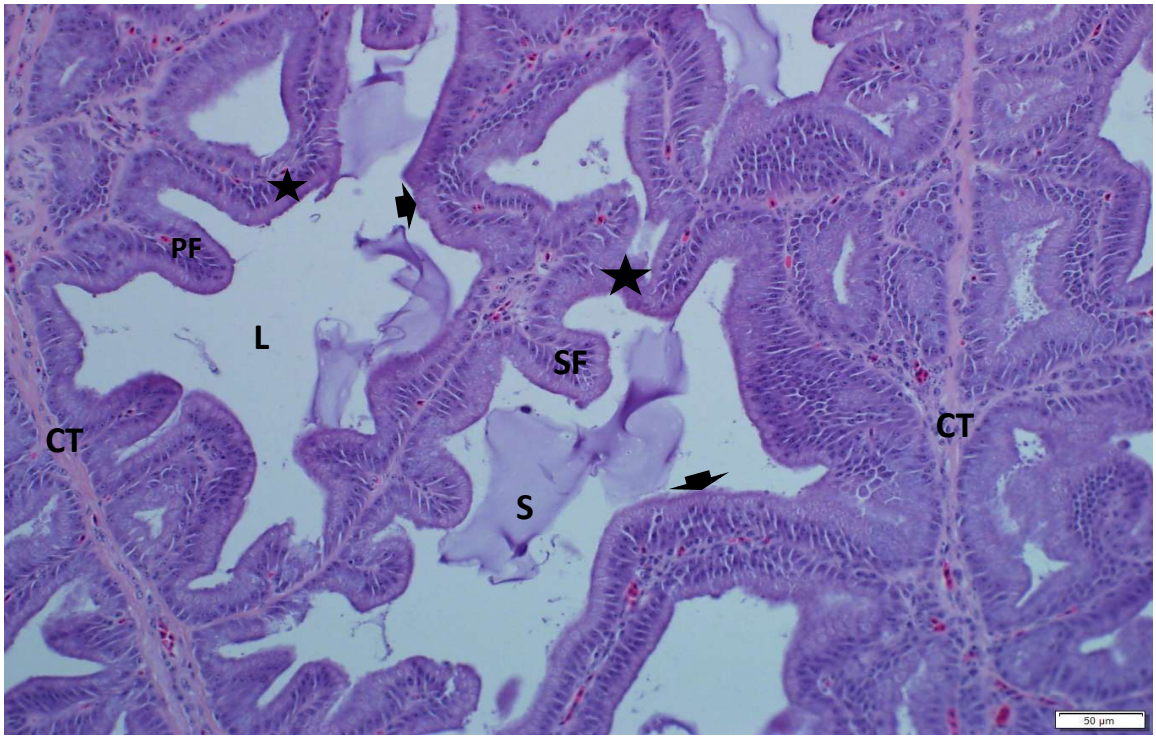

Figure 2.15: Light photomicrograph of a cloacal gland from an adult quail showing the mucosa of glandular units arranged in primary (PF), secondary (SF) and anastomosing (asterisks) folds. Arrowheads: simple columnar epithelium. L: lumen. S: secretory material. CT: connective tissue trabeculae. Haematoxylin and eosin stain.

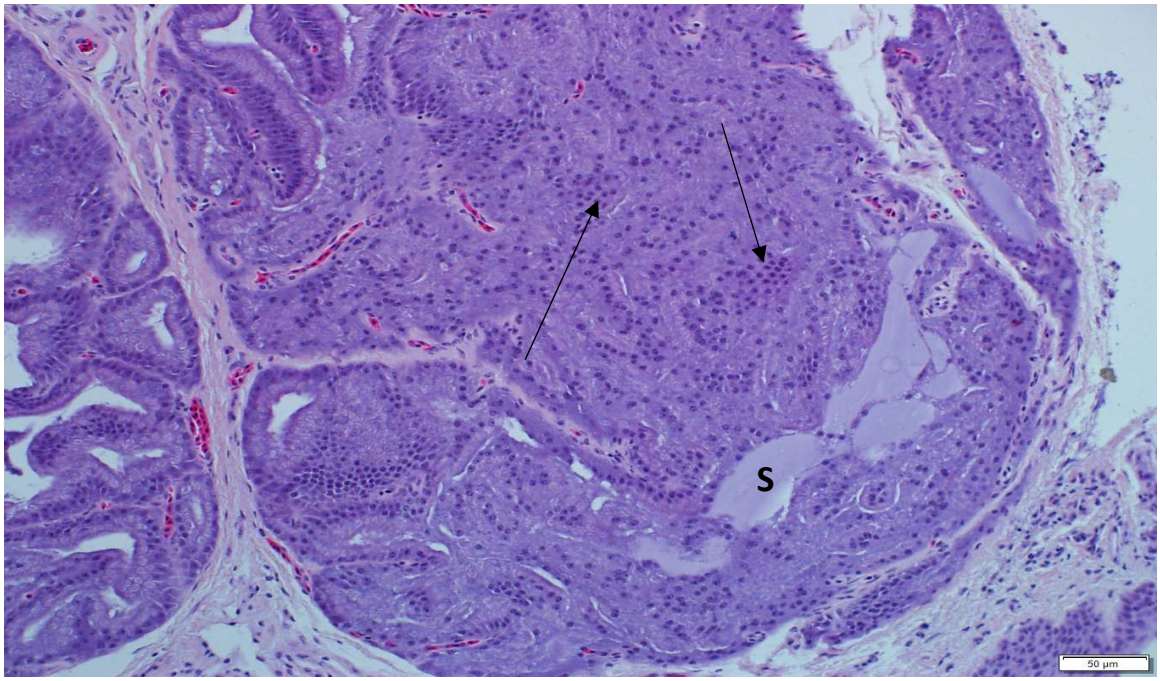

Figure 2.16: Light photomicrograph of a cloacal gland from an adult quail showing a glandular unit filled with cellular debris (arrows) and a small amount of secretory material (S). Haematoxylin and eosin stain.

2.3.4 Morphometry of secretory epithelial cells

The data on secretory epithelial cell heights was tested for homogeneity and normality. The Shapiro Wilks test showed that the data was not normally distributed (p<0.05). Therefore, the data was analyzed using the Kruskal-Wallis test. The data on changes in secretory epithelial cell heights in pre-pubertal, pubertal and adult birds is presented in Table 2.7 and Graph 2.6. Statistically significant differences (p<0.05) were observed between pre-pubertal and pubertal birds as well as between pre-pubertal and adult birds. Correlations between plasma testosterone concentrations and secretory epithelial cell heights were determined using Pearson's correlation test. Data on the correlation between epithelial cell heights and plasma testosterone concentrations is presented in Table 2.8. Analysis of the correlation

between epithelial cell heights and plasma testosterone concentrations revealed a moderate positive correlation that was not statistically significant (r (19) = .42; p=.57).

Table 2.7: Cloacal gland secretory epithelial cell heights in pre-pubertal, pubertal and adult Japanese quails.

Age group	Epithelial cell height (µm)
Pre-pubertal	19.95 ± 0.36^{ab}
Pubertal	24.68 ± 0.45^{a}
Adult	24.54 ± 0.32^{b}

All data is expressed as mean ± standard error. $p<0.05$ is considered to be statistically significant. There are statistically significant differences between means sharing the same superscript.

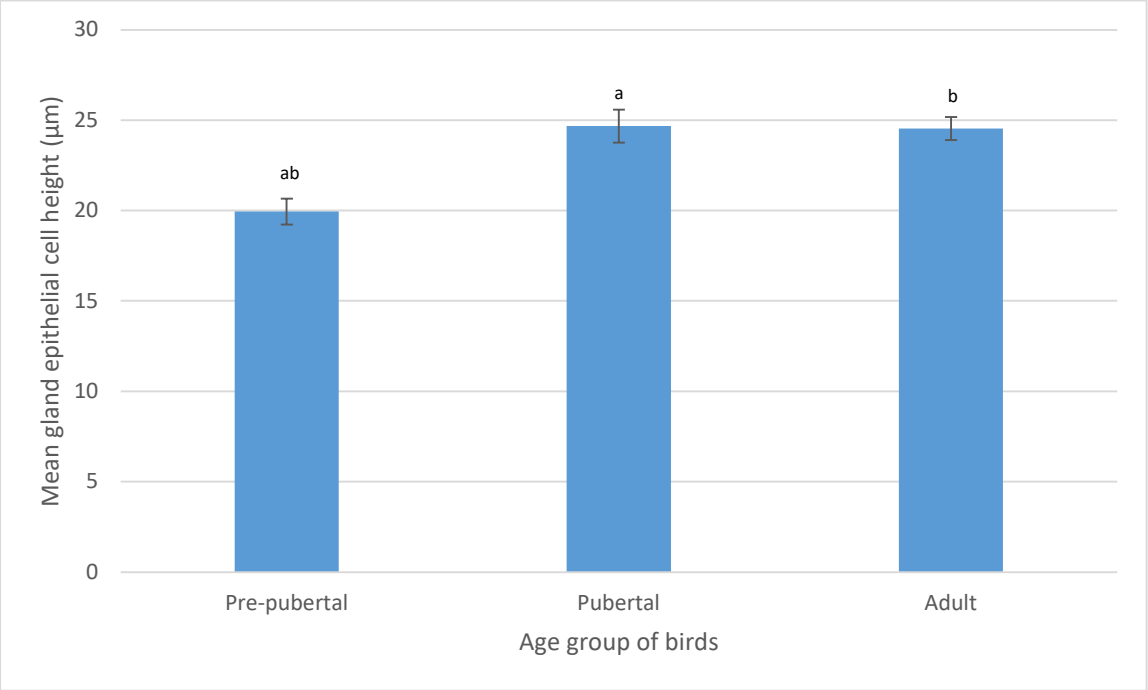

Graph 2.6: Cloacal gland secretory epithelial cell heights in pre-pubertal, pubertal and adult birds. Data is expressed as mean ± standard error. There are statistically significant differences between means sharing the same lettering ($p<0.05$). The data was analyzed using the Kruskal-Wallis test.

Table 2.8: Correlation of cloacal gland epithelial cell heights with plasma testosterone concentrations.

		Plasma testosterone concentration	Epithelial cell heights
Plasma testosterone concentrations	Pearson Correlation	1	.421
	Sig. (2-tailed)		.057
	N	21	21
Epithelial cell heights	Pearson Correlation	.421	1
	Sig. (2-tailed)	.057	
	N	21	21

2.3.5 Periodic acid Schiff and alcian blue histochemistry

Pre-pubertal birds

In pre-pubertal birds, positive periodic acid Schiff (PAS) and alcian blue staining was observed in the simple columnar secretory cells of the cloacal gland (Figures 2.17 and 2.18). Application of the enzyme, diastase, to the cloacal gland sections did not result in a loss of PAS positive staining (Figure 2.19).

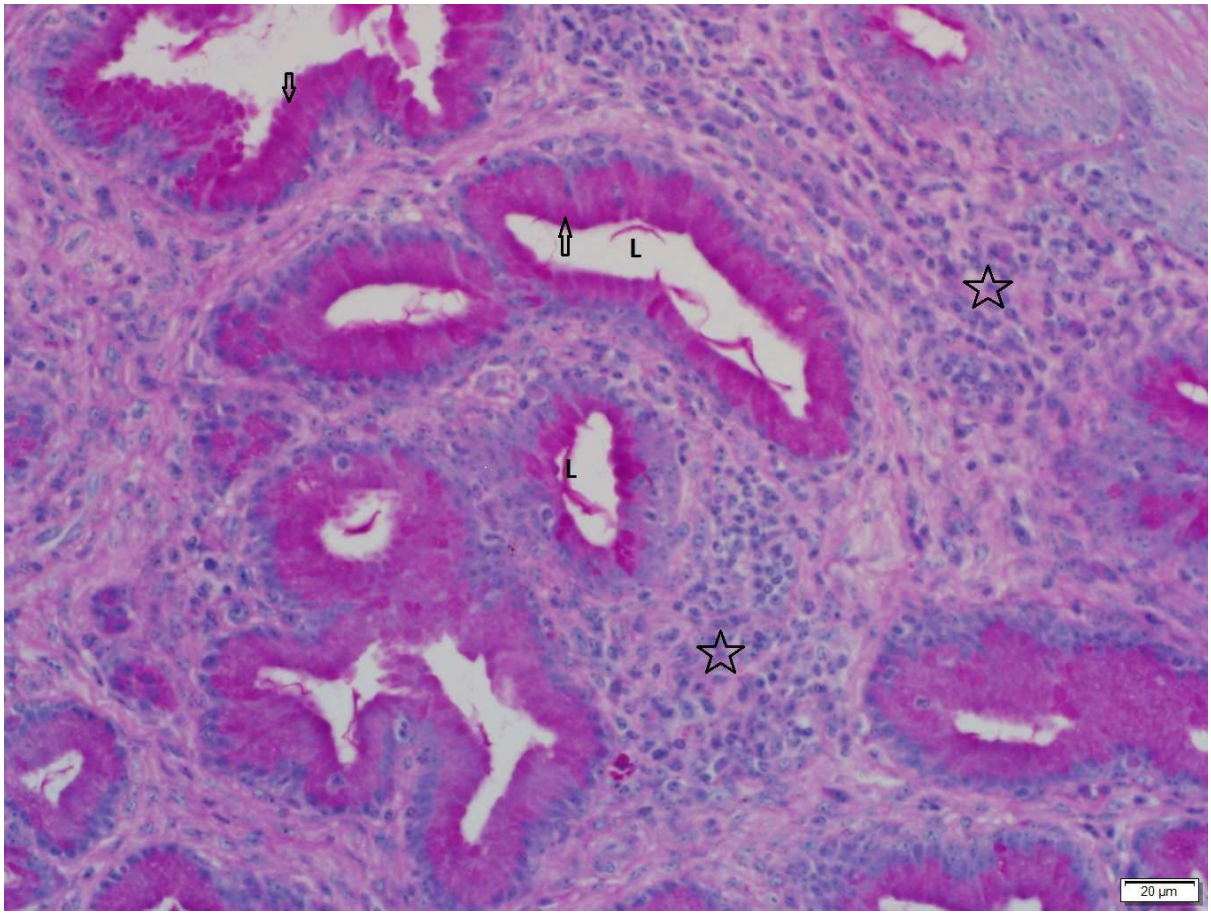

Figure 2.17: Light photomicrograph of the cloacal gland in a pre-pubertal bird. Arrows: PAS-positive glandular secretory cells. L: lumen. Asterisks: connective tissue. PAS stain.

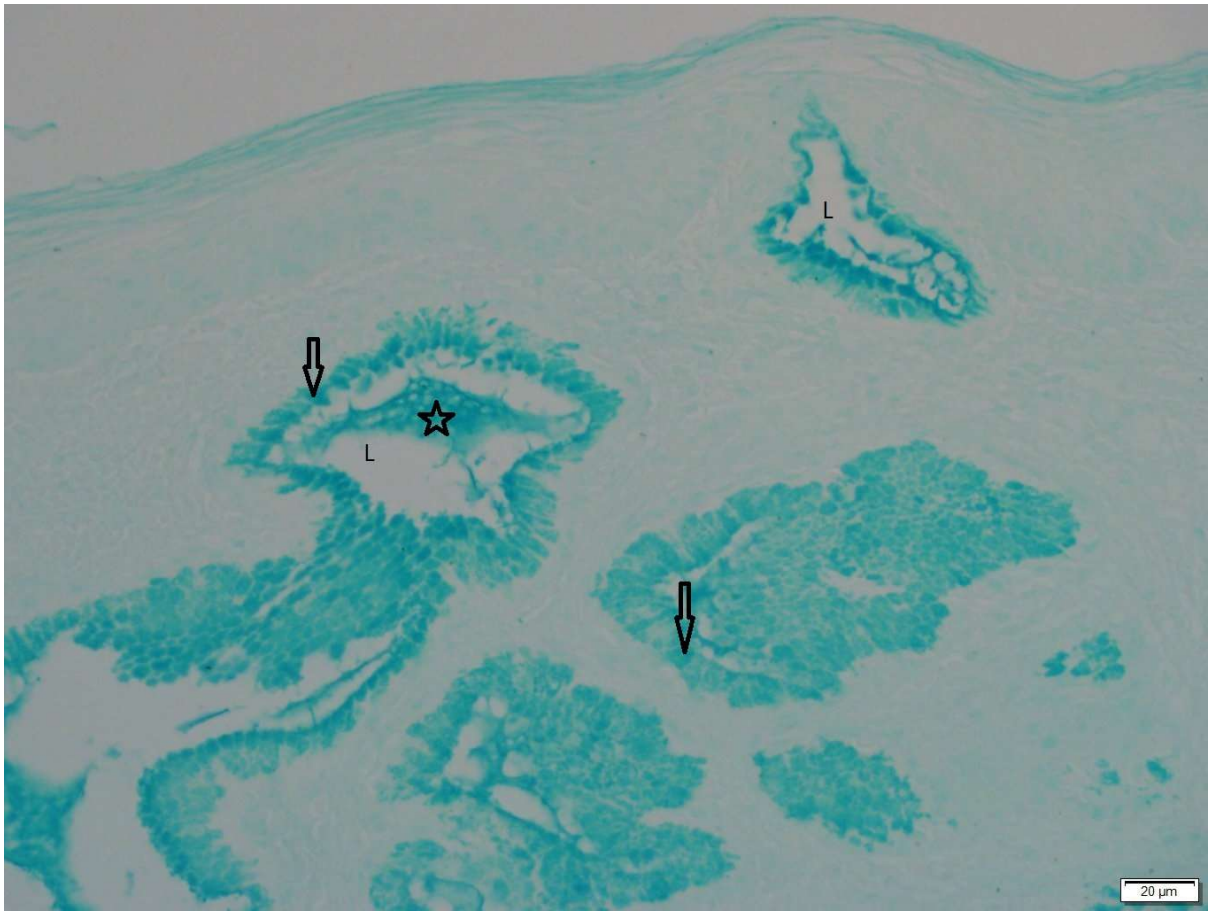

Figure 2.18: Light photomicrograph of the cloacal gland in a pre-pubertal bird. Arrows: alcian blue positive cells. L: lumen. Asterisk: secretory material. Alcian blue stain.

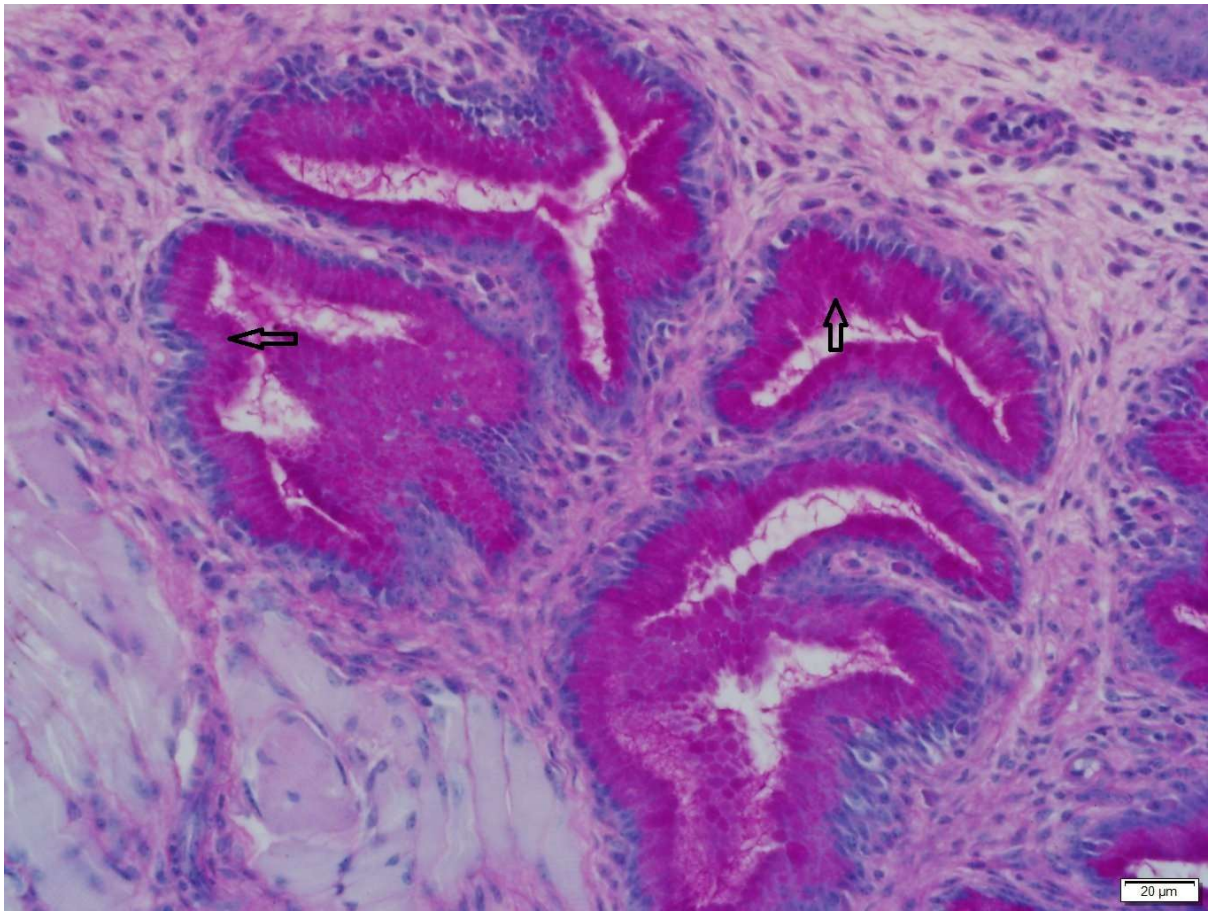

Figure 2.19: Light photomicrograph of the cloacal gland in a pre-pubertal bird showing the PAS reactivity (arrows) of secretory cells after diastase treatment. PAS stain.

Pubertal birds

In pubertal birds, strong PAS and alcian blue staining was demonstrated in the secretory cells of glandular units (Figures 2.20 and 2.21). The PAS product in the cells was diastase-resistant (Figure 2.22).

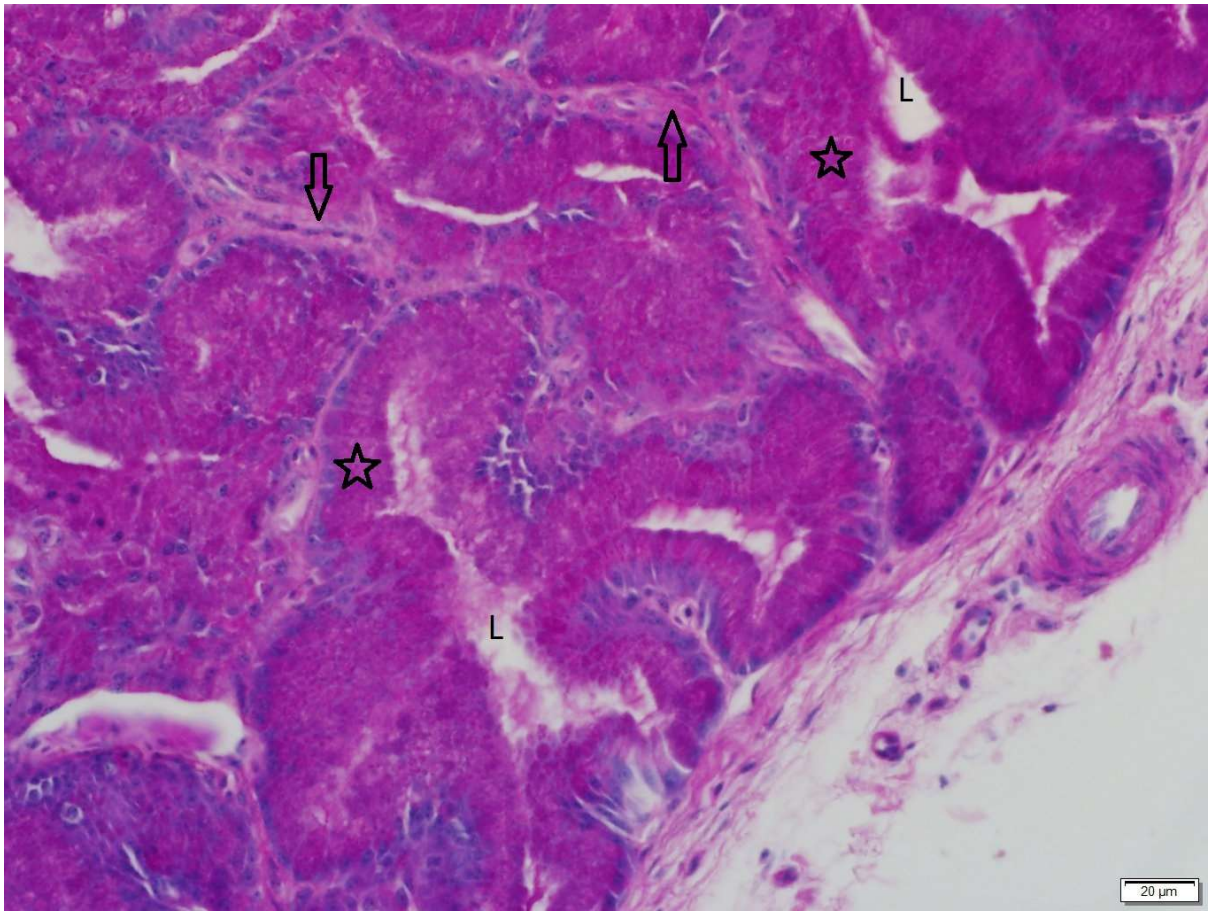

Figure 2.20: Light photomicrograph showing PAS staining in the cloacal gland of a pubertal bird. Asterisks: PAS-positive cells. Arrows: connective tissue trabeculae between glandular units. L: lumina of glandular units. PAS stain.

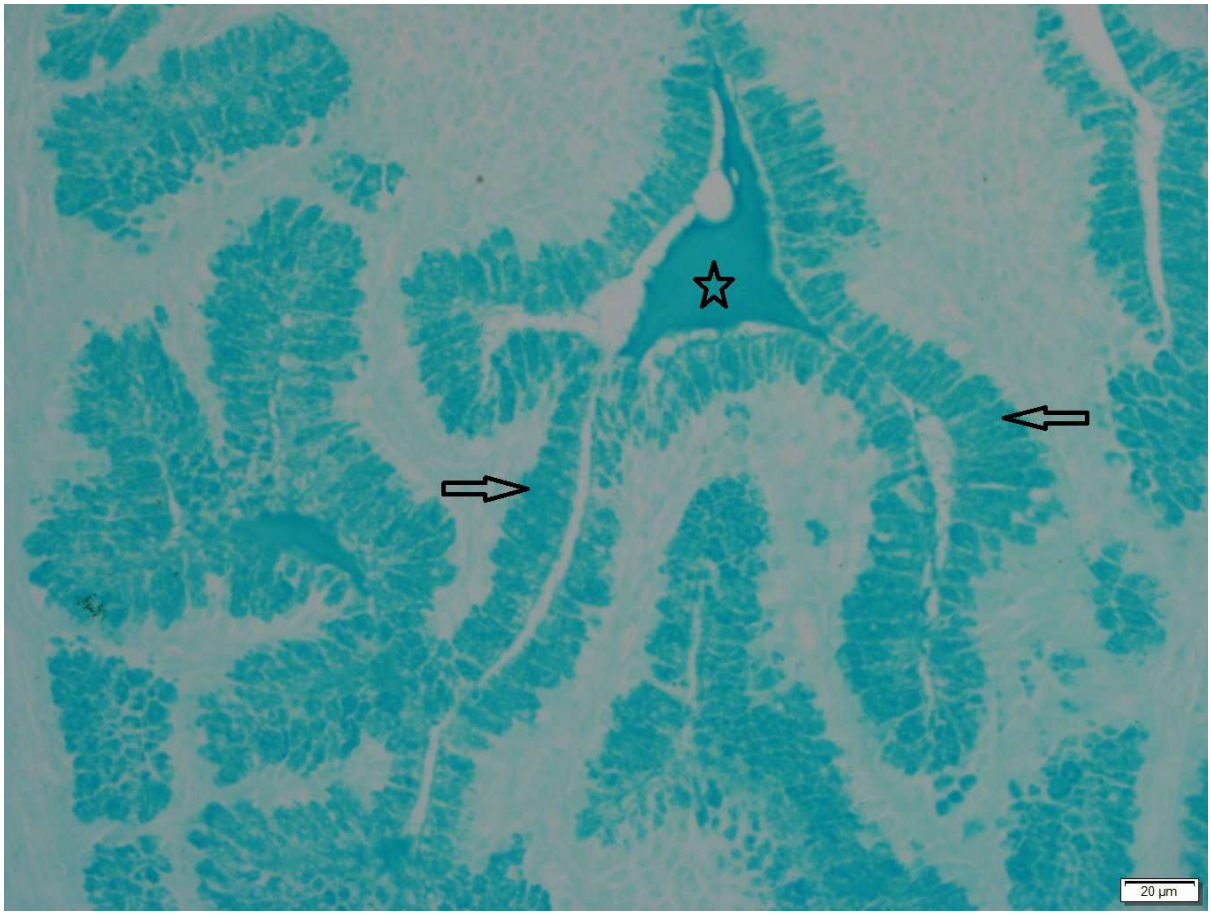

Figure 2.21: Light photomicrograph showing alcian blue staining in the cloacal gland of a pubertal bird. Arrows: alcian blue positive cells. Asterisk: secretory product in the lumen of a glandular unit. Alcian blue stain.

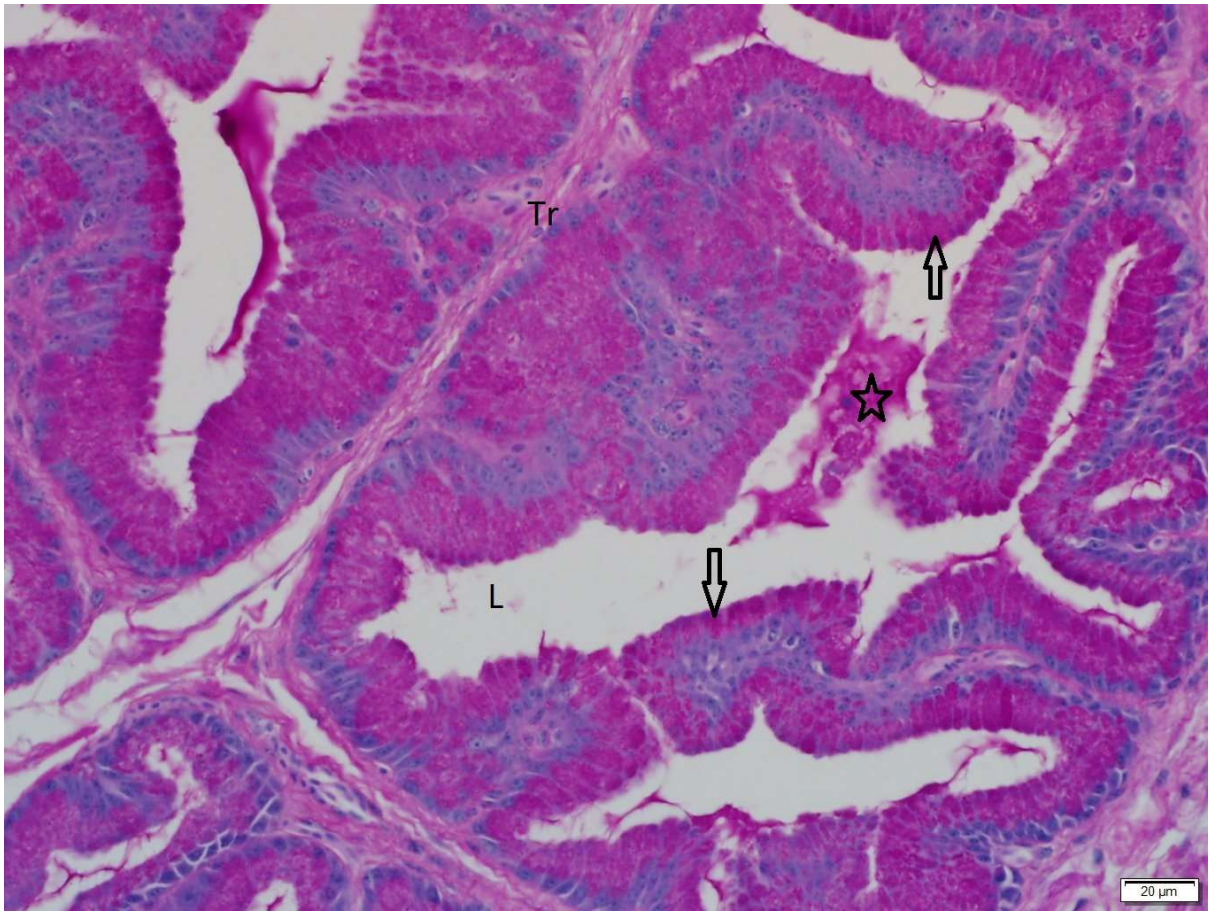

Figure 2.22: Light photomicrograph of the cloacal gland of a pubertal quail showing PAS positive material within a glandular unit in the cloacal gland, following treatment with diastase. Arrows: diastase-resistant PAS product in the supranuclear cytoplasm of secretory cells. Tr: connective tissue trabeculae between adjacent glandular units. PAS stain.

Adult birds

A moderate to strong diastase-resistant PAS staining, as well as alcian blue staining was observed in the majority of cells lining the glandular units in adult birds (Figures 2.23, 2.24 & 2.25). Degenerating cells in the glandular units exhibited weak PAS staining.

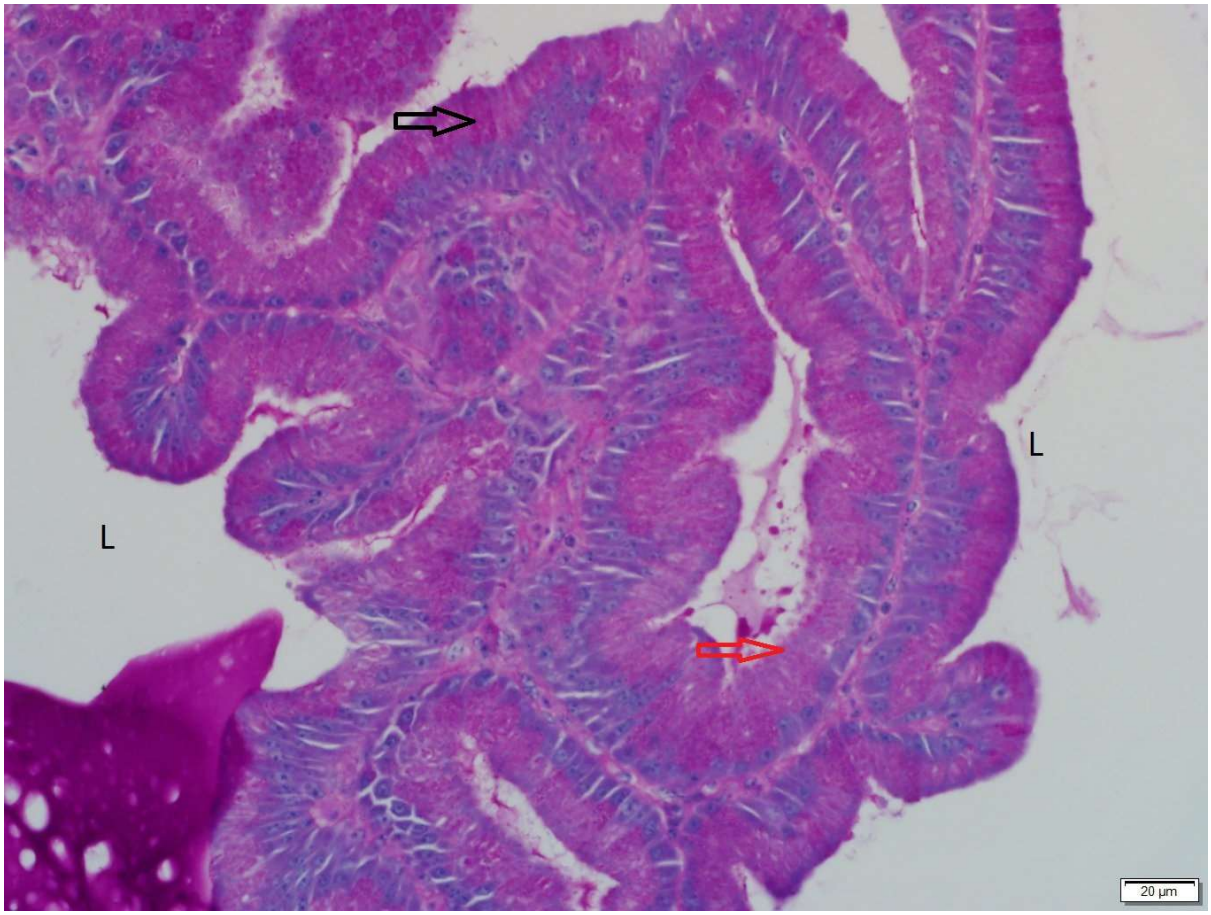

Figure 2.23: Light photomicrograph of the cloacal gland in an adult bird showing strong (black arrow) and moderate (red arrow) PAS staining. L: lumen of glandular units. PAS stain.

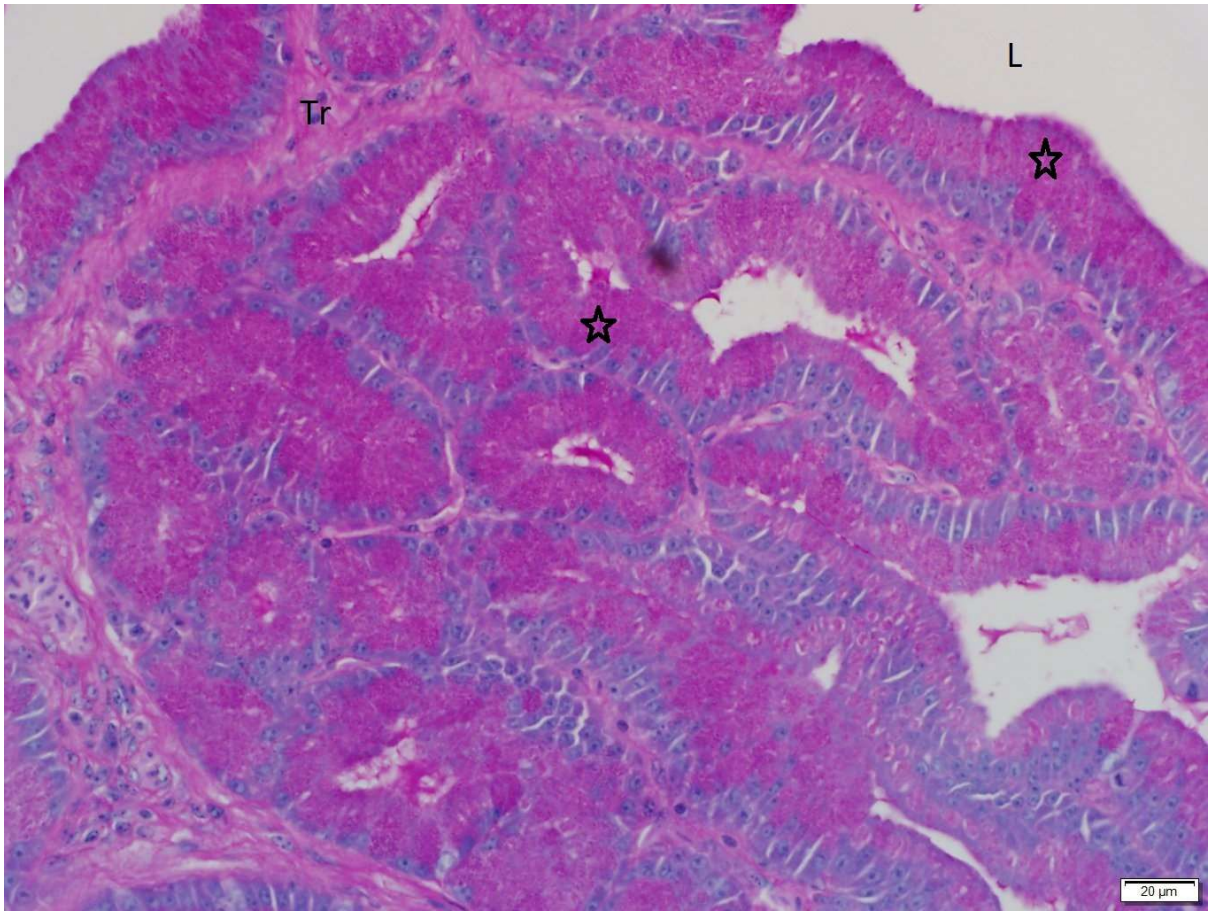

Figure 2.24: Light photomicrograph of the cloacal gland in an adult bird showing PAS staining following diastase treatment. Asterisks: diastase-resistant PAS product. Tr: connective tissue trabeculae. L: lumen. PAS stain.

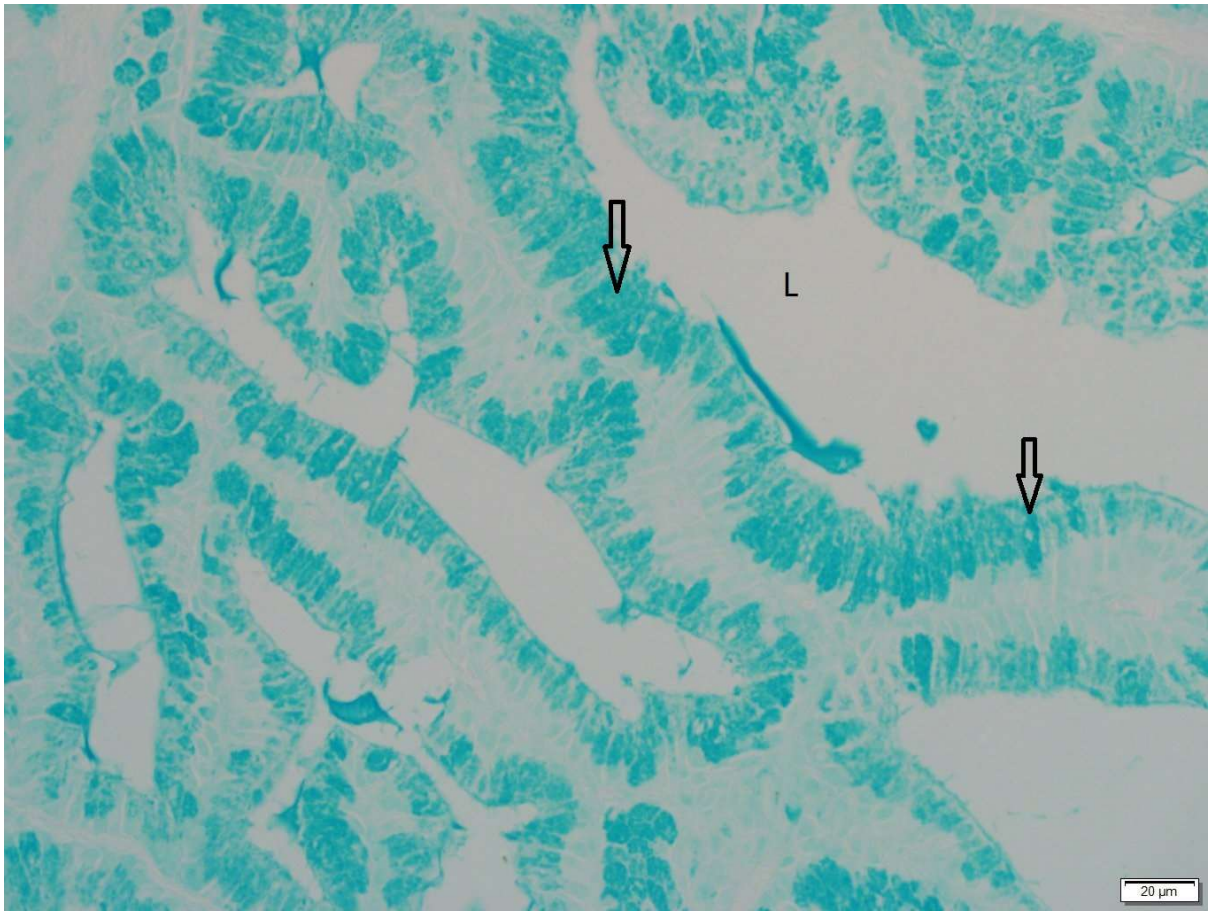

Figure 2.25: Light photomicrograph of the cloacal gland in an adult bird showing alcian blue staining. Arrows: alcian blue positive cells. L: lumen of a glandular unit. Alcian blue stain.

2.3.6 TUNEL staining

In pre-pubertal birds, the secretory cells lining the glandular units of the cloacal glands did not exhibit TUNEL staining (Figure 2.26). Several TUNEL positive cells were observed in the secretory cells forming the lining of the glandular units in pubertal birds (Figure 2.27), while numerous TUNEL positive cells were observed in the adult birds (Figure 2.28). The TUNEL positive staining in adult birds occurred in the nuclei of degenerating secretory cells (Figure 2.28), as well as in desquamated cells located within the lumina of the glandular units (Figure 2.29).

No positive staining for TUNEL was demonstrated in the negative control sections (Figure 2.30).

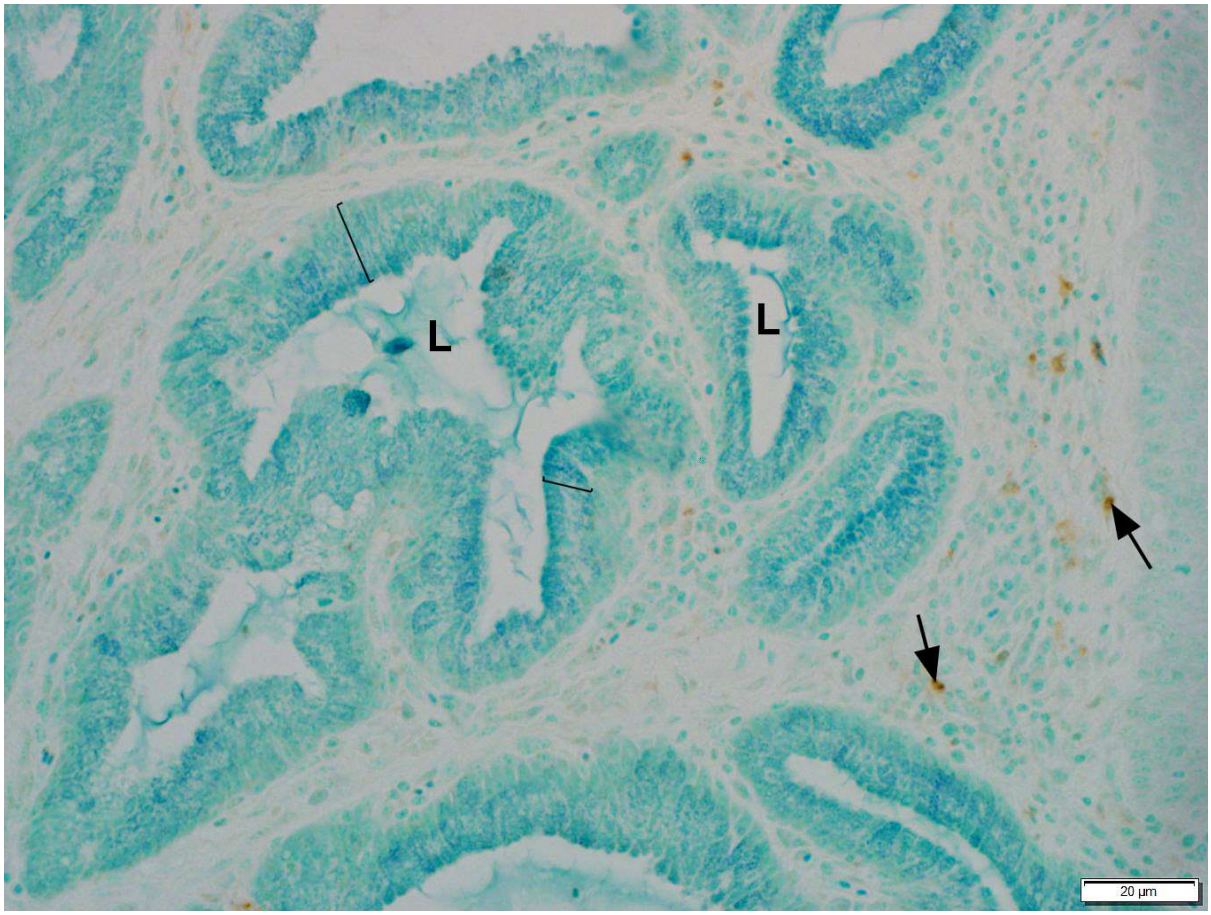

Figure 2.26: Light photomicrograph showing negative staining for TUNEL in the secretory cells lining the glandular units in a pre-pubertal bird. Brackets: TUNEL negative secretory cells. Arrows: TUNEL positive nuclei of leukocytes. L: lumen.

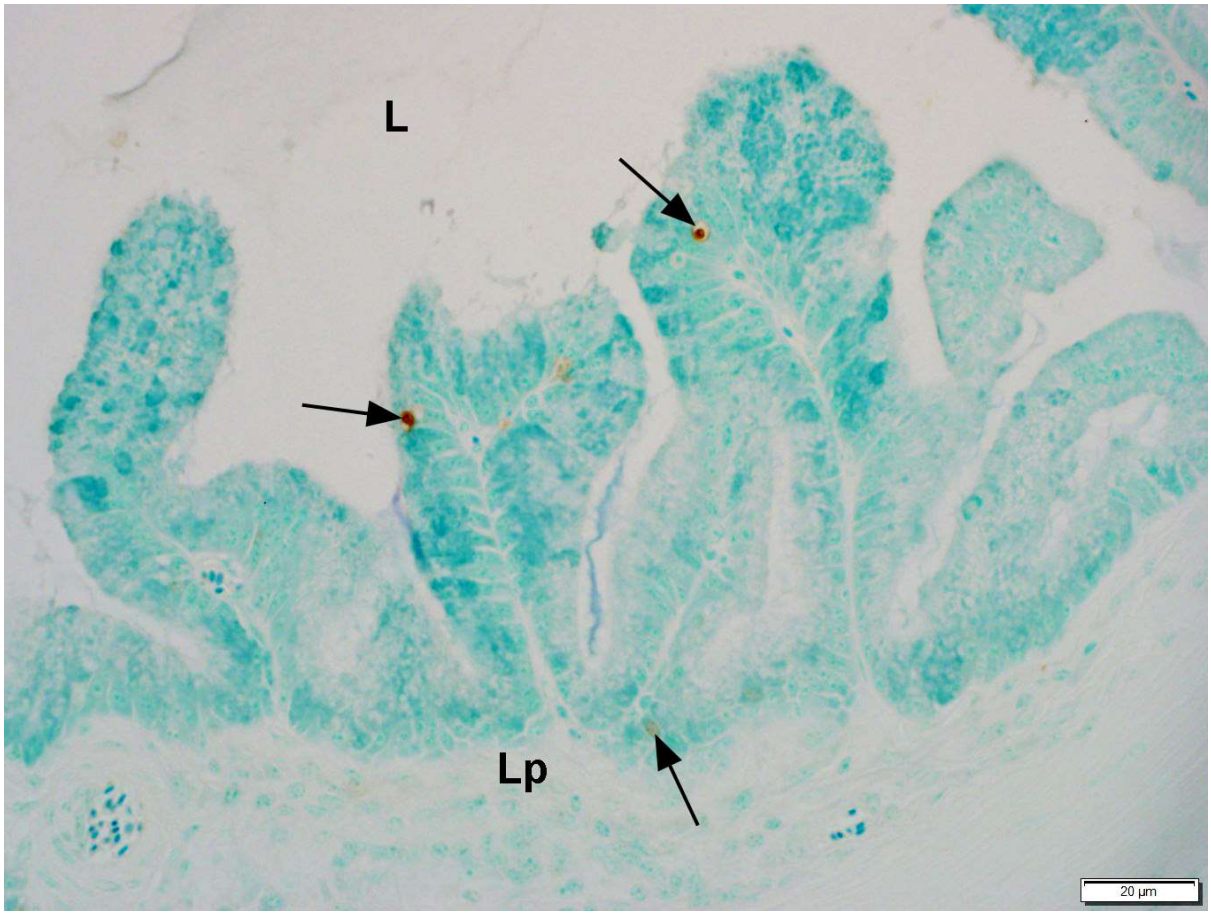

Figure 2.27: Light photomicrograph showing TUNEL positive nuclei (arrows) of secretory cells in the cloacal gland of a pubertal bird. L: lumen. Lp: *lamina propria*.

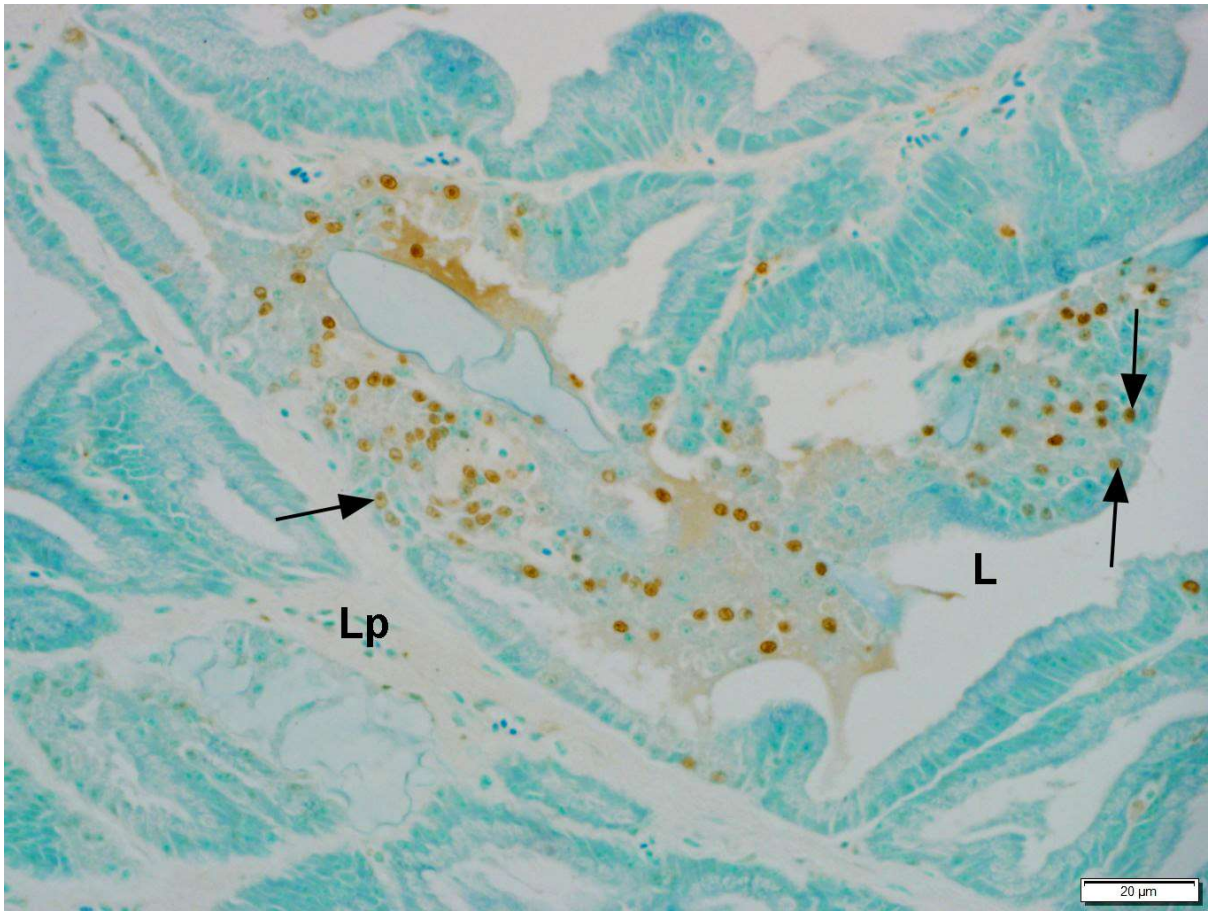

Figure 2.28: Light photomicrograph showing TUNEL staining in the cloacal gland of an adult bird. TUNEL positive nuclei (arrows) are observed in degenerating secretory cells of the glandular units. Lp: *lamina propria*. L: lumen.

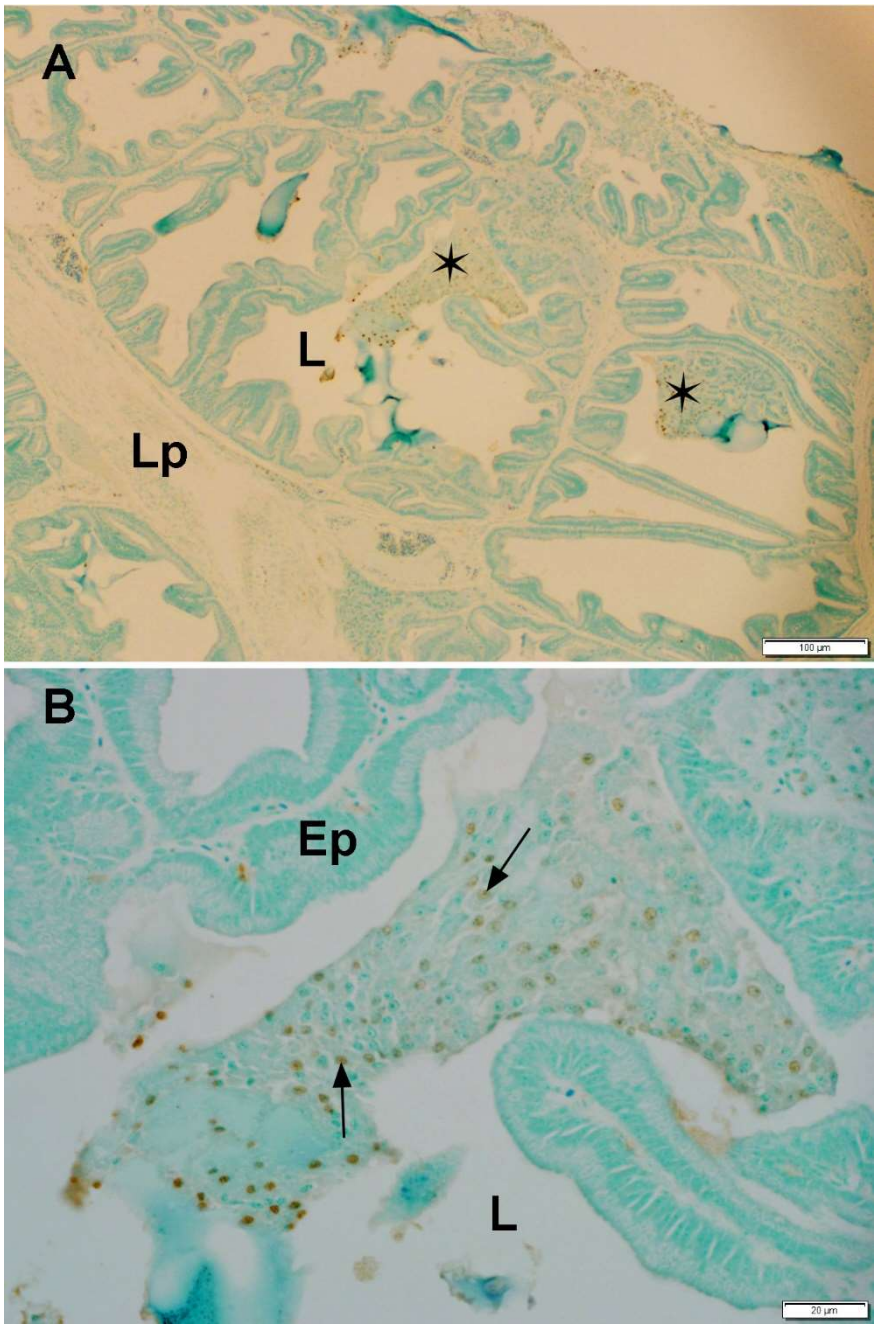

Figure 2.29: Low (A) and high (B) magnification light photomicrographs showing TUNEL staining in the cloacal gland of an adult bird.

A. Asterisks: cellular debris containing TUNEL positive nuclei. L: lumen. Lp: *lamina propria*.

B. Arrows: TUNEL positive nuclei in cellular debris. Ep: secretory cells of the glandular units. L: lumen.

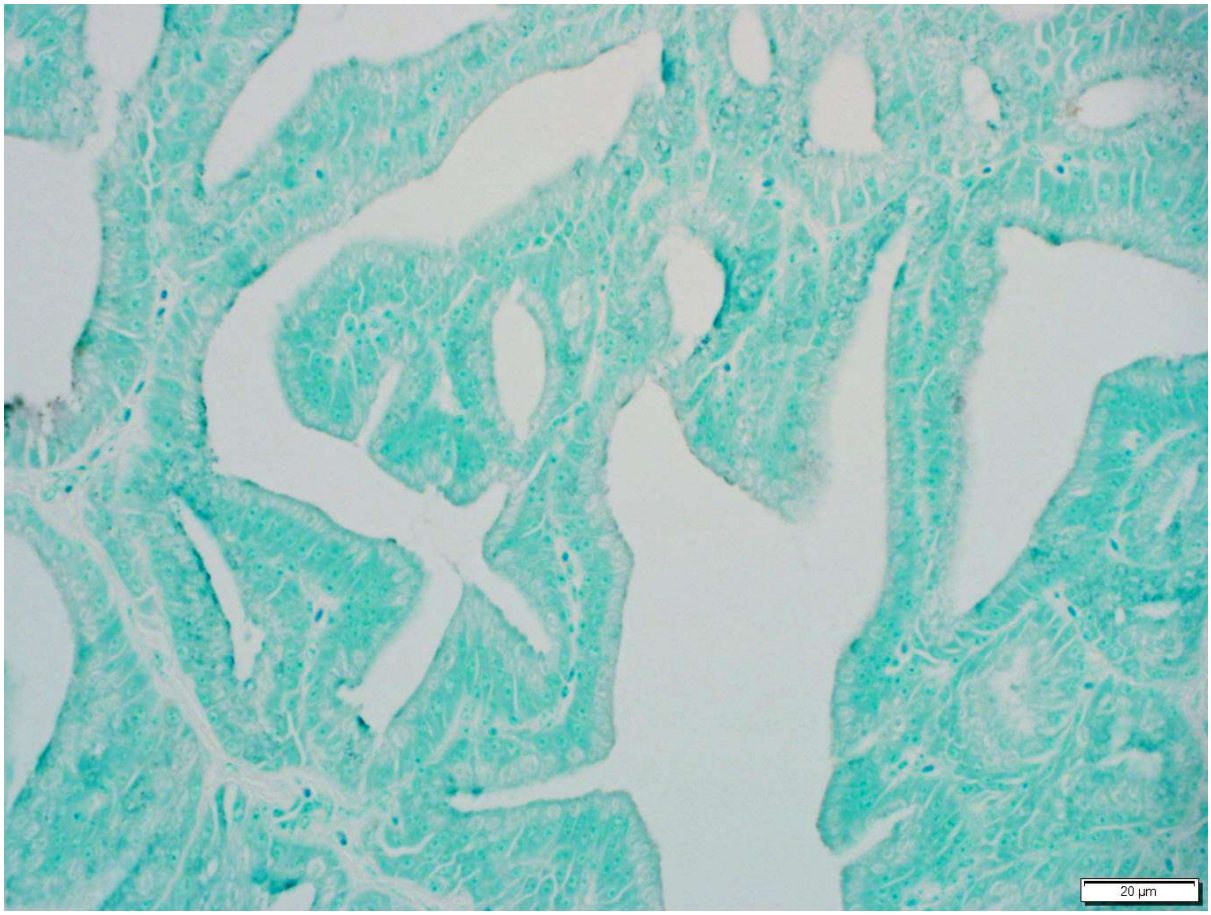

Figure 2.30: Light photomicrograph of the negative control section.

2.3.7 TUNEL morphometry

The data on the number of TUNEL positive nuclei observed in the cloacal glands of pre-pubertal, pubertal and adult birds was tested for homogeneity and normality. The Kolmogorov-Smirnov test showed that the data was not normally distributed (p<0.05). Therefore, the data was analyzed using the Kruskal-Wallis test. Statistically significant differences were observed between all age groups. The data on the number of TUNEL positive nuclei in the cloacal glands of birds of different age groups is presented in Table 2.9 and Graph 2.7.

Table 2.9: Table showing the number of TUNEL positive nuclei observed per field in the cloacal glands of pre-pubertal, pubertal and adult Japanese quails.

Age group of birds	Number of TUNEL positive nuclei per field
Pre-pubertal	00 ± 00 ^{ab}
Pubertal	15.53 ± 3.71 ^{ac}
Adult	48.73 ± 5.53 ^{bc}

All data is expressed as mean ± standard error with $p<0.05$ considered to be statistically significant. There are statistically significant differences between means sharing the same superscript.

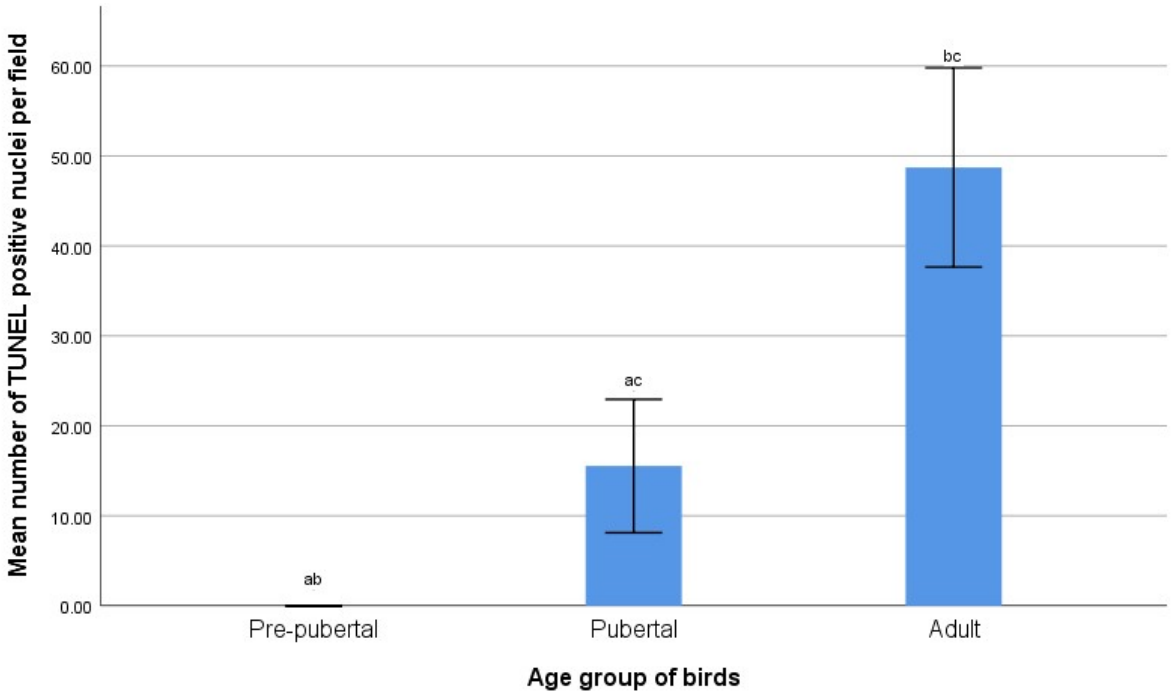

Graph 2.7: The number of TUNEL positive nuclei per field, observed in the cloacal glands of pre-pubertal, pubertal and adult birds. Data is expressed as mean ± standard error. There are statistically significant differences between means sharing the same letters ($p<0.05$). The data was analysed using the Kruskal-Wallis test.

2.3.8 Androgen receptor immunohistochemistry

Pre-pubertal birds

Weak to moderate androgen receptor immunostaining was observed in the nuclei of epithelial cells lining glandular units (Figures 2.31 & 2.32). In addition, the nuclei of some of the secretory cells were androgen receptor immunonegative (Figures 2.31 & 2.32). Androgen receptor immunoreactivity in the cytoplasm of secretory cells was weak or absent.

Leukocytic aggregations observed within the connective tissue separating the glandular units displayed strong positive immunostaining for the androgen receptor (Figure 2.33). Fibroblasts in the connective tissue separating the glandular units exhibited moderate androgen receptor immunostaining (Figures 2.31 & 2.32).

The *tunica media* and endothelial cells of the blood vessels located within the connective tissue showed weak to moderate positive immunoreactivity for the androgen receptor (Figure 2.34).

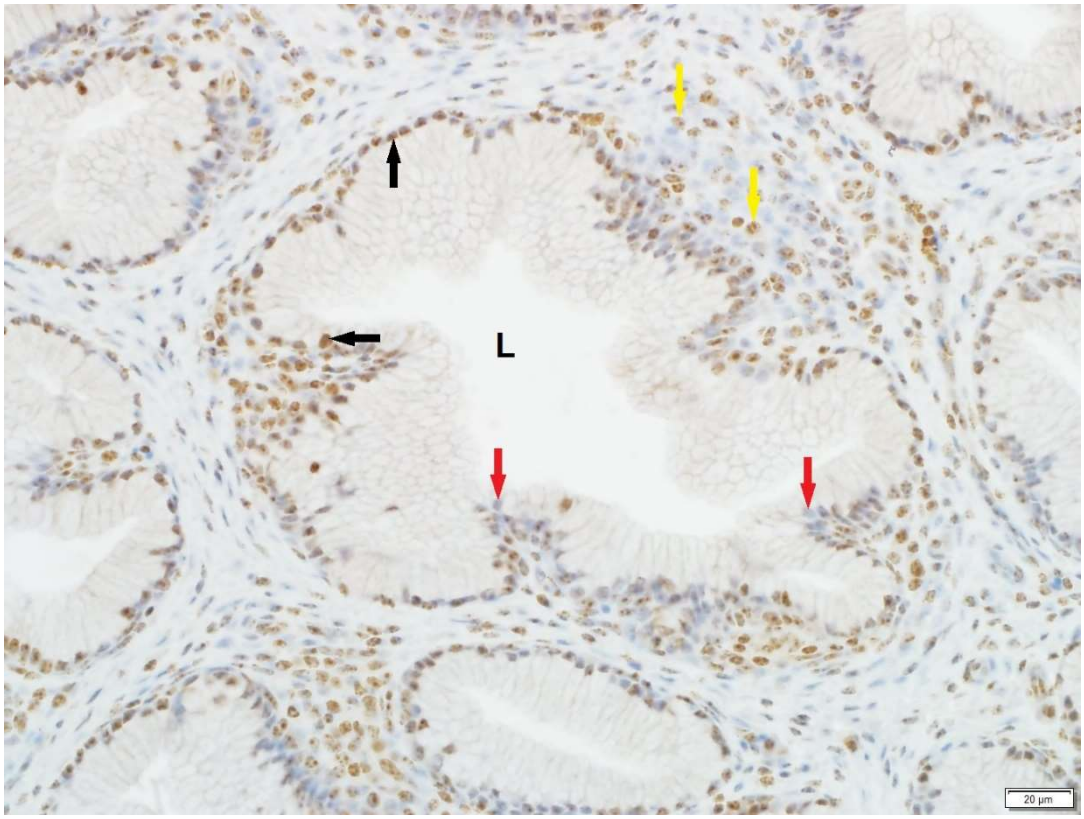

Figure 2.31: Light photomicrograph showing androgen receptor immunostaining in the cloacal gland of a pre-pubertal quail. Cells with androgen receptor positive (black arrows) and androgen receptor negative (red arrows) nuclei line the glandular units. Yellow arrows: androgen receptor immunopositive fibroblasts. L: lumen of a glandular unit.

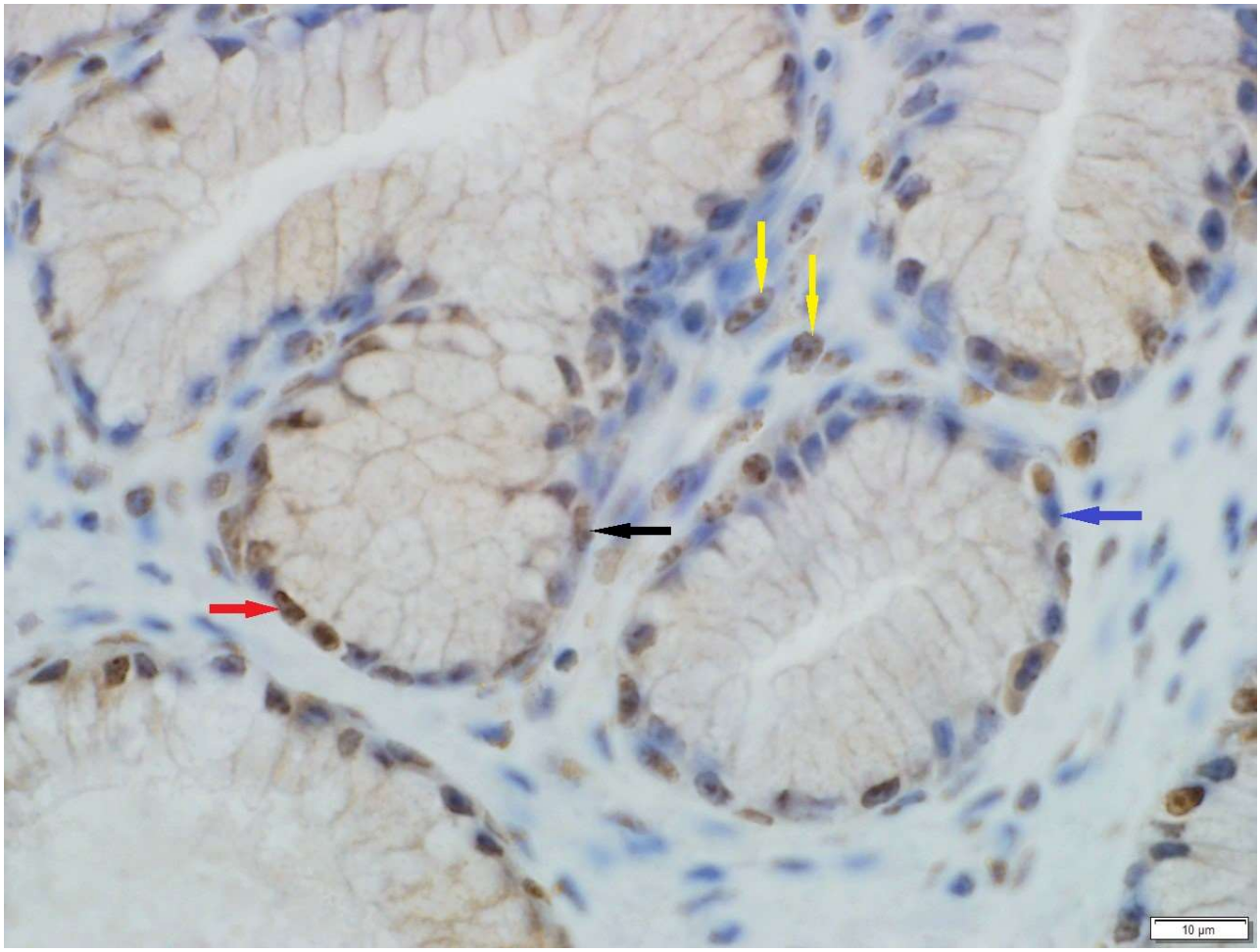

Figure 2.32: Light photomicrograph showing androgen receptor immunonegative (blue arrow), weakly immunopositive (black arrow) and moderately immunopositive (red arrow) nuclei in the cloacal gland of a pre-pubertal quail. Yellow arrows: fibroblasts.

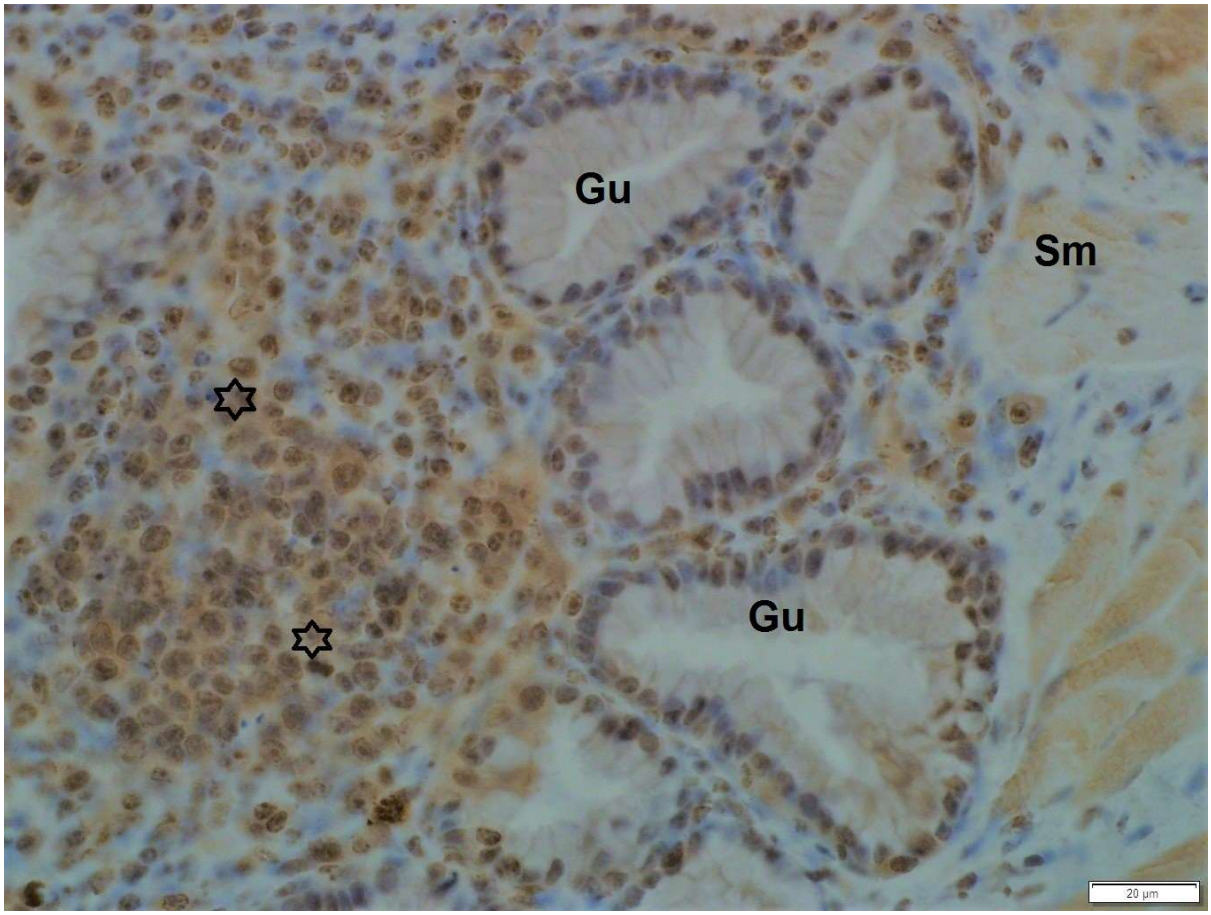

Figure 2.33: Light photomicrograph showing an androgen receptor positive leukocytic aggregation (asterisks) in the cloacal gland of a pre-pubertal quail. Gu: glandular units. Sm: smooth muscle.

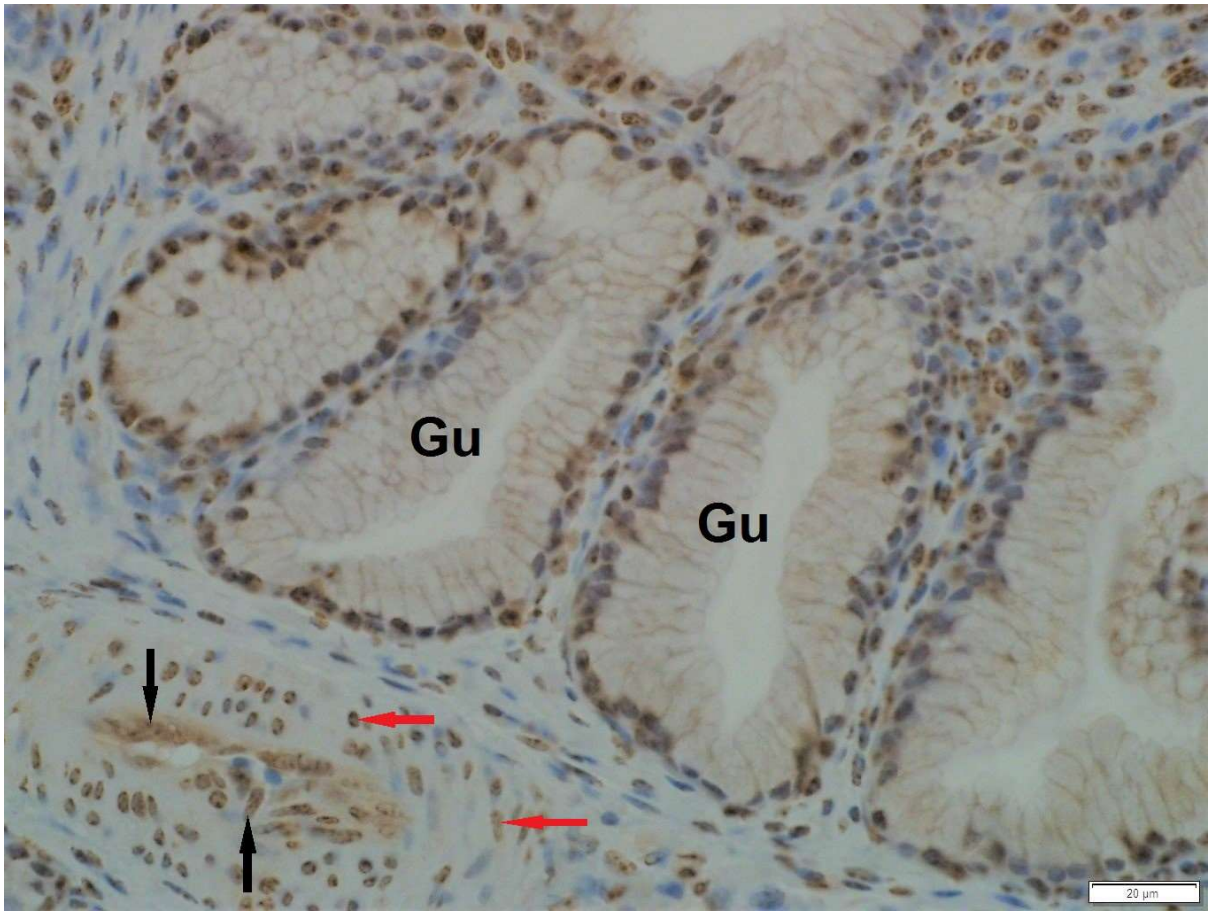

Figure 2.34: Light photomicrograph showing androgen receptor immunostaining in a blood vessel in the cloacal gland of a pre-pubertal quail. Black arrows: immunopositive endothelial cells. Red arrows: immunopositive smooth muscle cells of the *tunica media*.

Pubertal birds

In pubertal birds, moderate to strong androgen receptor immunoreactivity was demonstrated in the nuclei of secretory cells lining the glandular units (Figures 2.35 & 2.36). Weak immunostaining for the androgen receptor was observed in the cytoplasm of the secretory cells (Figure 2.36). Androgen receptor immunostaining in fibroblasts varied from absent to moderate (Figures 2.35 & 2.36). The endothelial

cells of blood vessels in the connective tissue between the glandular units displayed moderate androgen receptor immunoreactivity, while immunostaining in the enclosing smooth muscle cells was weak (Figure 2.35).

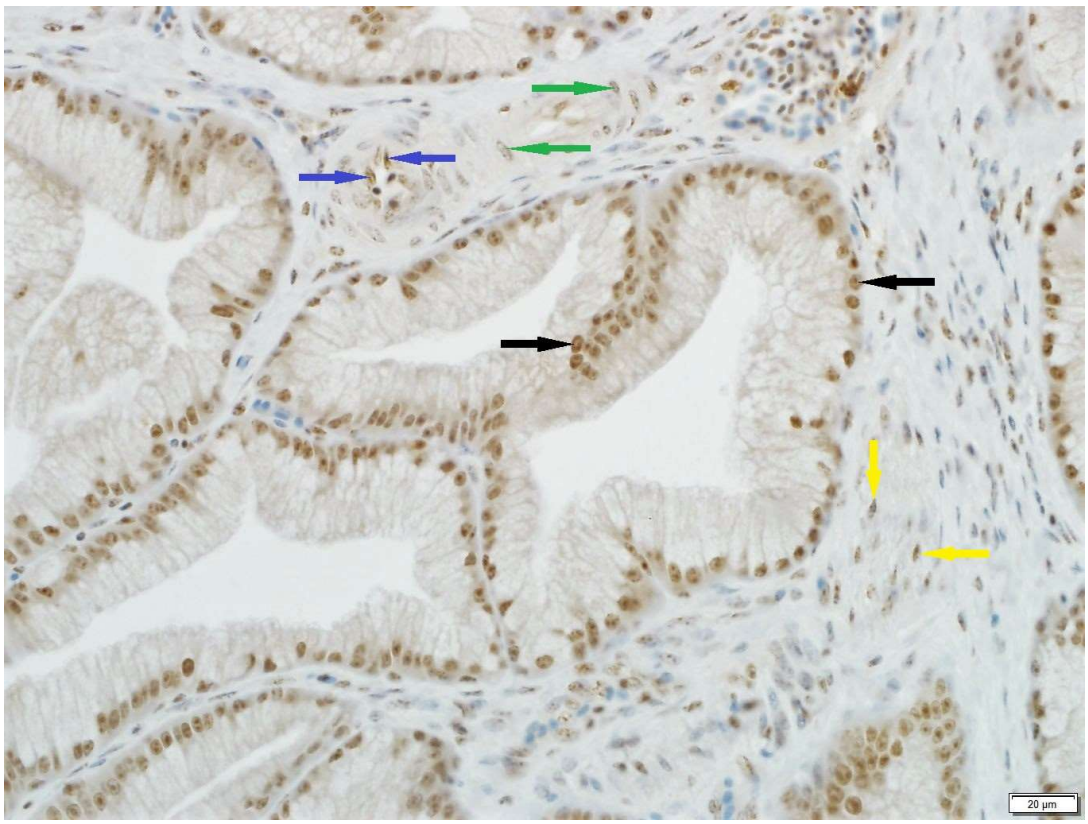

Figure 2.35: Light photomicrograph showing androgen receptor immunostaining in the cloacal gland of a pubertal bird. Strong immunoreactivity is observed in the nuclei (black arrows) of secretory cells. Yellow arrows: weakly immunostained fibroblasts. Blue arrows: moderate immunostaining in endothelial cells. Green arrows: weak immunostaining in smooth muscle cells of a blood vessel.

Figure 2.36: Light photomicrograph showing androgen receptor immunostaining in the cloacal gland of a pubertal bird. Black arrows: strong androgen receptor immunostaining in the nuclei of secretory cells. White arrow: weak immunoreactivity for the androgen receptor in the cytoplasm of a secretory cell. Yellow arrows: weak androgen immunostaining in fibroblasts.

Adult birds

The cloacal glands of adult quails contained both apparently healthy and degenerating glandular units. The secretory cells lining the healthy glandular units displayed moderate to strong nuclear immunostaining for the androgen receptor (Figure 2.37). The cytoplasm of these cells displayed weak to moderate androgen receptor immunostaining (Figure 2.37). The nuclei of secretory cells lining

degenerating glandular units were predominately androgen receptor immunonegative (Figure 2.38).

Fibroblasts in the connective tissue trabeculae separating the glandular units showed moderate to strong immunostaining for the androgen receptor (Figure 2.37), while fibrocytes were androgen receptor immunonegative. Moderate androgen receptor immunostaining was observed in the endothelial cells of interglandular blood vessels, while weak immunostaining was present in the smooth muscle cells forming the walls of the blood vessels (Figure 2.39).

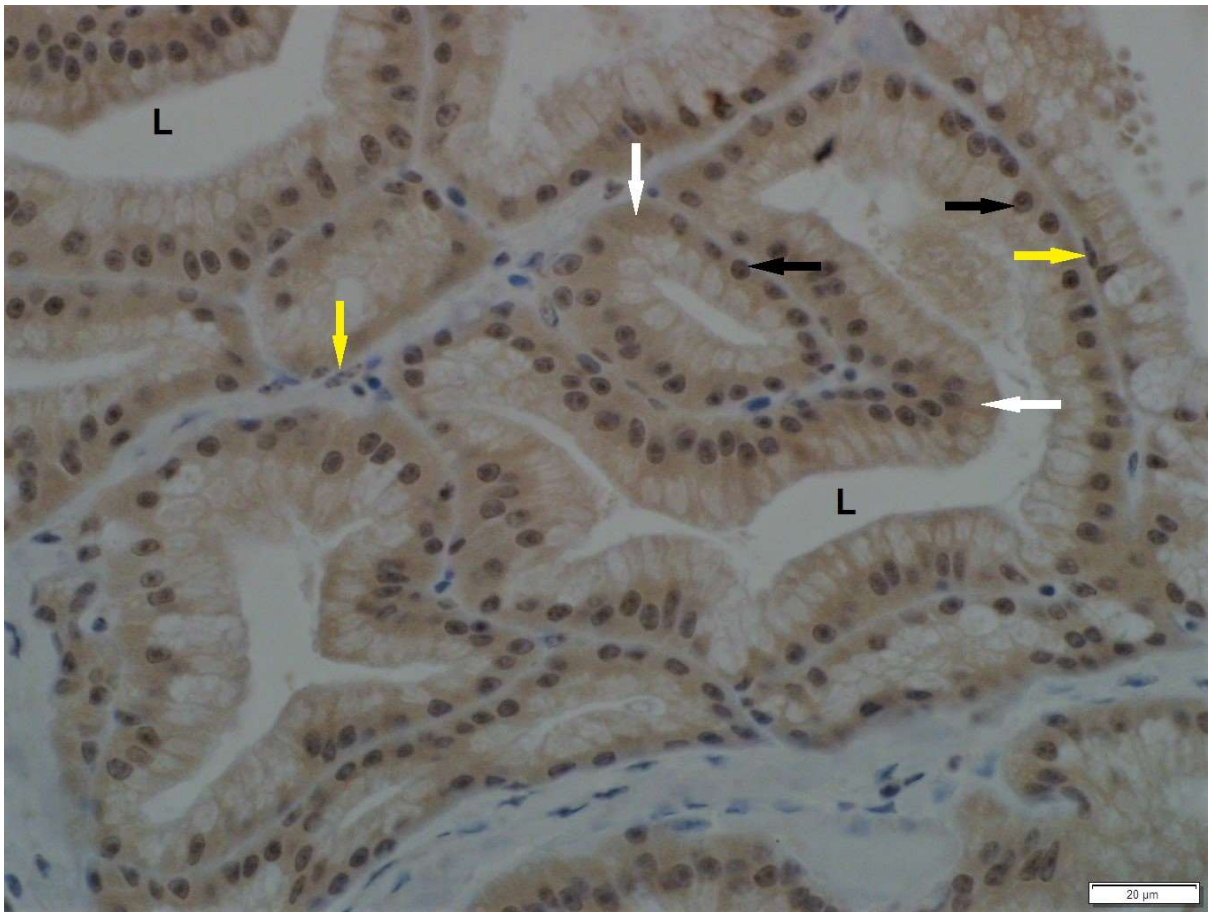

Figure 2.37: Light photomicrograph of androgen receptor immunostaining in the cloacal gland of an adult bird. Black arrows: Moderate androgen receptor immunostaining in the nuclei of epithelial secretory cells. White arrows: weak

androgen receptor immunostaining in the cytoplasm of secretory cells. Yellow arrows: immunopositive fibroblasts. L: lumina of glandular units.

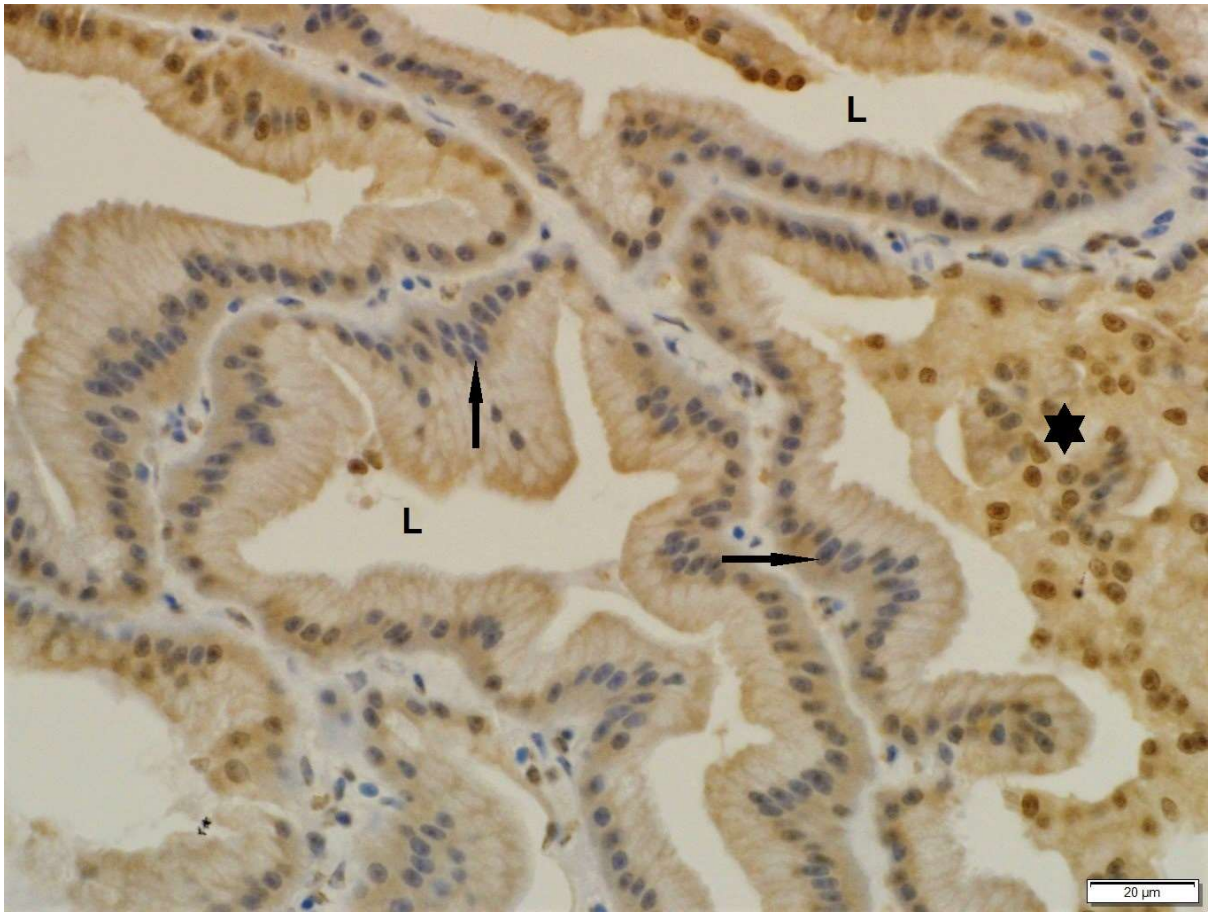

Figure 2.38: Light photomicrograph of androgen receptor immunostaining in the cloacal gland of an adult bird. Black arrows: immunonegative nuclei of secretory cells lining degenerating glandular units. Asterisk: cellular debris. L: lumina of glandular units.

Figure 2.39: Light photomicrograph of androgen receptor immunostaining in the cloacal gland of an adult bird. Immunostaining is demonstrated in the endothelial cells (yellow arrows) and smooth muscle cells (black arrows) of a blood vessel. L: lumen of a glandular unit.

2.3.9 Androgen receptor immunoreactive cell morphometry

The data on the number of epithelial secretory cells that showed positive immunostaining for the androgen receptor was tested for homogeneity and normality. The Kolmogorov- Smirnov test showed that the data was not normally distributed ($p<0.05$). Therefore, the data was analyzed using the Kruskal-Wallis test. There were statistically significant differences in the number of androgen receptor immunopositive and immunonegative cells between the pre-pubertal and pubertal groups, as well as the pre-pubertal and adult groups. The data on the androgen

receptor immunopositive cells in the cloacal glands of birds of different age groups is presented in Table 2.10 and Graph 2.8.

Table 2.10: Percentage of androgen receptor immunopositive and immunonegative epithelial secretory cells in pre-pubertal, pubertal and adult Japanese quails.

Age group of birds	% AR positive cells	% AR negative cells
Pre-pubertal	96.58 ± 1.23 ^{ab}	3.42 ± 1.23 ^{ab}
Pubertal	99.20 ± 0.53 ^{a}	0.80 ± 0.53 ^{b}
Adult	99.90 ± 0.08 ^{b}	0.10 ± 0.08 ^{a}

All data is expressed as mean ± standard error with $p<0.05$ considered to be statistically significant. There are statistically significant differences between means sharing the same superscript.

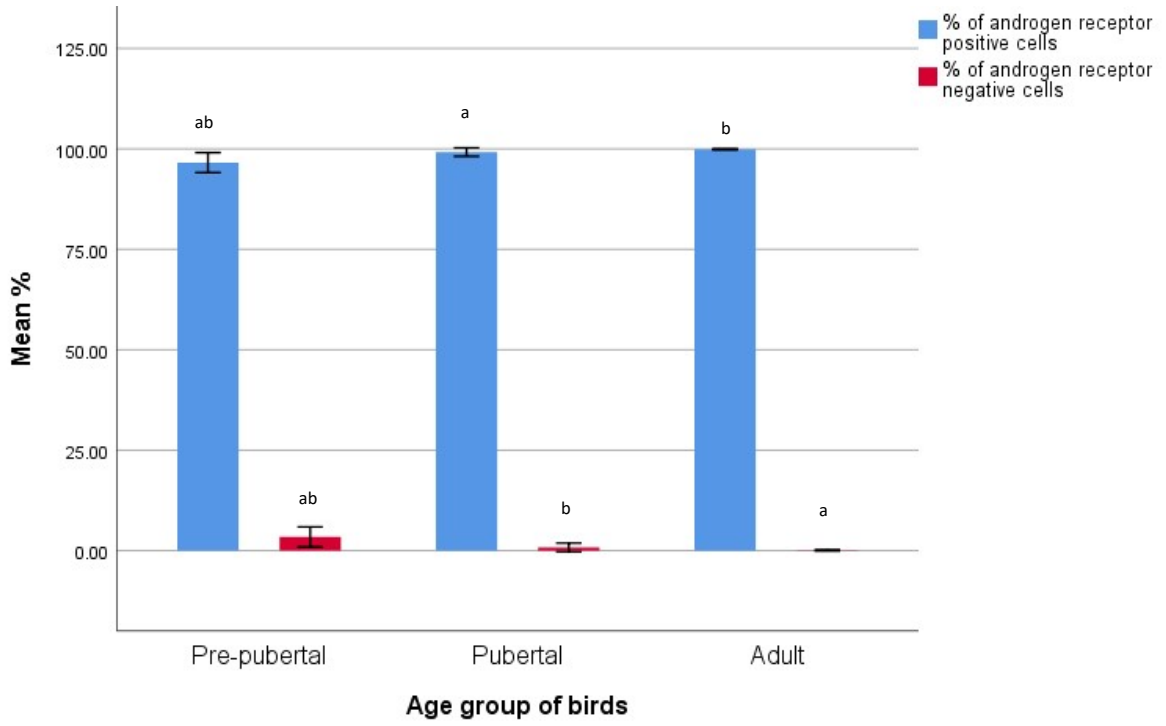

Graph 2.8: The percentage of secretory cells showing androgen receptor immunopositive and immunonegative nuclear staining in the cloacal glands of pre-pubertal, pubertal and adult birds. There are statistically significant differences between means sharing the same letters ($p<0.05$). Data is expressed as mean ± standard error. The data was analyzed using the Kruskal-Wallis test.

2.3.10 Transmission electron microscopy (TEM)

Pre-pubertal birds

The epithelial lining of glandular units in pre-pubertal birds was formed by columnar secretory cells, as well as basal cells.

Secretory cells

Secretory cells in pre-pubertal birds contained electron dense cytoplasm and basally-located, irregular-shaped heterochromatic nuclei (Figure 2.40 A). Contained within the supranuclear cytoplasm were Golgi complexes and secretory vacuoles (Figure 2.40 B), while several elongated mitochondria were observed in the infranuclear cytoplasm. The secretory vacuoles contained a material of variable form and electron density (Figure 2.40 B). The apical plasma membranes of the secretory

cells exhibited microvilli, which were occasionally branched (Figure 2.40 C). In addition, pits formed by discharged secretory vacuoles were observed (Figure 2.40 D).

Basal cells

Basal cells observed in the epithelial lining of the glandular units included lymphocytes (Figure 2.41 A), plasma cells (Figure 2.41 B), as well as elongated cells (Figure 2.41 C). The lymphocytes were characterised by the presence of round, centrally-placed heterochromatic nuclei surrounded by moderate amounts of cytoplasm (Figure 2.41 A). Mitochondria, rough endoplasmic reticulum (RER) cisternae and a few lysosomes were observed in the cytoplasm (Figure 2.41 A). The plasma cells contained heterochromatic nuclei enclosed by abundant cytoplasm. Dilated RER profiles were observed in these cells (Figure 2.41 B).

The third type of basal cells were termed “elongated cells”. The cells contained elongated nuclei which were enclosed in a moderate amount of cytoplasm (Figure 2.41 C).

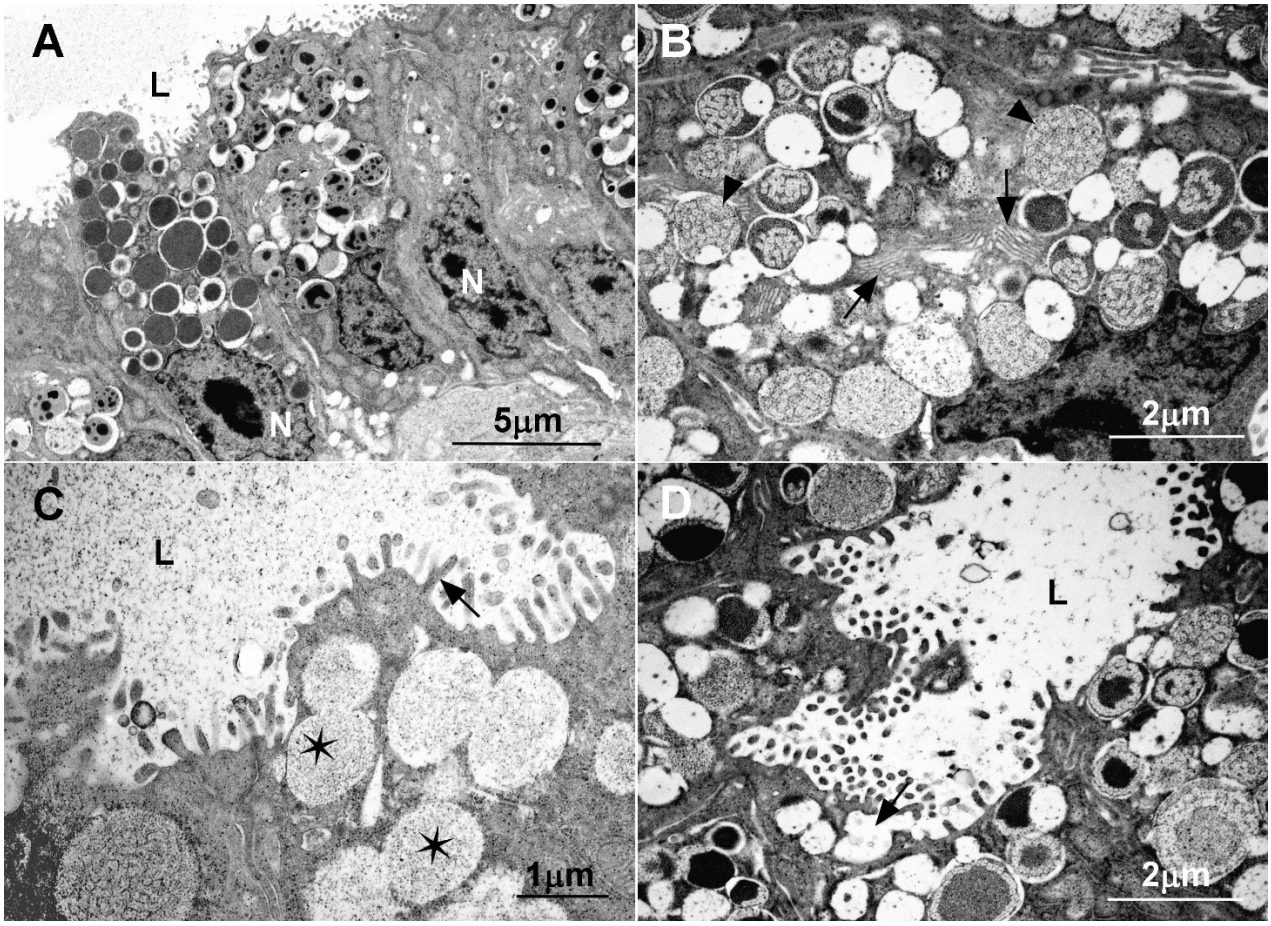

Figure 2.40: Transmission electron photomicrographs of glandular units in the cloacal glands of pre-pubertal quails.

A. Survey photomicrograph of the secretory cells lining a glandular unit. N: nucleus. L: lumen.

B: Supranuclear region of a secretory cell. Arrows: Golgi complexes. Arrowheads: secretory vacuoles.

C: Apical regions of secretory cells. Arrow: branched microvillous. L: lumen. Asterisks: secretory vacuoles.

D: Apical regions of secretory cells. Arrow: pit formed by a discharged secretory vacuole. L: lumen.

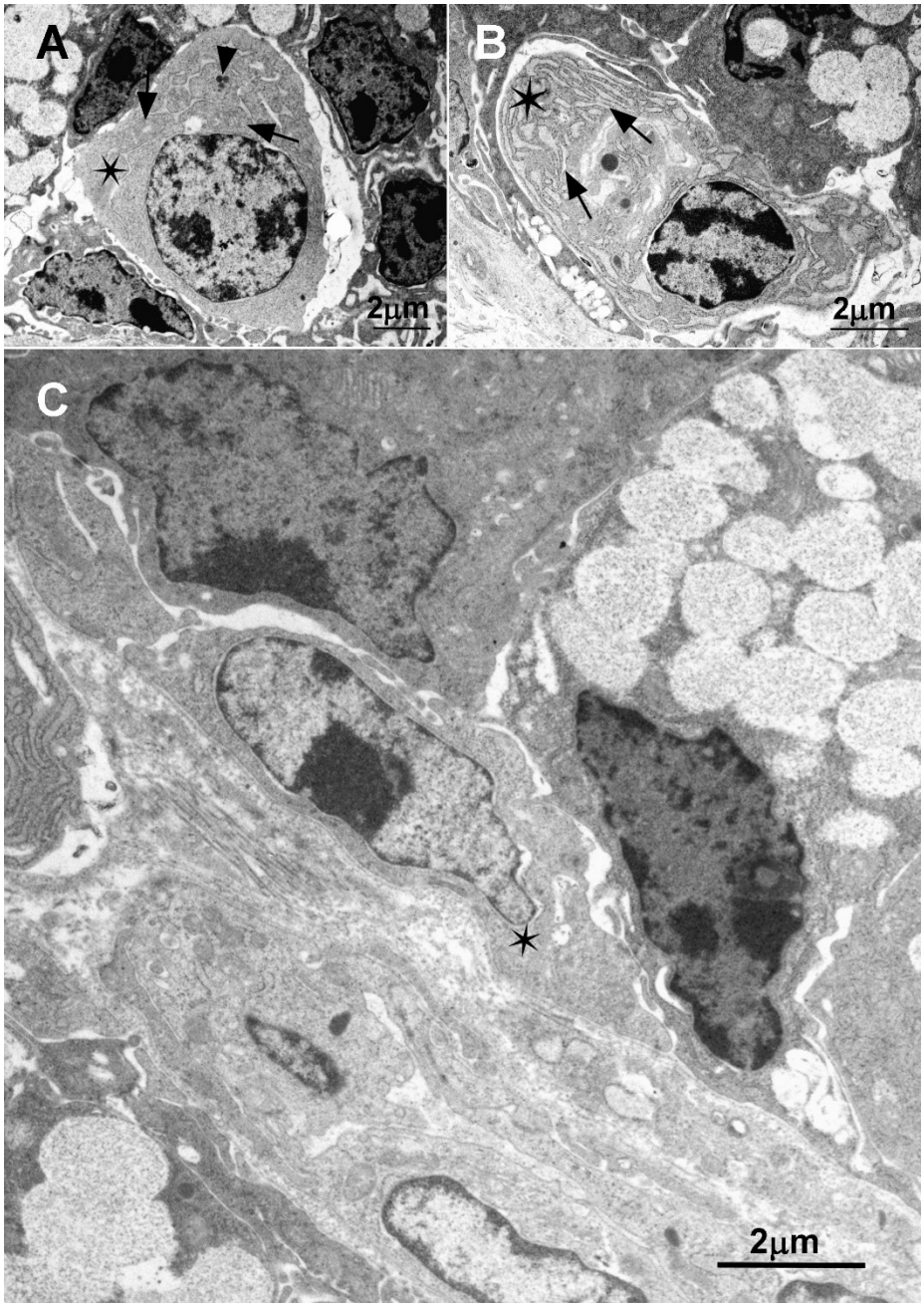

Figure 2.41: Transmission electron photomicrographs of basal cells in the epithelia lining glandular units in the cloacal glands of pre-pubertal quails.

A: Asterisk: lymphocyte. Arrows: mitochondria. Arrowhead: group of lysosomes.

B: Asterisk: plasma cell. Arrows: RER cisternae.

C: Asterisk: elongated basal cell.

Pubertal birds

The glandular units of the cloacal gland in pubertal birds were lined by cells of low, intermediate and high electron density, which will be designated as types 1, 2 and 3 respectively (Figure 2.42). In addition, a few basal cells were observed.

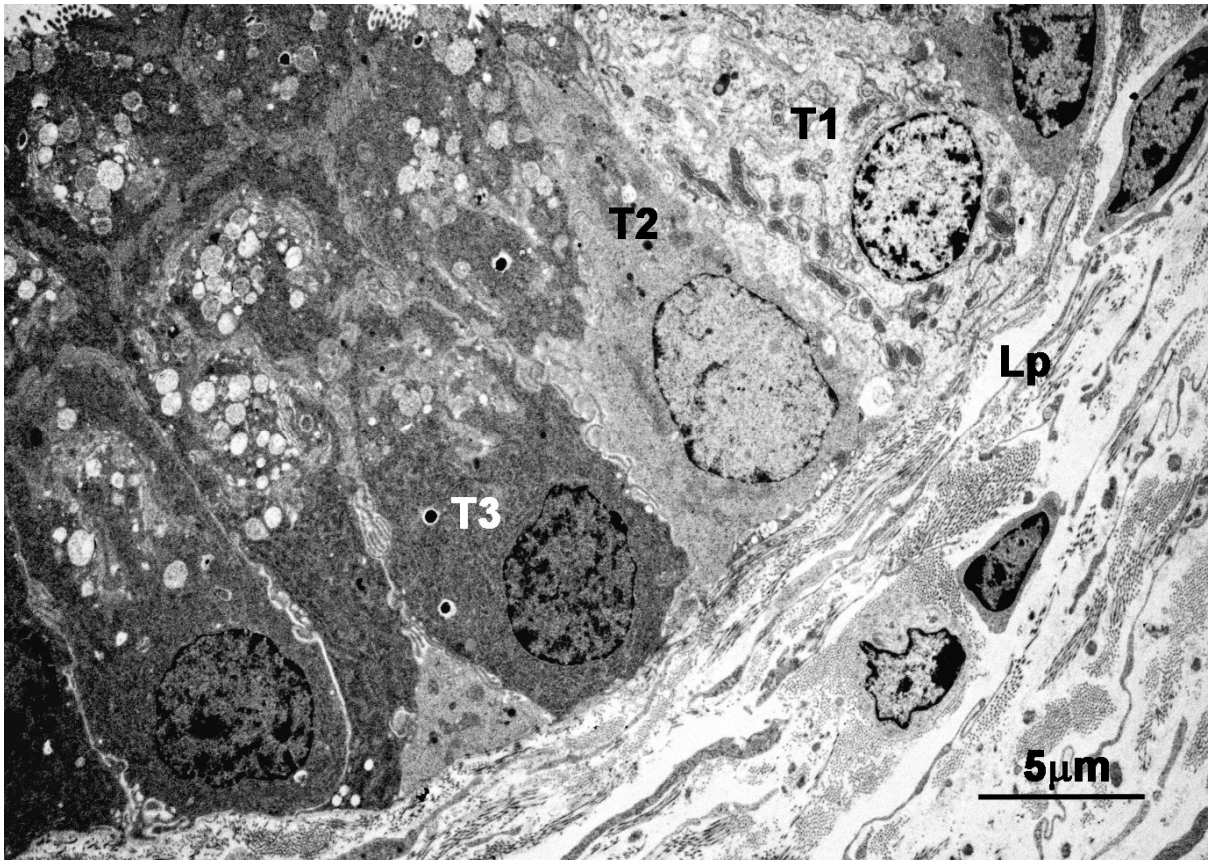

Figure 2.42: Transmission electron photomicrograph of type 1 (T1), 2 (T2) and 3 (T3) cells in the epithelial lining of a glandular unit in the cloacal gland of a pubertal quail. Lp: *lamina propria*.

Type 1 cells

Type 1 cells were characterised by cytoplasm of low electron density which contained evenly distributed, long, dilated profiles of RER (Figure 2.43 A). The RER profiles partially or totally enclosed mitochondria (Figure 2.43 A). Contained within the type 1 cells were oval-shaped nuclei with clumps of heterochromatin (Figure 2.43

A). Multiple Golgi complexes with developing secretory vacuoles were prominent features of the supranuclear cytoplasm (Figure 2.43 B).

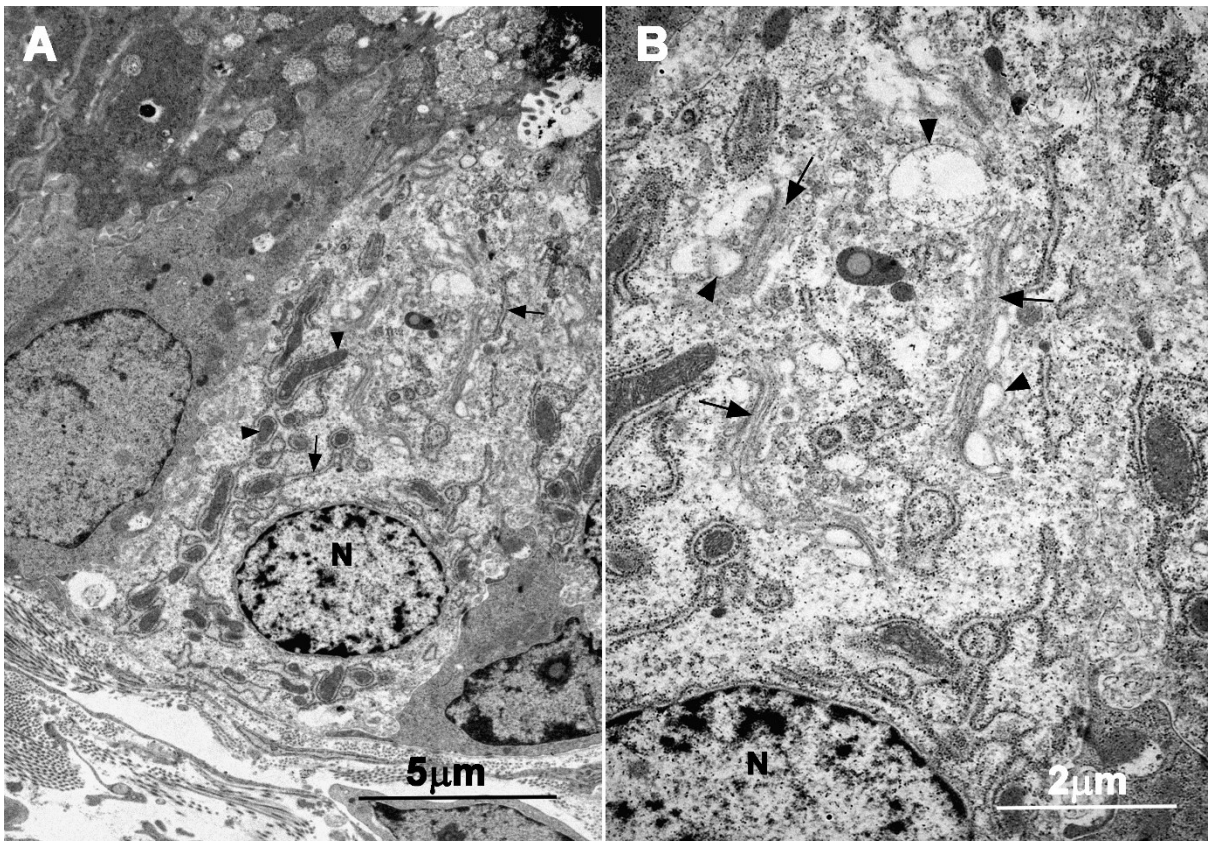

Fig 2.43: Transmission electron photomicrographs of electron lucent cells (type 1) in the epithelia lining glandular units in the cloacal glands of pubertal quails.

A: Arrows: RER cisternae. Arrowheads: mitochondria. N: nucleus.

B: Supranuclear cytoplasm of a type 1 cell. Arrows: Golgi complexes. Arrowheads: secretory vacuoles in various stages of formation. N: nucleus.

Type 2 cells

Type 2 cells contained cytoplasm of an intermediate electron density (Figure 2.44). These cells contained basally-located euchromatic nuclei. The peri- and

supranuclear cytoplasm contained elongated mitochondria, small vesicles, and lysosomes (Figure 2.44).

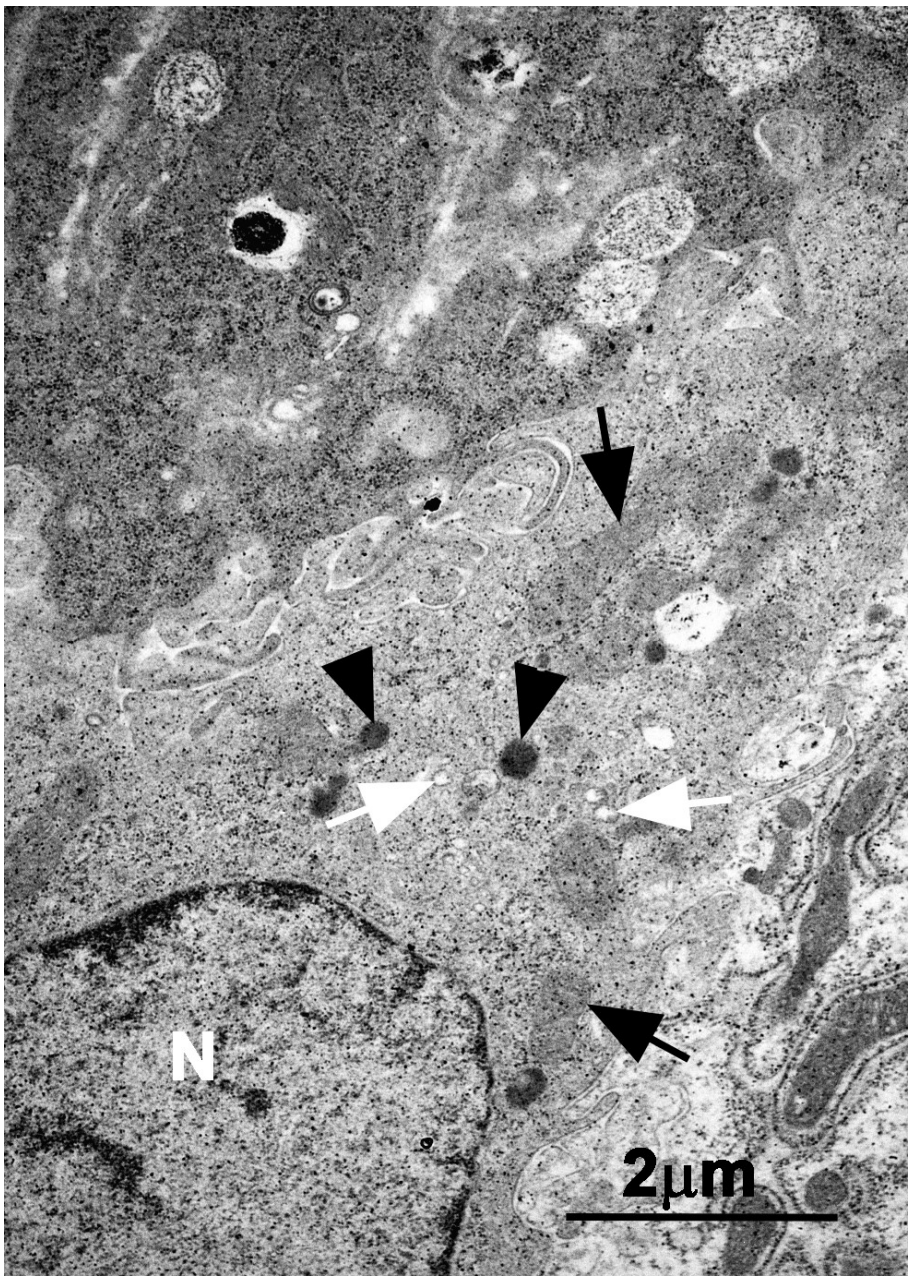

Fig 2.44: Transmission electron photomicrograph of a type 2 cell in the epithelia lining glandular units in the cloacal gland of a pubertal quail. Black arrows: mitochondria. White arrows: vesicles. Arrowheads: lysosomes. N: nucleus.

Type 3 cells

Type 3 cells contained basally-located heterochromatic nuclei. The basal, perinuclear and supranuclear cytoplasm was electron dense, while cytoplasm of an intermediate electron density was observed in the apical regions of the cells (Figure 2.45 A). Located in the cytoplasmic regions of intermediate electron density were several Golgi complexes and developing secretory vacuoles of varying sizes and quantities (Figure 2.45B). The material contained within the secretory vacuoles exhibited a variable configuration and electron density (Figure 2.46). Some secretory vacuoles contained an electron dense core, while others exhibited a granular material of intermediate electron density (Figure 2.46). In addition, secretory vacuoles containing material arranged in beaded strands of an intermediate electron density were also observed (Figure 2.46).

The apical regions of type 3 cells displayed cytoplasmic protrusions which were at varying stages of detachment (Figure 2.47A). The commencement of detachment was preceded by the formation of linear electron dense areas directly below the cytoplasmic protrusions (Figure 2.47B).

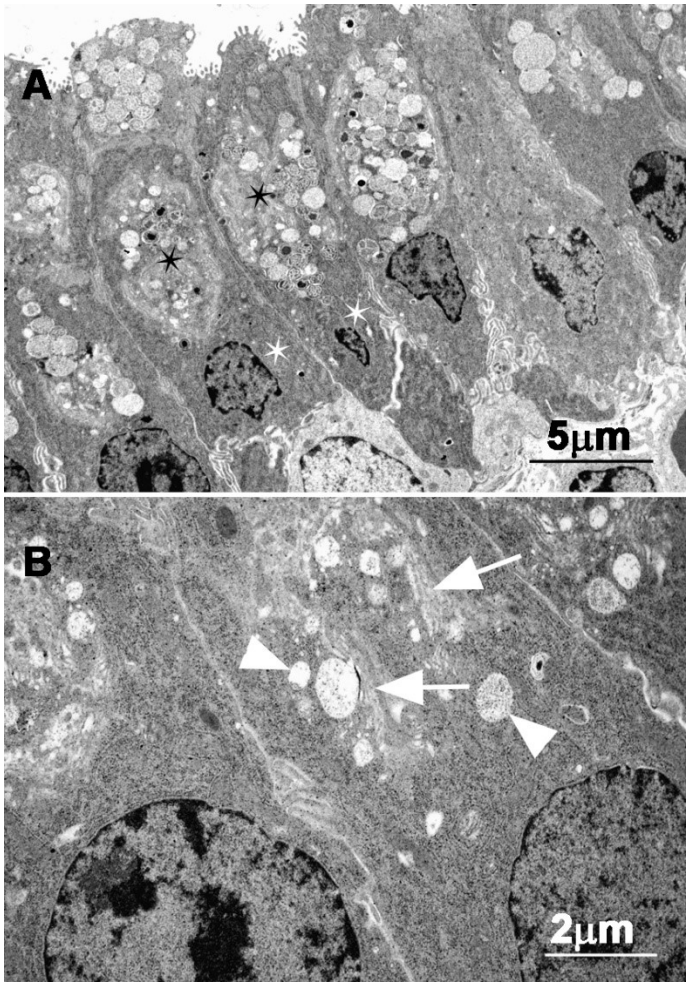

Figure 2.45: Transmission electron photomicrographs of the epithelial lining of glandular units in the cloacal glands of pubertal quails.

A: Type 3 cells contain cytoplasm of intermediate (black asterisks) and high (white asterisks) electron density.

B: Supranuclear regions of type 3 cells. Arrows: Golgi complexes. Arrowheads: developing secretory vacuoles.

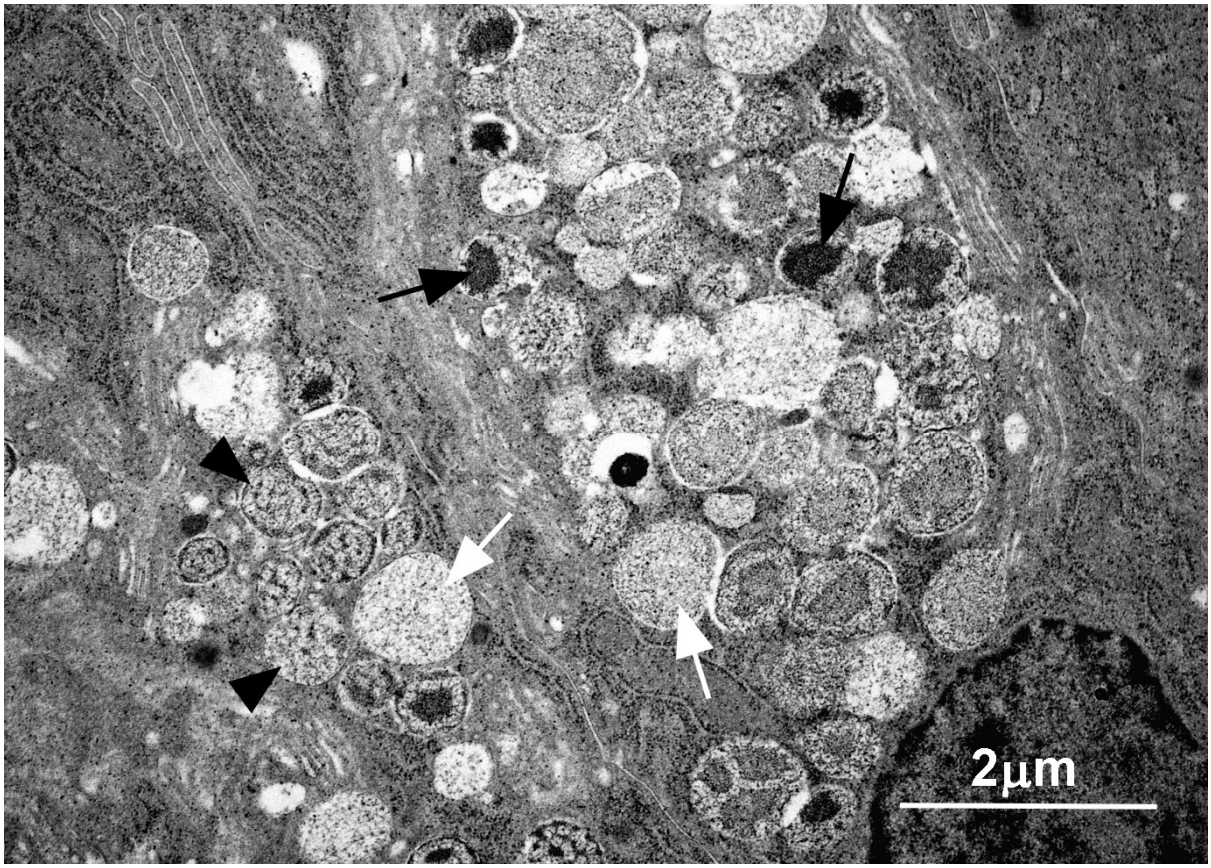

Figure 2.46: Transmission electron photomicrograph of type 3 cells in the epithelial lining of glandular units in the cloacal glands of pubertal quails. Secretory vacuoles with electron dense cores (black arrows), granular intermediate electron dense material (white arrows) and beaded material (arrowheads) are observed.

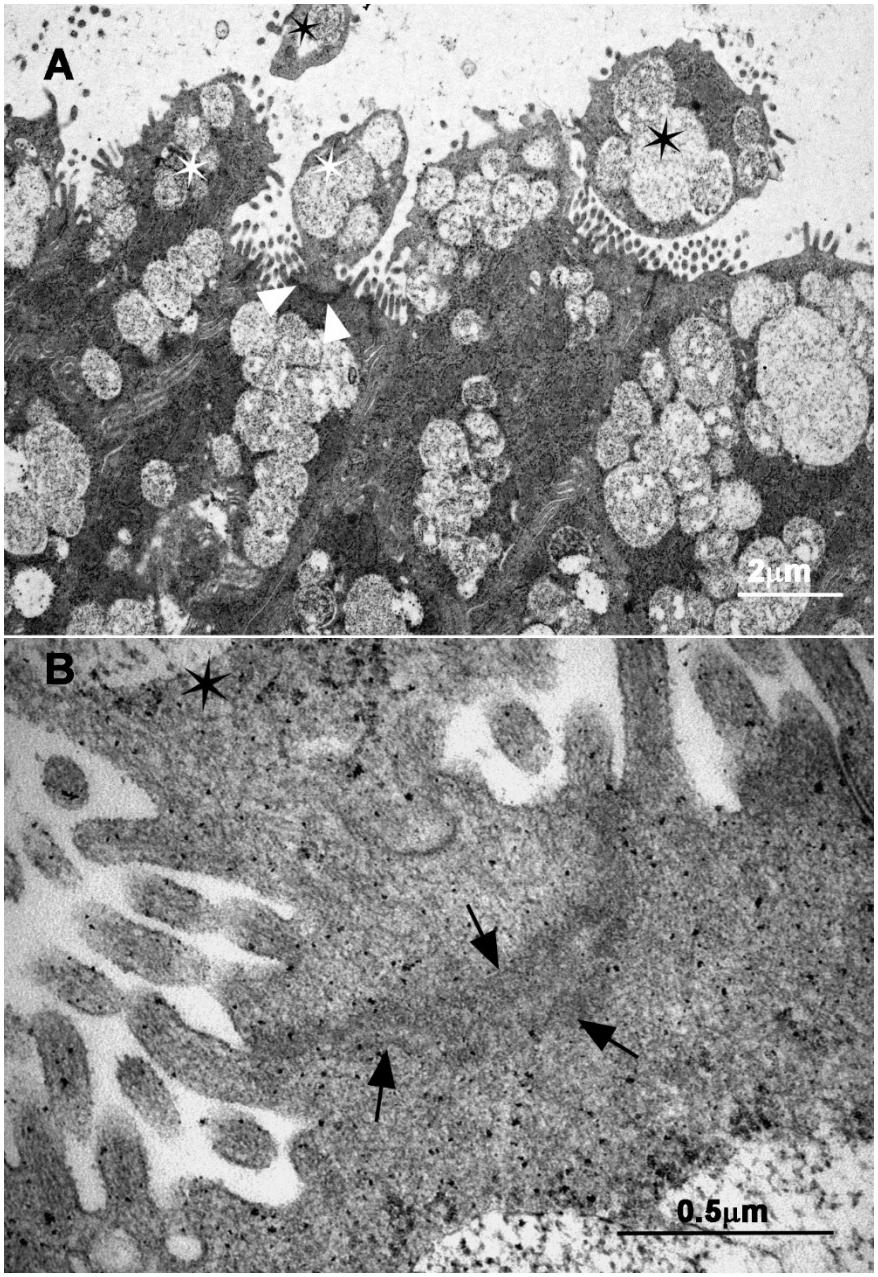

Figure 2.47: Transmission electron photomicrographs of type 3 cells in the epithelia lining glandular units in the cloacal glands of pubertal quails.

A: Detaching (white asterisks) and detached (black asterisks) cytoplasmic protrusions. Arrowheads: site of increased electron density.

B: Arrows: electron dense area in the site of protrusion detachment. Asterisk: cytoplasmic protrusion.

Basal cells

Basal cells in the lining epithelium of glandular units typically contained elongated nuclei enclosed by scant cytoplasm (Figure 2.48A). Few organelles were identified in the cytoplasm of the basal cells (Figure 2.48B).

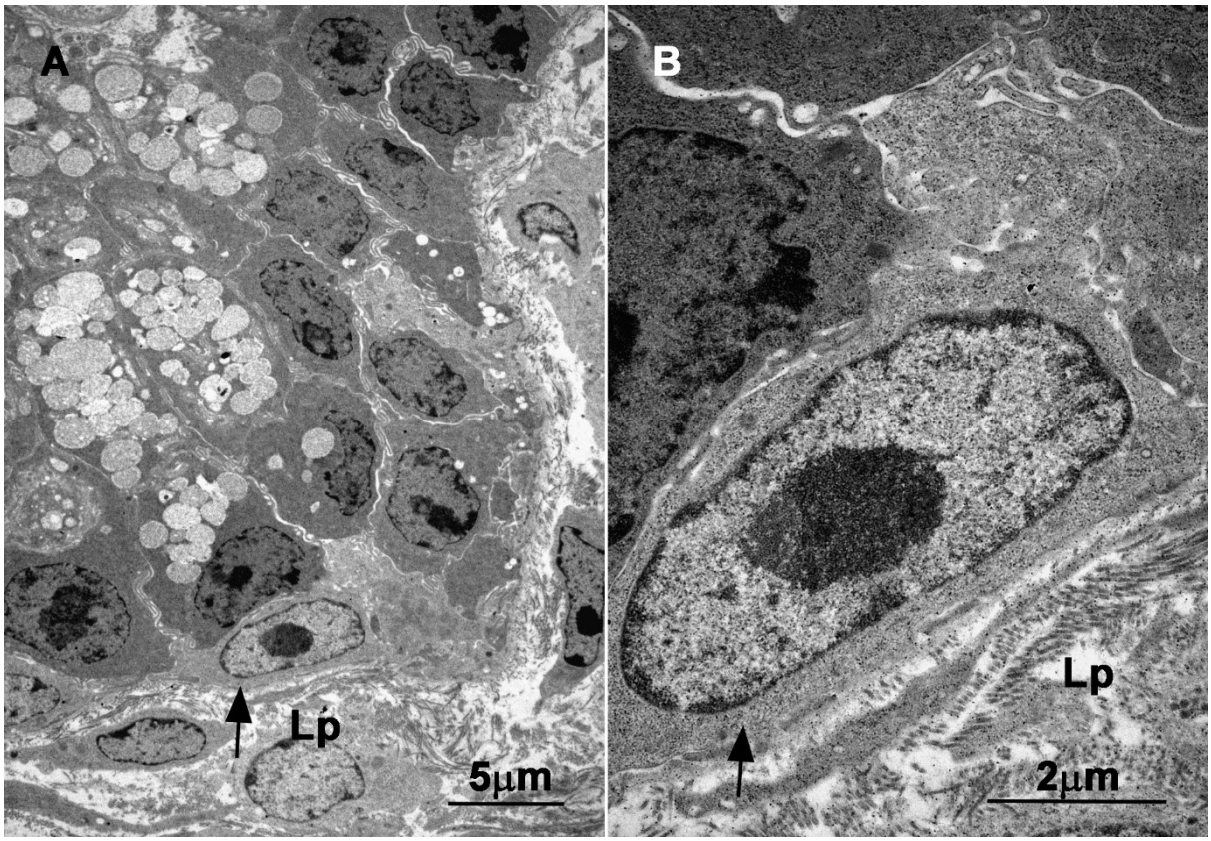

Figure 2.48: Low (A) and high (B) magnification transmission electron photomicrographs of a basal cell (arrows) in the epithelium lining a glandular unit in the cloacal gland of a pubertal quail. Lp: *lamina propria*.

Adult birds

In adult birds, the glandular units of the cloacal gland were lined by a pseudostratified columnar epithelium (Figure 2.49) comprising of: (1) columnar cells with electron lucent cytoplasm; (2) columnar cells with cytoplasm of an intermediate electron density; (3) basal cells; (4) degenerating cells. The cells with low and intermediate electron density cytoplasm will be designated as types 1 and 2 respectively. Various stages of secretory differentiation of both cell types were identified.

The epithelial cells lined lumina which contained a combination of secretory material and cellular debris (Figure 2.50).

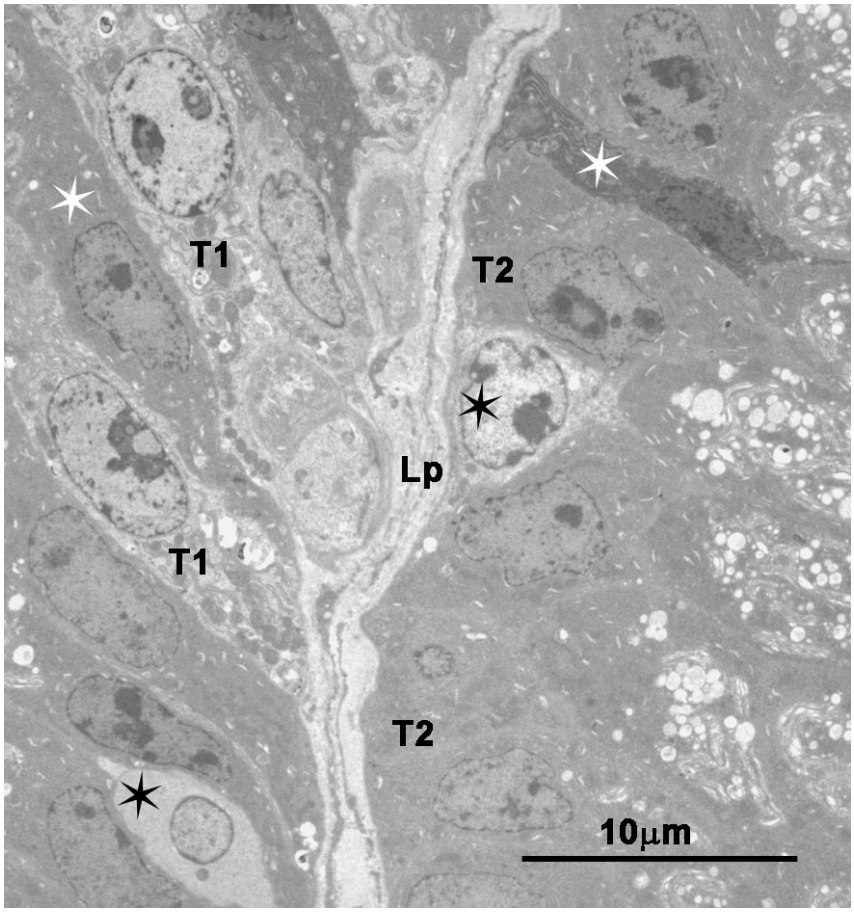

Figure 2.49: Transmission electron photomicrograph of type 1 (T1), type 2 (T2), basal (black asterisks) and degenerating (white asterisks) cells lining a primary fold in a glandular unit in the cloacal gland of an adult quail.

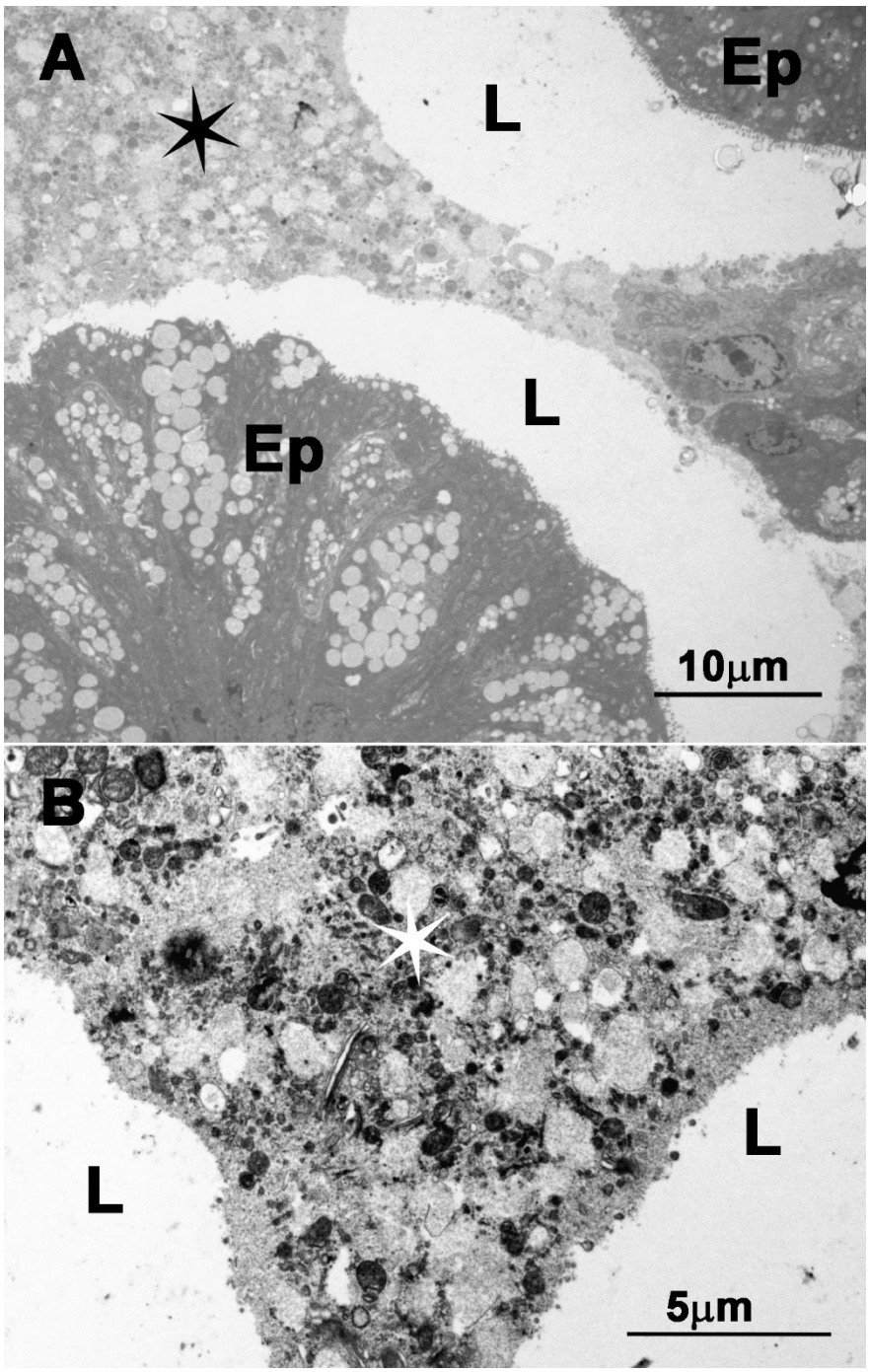

Figure 2.50: Transmission electron photomicrographs (A and B) of secretory material and cellular debris (asterisks) in lumina (L) of glandular units in the cloacal glands of adult quails. Ep: glandular unit epithelium.

Type 1 cells

Stage 1

Stage 1 was the earliest form of the secretory process observed in type 1 cells. During stage 1 the cells exhibited tapered apical regions which did not extend to the glandular lumen (Figure 2.51A). The nuclei during this stage of the secretory process were euchromatic with clumps of chromatin. Basally the cells contained long RER cisternae, several mitochondria and masses of clear vacuoles (Figure 2.51B). Contained within the supranuclear cytoplasm were RER cisternae, mitochondria and occasional secretory vacuoles (Figure 2.51C). The cells lacked distinct Golgi complexes.

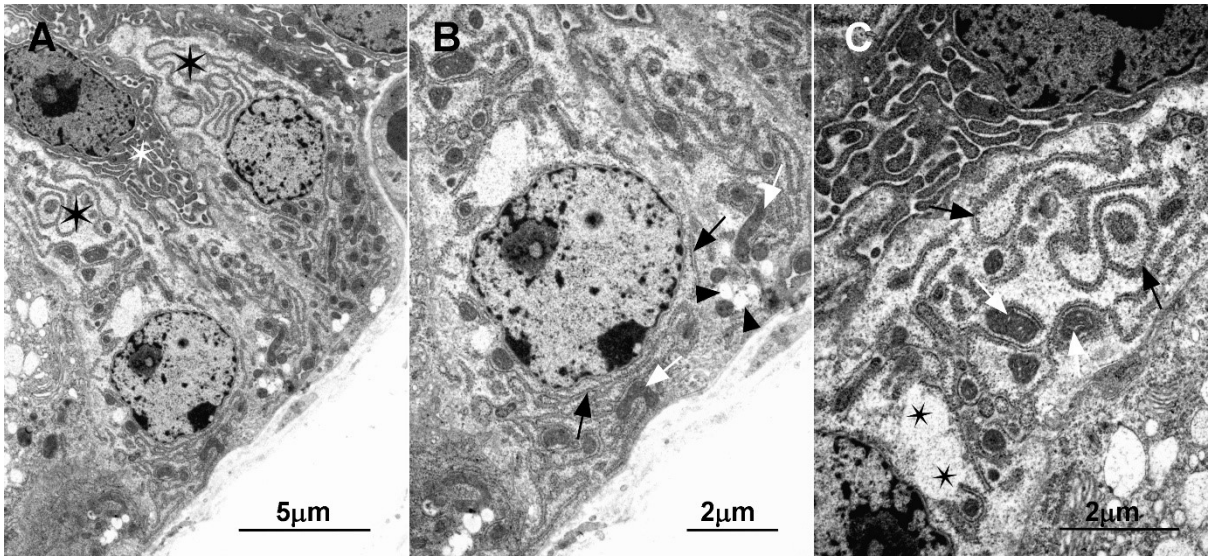

Figure 2.51: Transmission electron photomicrographs of type 1 (stage 1) cells and degenerating cells in the epithelial lining of a glandular unit in the cloacal gland of an adult quail.

A: Black asterisks: type 1 cells in stage 1 of the secretory process. White asterisk: degenerating cell.

B: Black arrows: RER cisternae. White arrows: mitochondria. Arrowheads: vacuoles.

C: Black arrows: RER cisternae. White arrows: mitochondria. Asterisks: secretory vacuoles.

Stage 2

The apices of type 1 cells in stage 2 of the secretory process did not extend to the glandular lumen. These contained basally-located euchromatic nuclei surrounded by long profiles of RER, which were associated with masses of mitochondria (Figure 2.52). In addition, the cytoplasm contained numerous, partially coalesced secretory vacuoles (Figure 2.52).

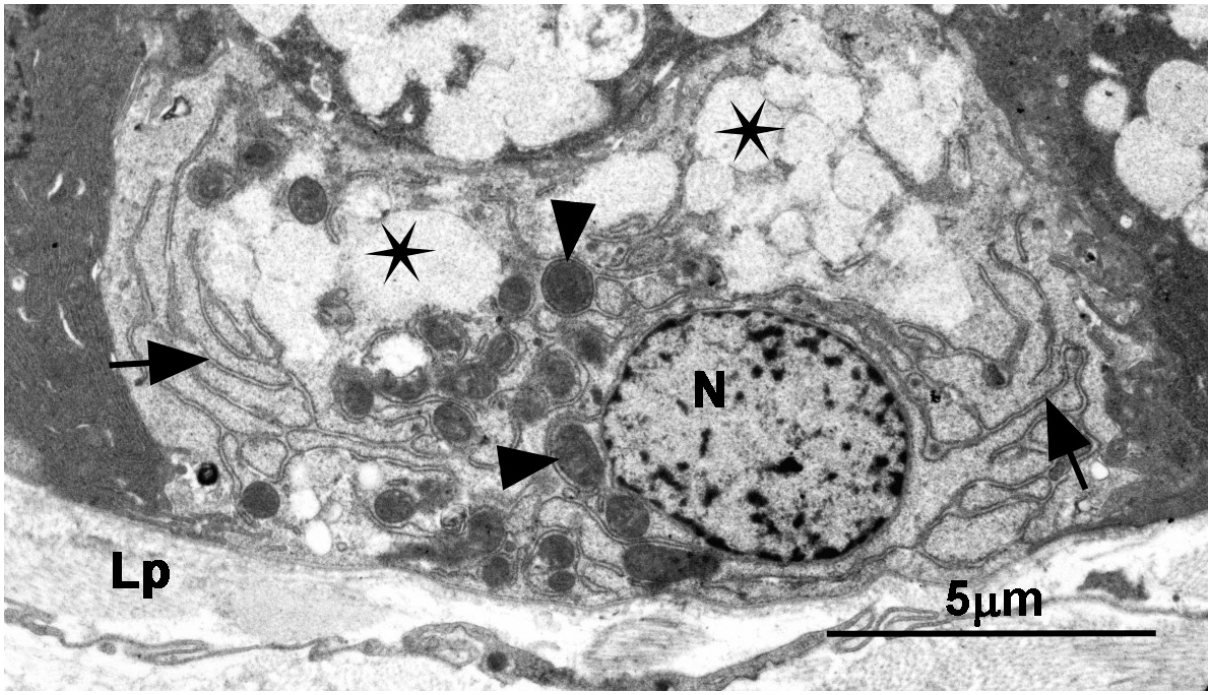

Figure 2.52: Transmission electron photomicrograph of a type 1 (stage 2) cell in the epithelial lining of a glandular unit in the cloacal gland of an adult quail. Arrows: RER cisternae. Arrowheads: mitochondria. Asterisks: secretory vacuoles. N: nucleus. Lp: *lamina propria*.

Stage 3

Type 1 cells in stage 3 of the secretory process were columnar in shape, with apices which extended to the glandular lumen. Contained within these cells were centrally-located, oval-shaped, euchromatic nuclei (Figure 2.53). The perinuclear cytoplasm contained short profiles of RER, as well as a few mitochondria. Located in the basal regions of the cells were long profiles of RER, mitochondria and groups of small vacuoles. The supranuclear cytoplasm contained varying quantities of secretory vacuoles. The secretory vacuoles contained a flocculent material of an intermediate electron density. Coalescence of the secretory vacuoles was common.

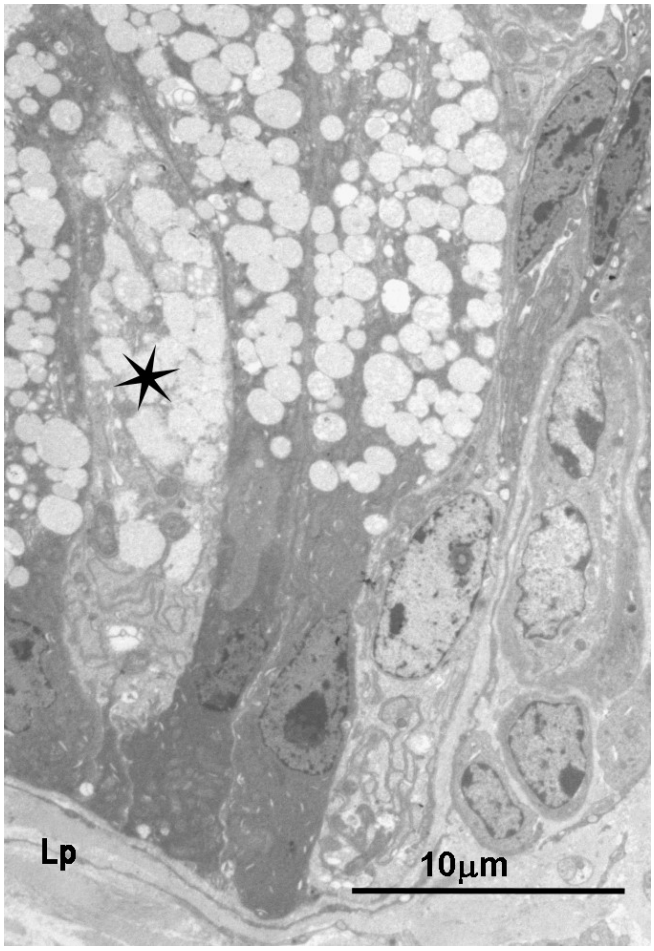

Figure 2.53: Transmission electron photomicrograph of the epithelial lining of a glandular unit in the cloacal gland of an adult quail. Asterisk: type 1 (stage 3) cell. Lp: *lamina propria*.

Type 2 cells

Stage 1

In stage 1 of the secretory process the apical regions of type 2 cells did not extend to the lumen (Fig 2.54A). At this stage of development, the cells were characterised by the presence of extensive basally-located RER, which was either arranged in whorls (Fig 2.54B) or stacks (Fig 2.54C). A euchromatic nucleus with a distinct nucleolus was placed in the central region of the cell. The supranuclear region of the cell

contained long profiles of RER and occasional secretory vacuoles (Fig 2.54B). Golgi complexes were not prominent at this stage of the secretory process.

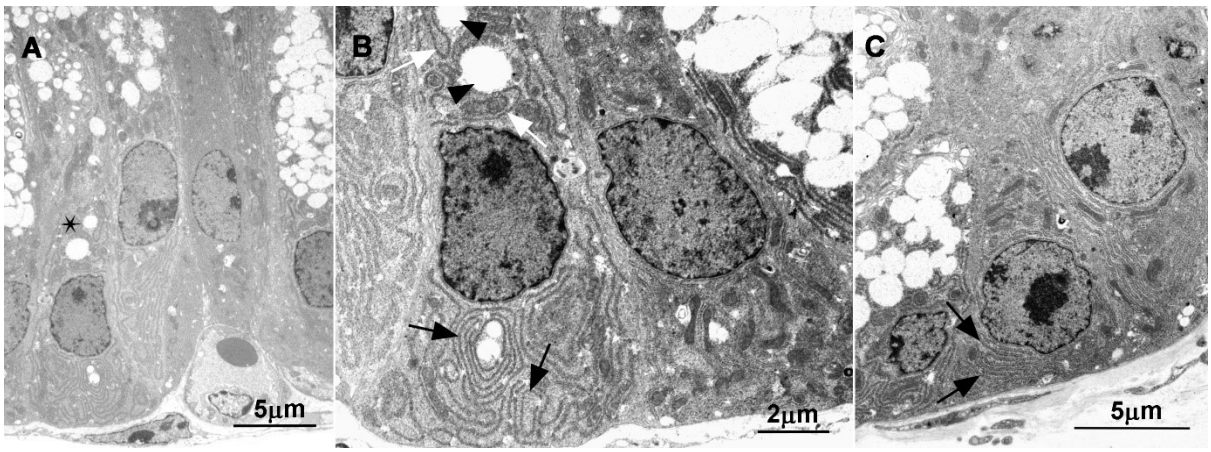

Fig 2.54: Transmission electron photomicrographs of the epithelial lining of glandular units in the cloacal gland of adult quails.

A: Asterisk: type 2 (stage 1) cell.

B: Black arrows: whorls of RER profiles. White arrows: RER profiles in the supranuclear cytoplasmic region. Arrowheads: secretory vacuoles.

C: Arrows: RER profiles arranged in stacks.

Stage 2

The apical surfaces of type 2 cells in stage 2 of the secretory process did not extend to the lumen of the glandular unit. During this stage of the secretory process, type 2 cells contained oval-shaped nuclei with prominent nucleoli (Fig 2.55A). The infranuclear region was dominated by numerous mitochondria and RER profiles arranged in stacks (Fig 2.55B) or whorls (Fig 2.55C). In addition, occasional vacuoles were observed in the infranuclear region (Fig 2.55B). The supranuclear cytoplasm closest to the nucleus contained profiles of RER, as well as a few coated

vesicles. The remainder of the supranuclear cytoplasm contained multiple Golgi complexes and several secretory vacuoles (Fig 2.55 A & C).

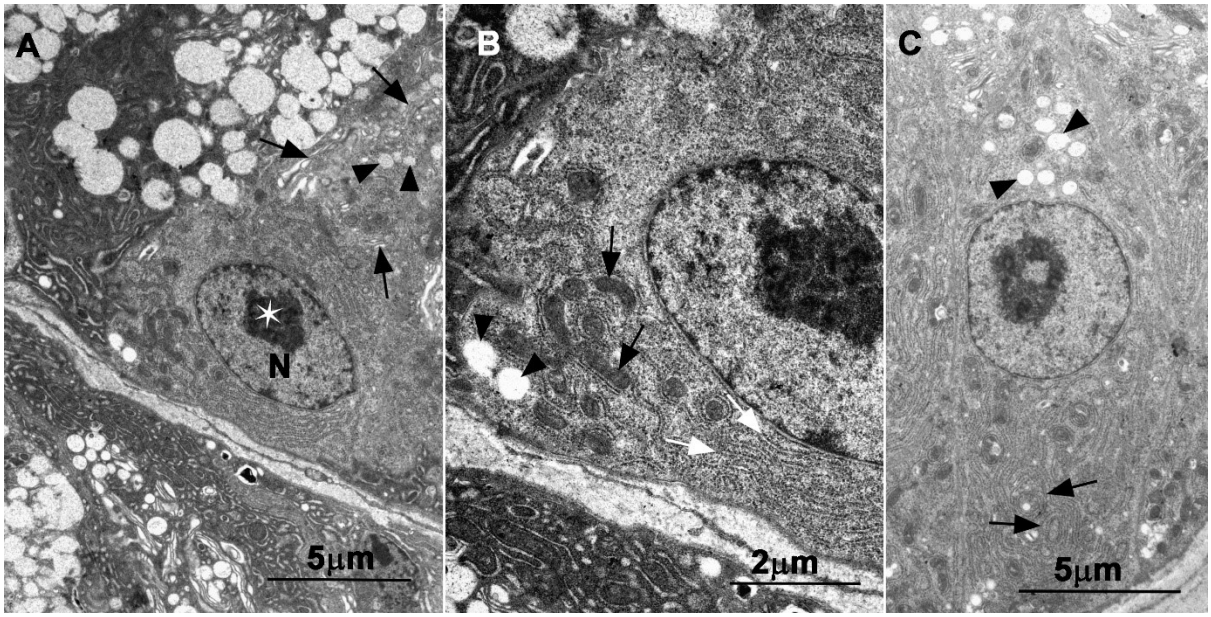

Figure 2.55: Transmission electron photomicrographs of the epithelial lining of glandular units in the cloacal gland of adult quails.

A: N: nucleus. Asterisk: nucleolus. Arrows: Golgi complexes. Arrowheads: secretory vacuoles.

B: Black arrows: mitochondria. White arrows: RER profiles. Arrowheads: vacuoles.

C: Arrows: whorls of RER profiles. Arrowheads: secretory vacuoles.

Stage 3

Type 2 cells in stage 3 of the secretory process were typically tall columnar in form, with broad apical and narrow basal regions (Figure 2.56A). The cells contained oblong-shaped euchromatic nuclei which were located towards the basal regions of the cells. Numerous profiles of RER were contained in the infranuclear cytoplasm

(Figure 2.56A). The supranuclear and apical cytoplasmic regions contained mitochondria, multiple Golgi complexes, as well as varying quantities of large secretory vacuoles (Figure 2.56B). Apical plasma membranes exhibited a few short microvilli (Figure 2.56C). In addition, deep pits, indicative of recent secretory product discharge, were evident (Figure 2.56C).

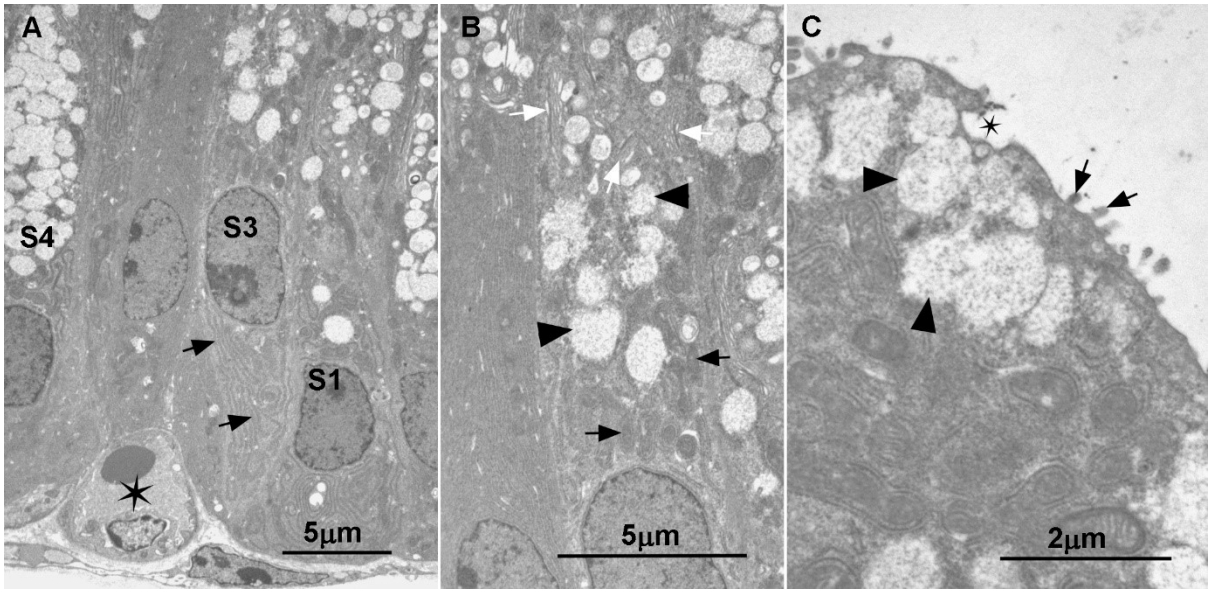

Figure 2.56: Transmission electron photomicrographs of the epithelial lining of a glandular unit in the cloacal gland of an adult quail.

A: Type 2 cells in stages 1 (S1), 3 (S3) and 4 (S4) of the secretory process. Arrows: RER cisternae. Asterisk: blood vessel in the *lamina propria*.

B: Black arrows: mitochondria. White arrows: Golgi complexes. Arrowheads: Secretory vacuoles.

C: Arrows: microvilli. Asterisk: discharge pit. Arrowheads: secretory vacuoles.

Stage 4

Type 2 cells in stage 4 of the secretory process contained oval to oblong-shaped nuclei, which were basally-located (Figure 2.57A). Located in the basal cytoplasm

were several mitochondria, a few long profiles of RER and vacuoles (Figure 2.57B). Multiple Golgi complexes and developing secretory vacuoles occupied the supranuclear cytoplasm (Figure 2.57C), while numerous mitochondria and coalescing secretory vacuoles were present in the apical cytoplasmic regions (Figure 2.58A). The apical plasma membrane exhibited numerous microvilli, which contained a central core of microfilaments (Figure 2.58B). The microfilaments were continuous with the terminal web located directly below the apical membrane (Figure 2.58B).

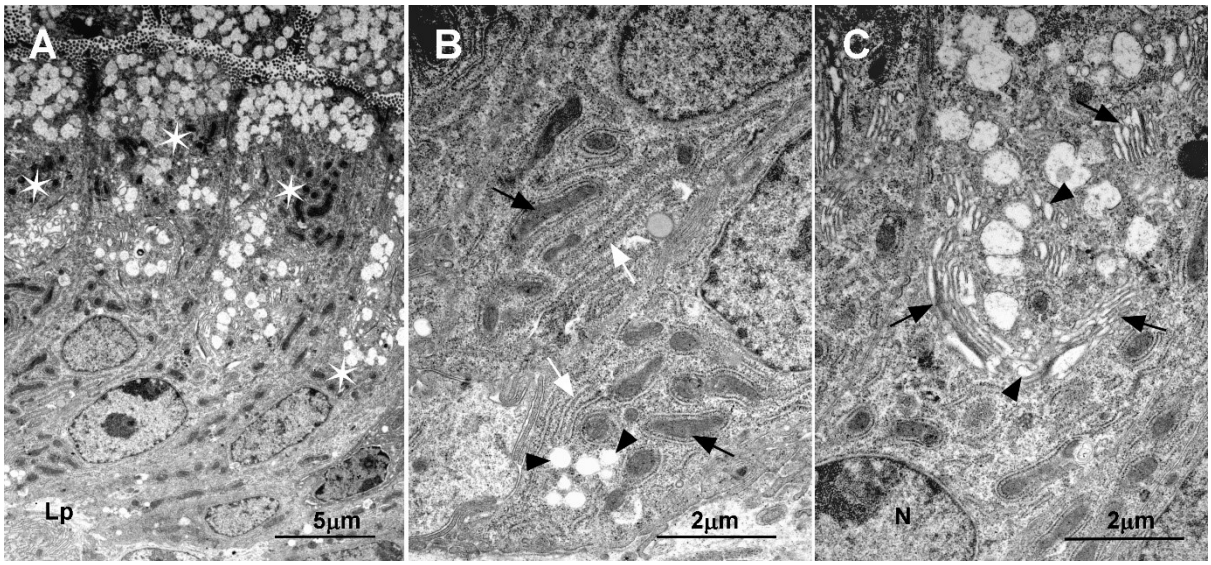

Figure 2.57: Transmission electron photomicrographs of the epithelial lining of a glandular unit in the cloacal gland of an adult quail.

A: Asterisks: Type 2 cells in stage 4 of the secretory process. Lp: *lamina propria*. B: Infranuclear cytoplasm. Black arrows: mitochondria. White arrows: RER cisternae. Arrowheads: vacuoles.

C: Supranuclear cytoplasm. Arrows: Golgi complexes. Arrowheads: developing secretory vacuoles.

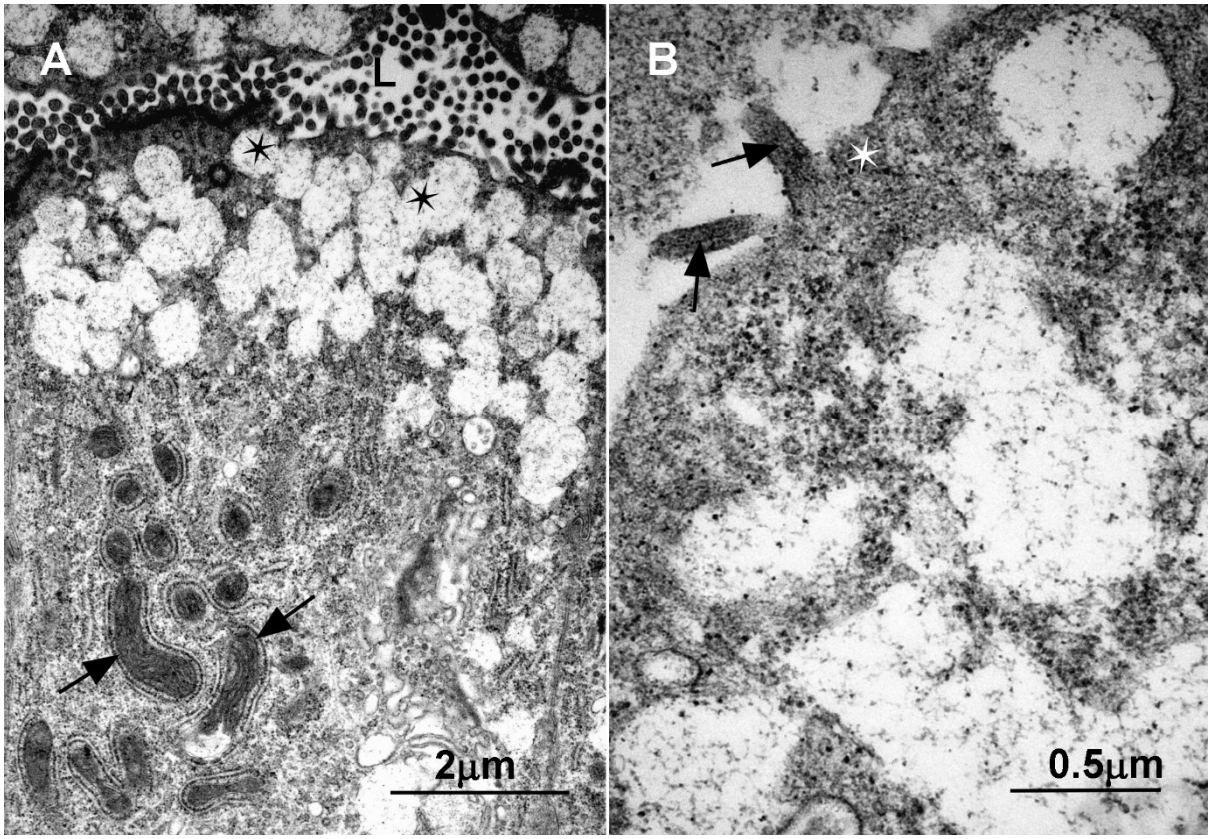

Figure 2.58: Transmission electron photomicrographs of the epithelial lining of a glandular unit in the cloacal gland of an adult quail.

A: Arrows: mitochondria. Asterisks: secretory vacuoles. L: lumen.

B: Arrows: microfilaments in microvilli. Asterisk: terminal web.

Basal cells

Various types of basal cells were present in the lining epithelium of glandular units in adult birds. Pyramidal (Figures 2.59A, B, & C), oval (Figures 2.60A & B) and elongated (Figure 2.66C) cells were observed. The pyramidal cells contained large oval or irregular-shaped nuclei, which dominated the cell. The enclosing cytoplasm contained a supranuclear Golgi complex, as well as a few mitochondria and fibrils (Figure 2.59C).

The oval-shaped cells contained centrally-placed euchromatic nuclei surrounded by abundant electron lucent cytoplasm (Figure 2.60A). In addition, occasional oval-shaped cells undergoing mitosis were observed (Figures 2.60A & B).

A typical elongated basal cell contained a large apically-placed nucleus and a long basal cytoplasmic process (Figure 2.60C). Contained within the cytoplasm were several mitochondria, a prominent Golgi complex, a few RER profiles, occasional multivesicular bodies and numerous small vesicles. The plasma membranes of these cells did not exhibit any junctional complexes.

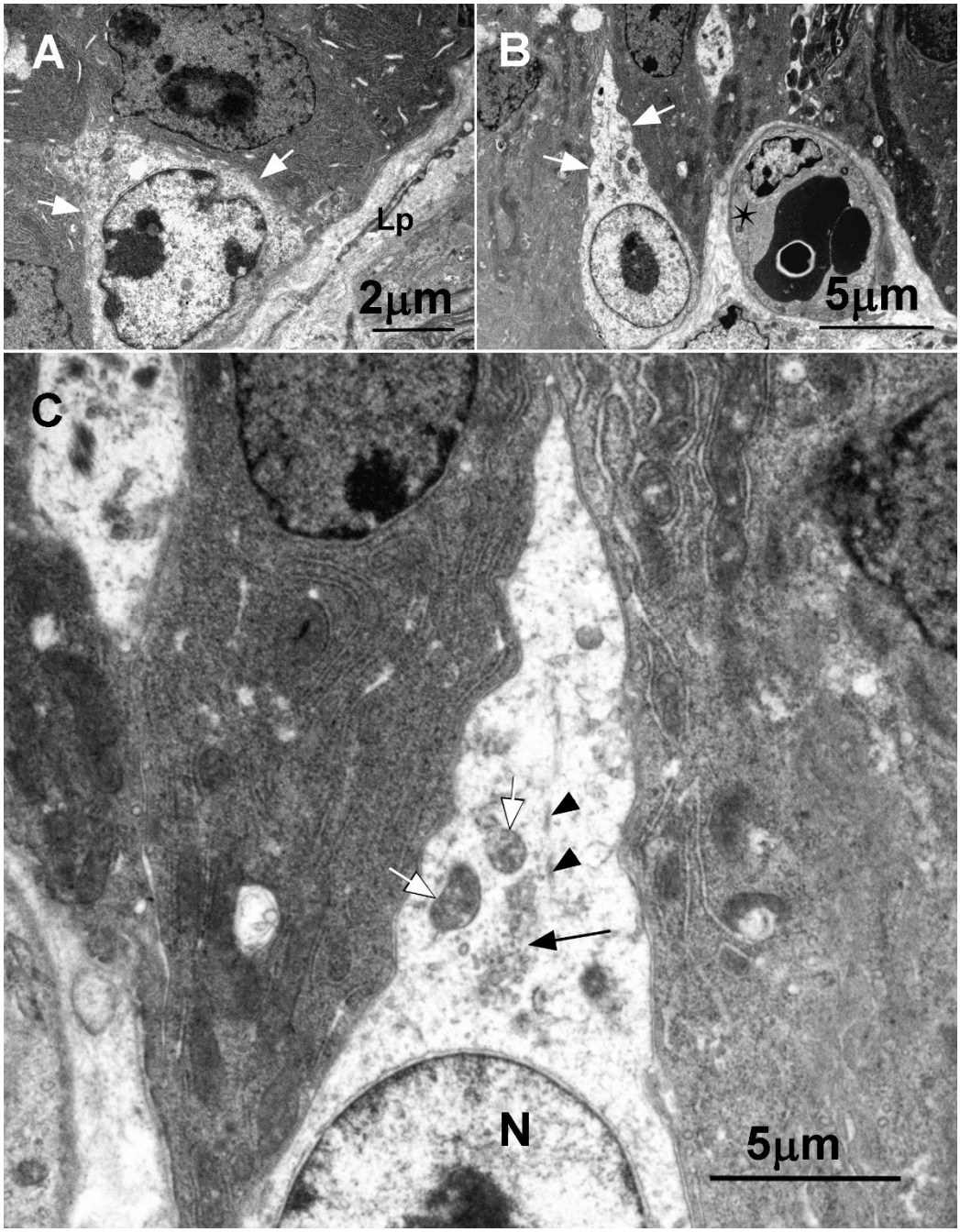

Figure 2.59: Transmission electron photomicrographs of the epithelial lining of a glandular unit in the cloacal gland of an adult quail.

A: Arrows: pyramidal-shaped basal cell. Lp: *lamina propria*.

B: Arrows: pyramidal-shaped basal cell. Asterisk: blood vessel.

C: Black arrow: Golgi complex. White arrows: mitochondria. Arrowheads: fibrils. N: nucleus.

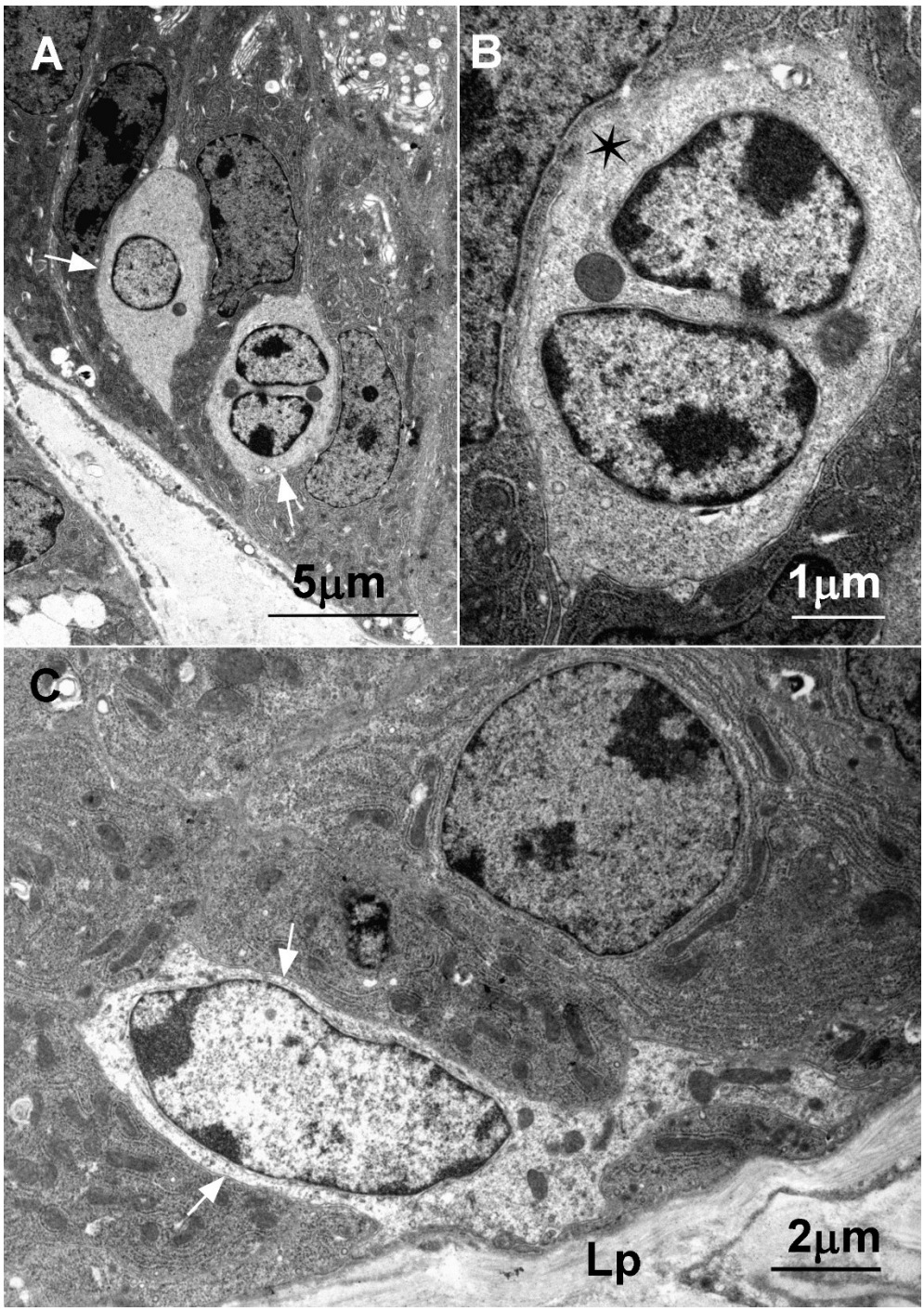

Figure 2.60: Transmission electron photomicrographs of the epithelial lining of glandular units in the cloacal gland of adult quails.

A: Arrows: oval-shaped basal cells with electron lucent cytoplasm.

B: Asterisk: oval-shaped cell undergoing mitosis.

C: arrows: elongated basal cell. Lp: *lamina propria*.

Degenerating cells

Cells undergoing apoptosis occurred either singly or in groups. The apoptotic process was identified in both type 1 and 2 cells.

Mitochondria partially or totally enclosed by dilated RER cisternae were observed in the early stages of apoptosis (Figures 2.61A & B). The nuclei in cells undergoing the early stages of apoptosis exhibited varying degrees of chromatin margination.

Cells undergoing the later stages of apoptosis were characterised by the presence of irregular-shaped nuclei, which exhibited chromatin condensation and margination. Degenerating nuclei were surrounded by prominent perinuclear spaces. In addition, the condensed cytoplasm of apoptotic cells contained dilated RER cisternae, as well as swollen, disintegrating mitochondria (Figure 2.62A). The apical regions of apoptotic cells exhibited cytoplasmic protrusions which were eventually released into the lumina of the glandular units (Figure 2.62B).

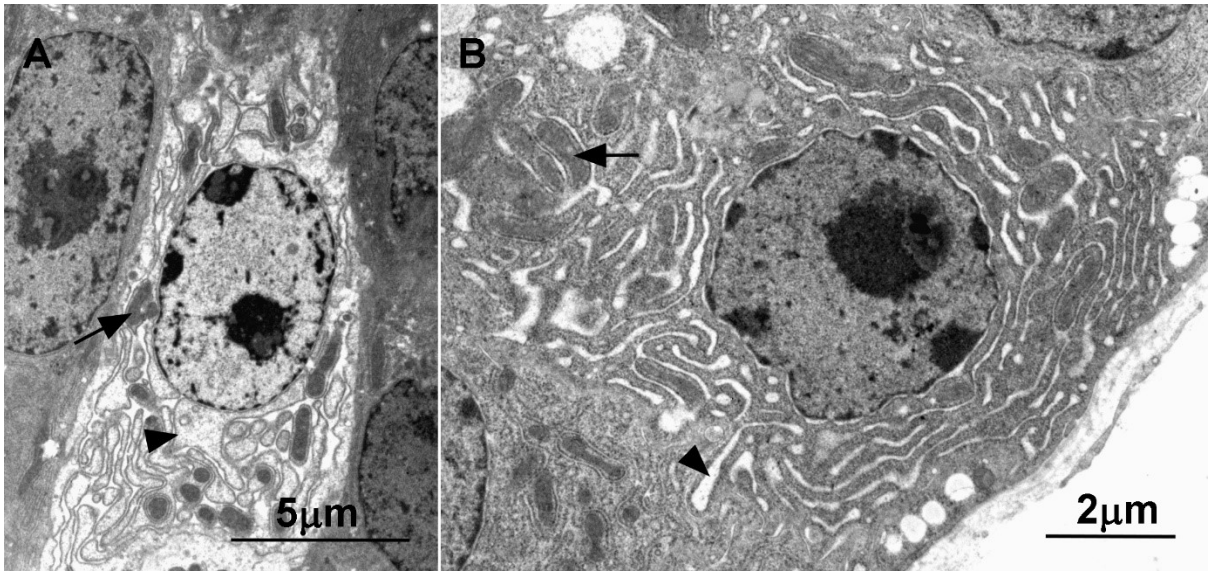

Figure 2.61: Transmission electron photomicrographs of apoptotic cells in the epithelial lining of glandular units in the cloacal gland of adult quails. Arrows: mitochondria. Arrowheads: dilated RER cisternae.

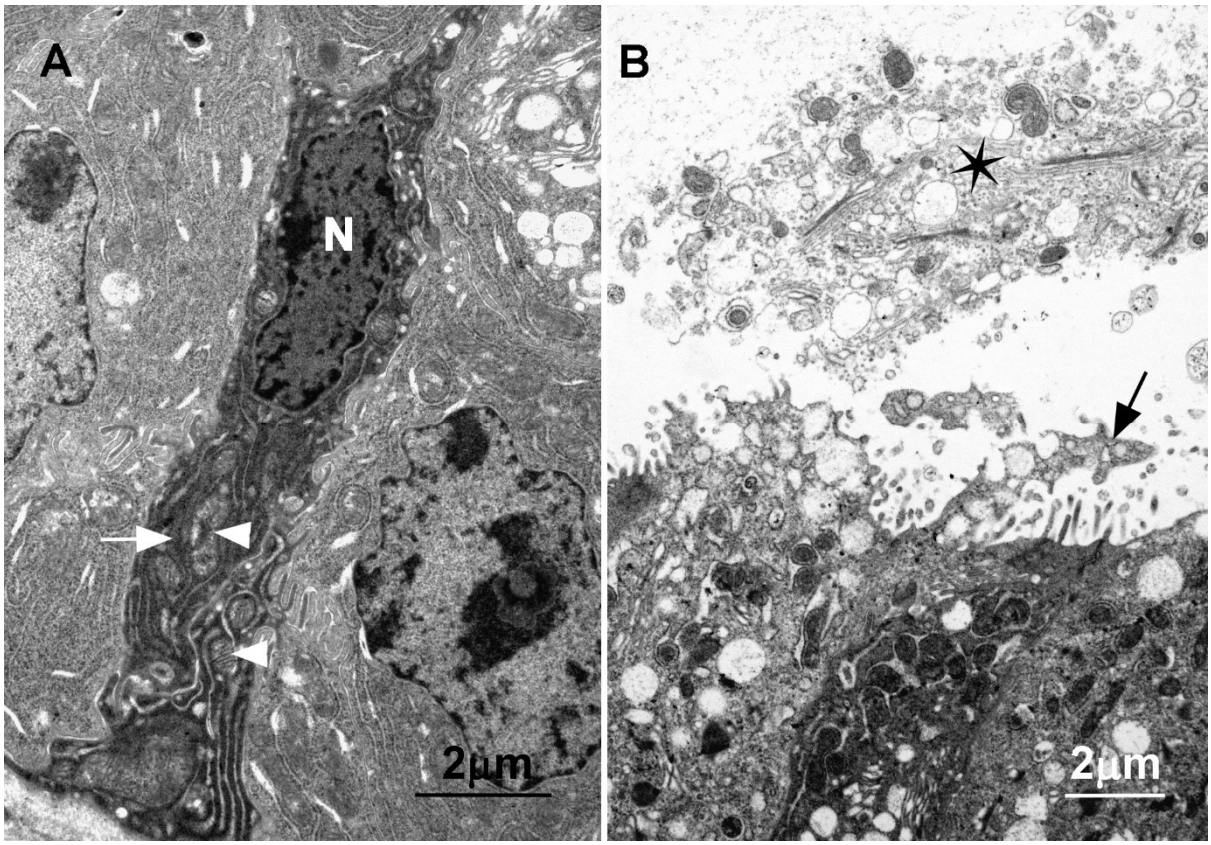

Figure 2.62: Transmission electron photomicrographs of the epithelial lining of glandular units in the cloacal gland of adult quails.

A: dilated RER cisterna (arrow) and disintegrating mitochondria (arrowheads) in an apoptotic cell. N: nucleus.

B: Arrow: cytoplasmic protrusion. Asterisk: cellular debris in the lumen of a glandular unit.

2.4 Discussion

2.4.1 Hormone analysis

The mean plasma testosterone concentrations in pre-pubertal, pubertal and adult birds were 0.04 ± 0.04 nmol/L, 1.05 ± 0.34 nmol/L and 2.73 ± 0.78 nmol/L, respectively, which indicated an increase in the levels of this hormone as sexual maturity progressed. These observations were in agreement with a previous report on hormonal levels in the maturing Japanese quail (Kouatcho *et al.*, 2015). It is known that testicular activity and testosterone production in the Japanese quail are stimulated by long daylengths (Sachs, 1967; Follett and Maung, 1978). Furthermore, Follett and Maung (1978) demonstrated a linear increase in plasma testosterone concentrations in quails that were exposed to increasing photoperiods. The increased photoperiods were shown to stimulate testicular growth. Follett and Maung (1978) further categorized testicular weights of birds into groups that would represent the testicular sizes that are usually observed in the different stages of development of Japanese quails. The relationship between testosterone concentration and testicular weights was analyzed, and plasma testosterone concentrations were found to be at their highest in quails exhibiting testicular weights that were equivalent to

those of adult individuals. In contrast, Rigaudiere *et al.* (1976) reported that pubertal male guinea pigs exhibited higher plasma testosterone levels than adult individuals. Rigaudiere *et al.* (1976) explained this as a consequence of the absence, in guinea pigs, of testosterone binding globulins. The absence of these testosterone binding globulins resulted in rapid hepatic catabolism and clearance of testosterone, and as a result, plasma testosterone concentrations were reduced in adult individuals.

In addition to photoperiods other factors such as the social dominance and interactions of the birds can cause variations in plasma testosterone concentrations (Follett and Maung, 1978; Abdul-Rahman *et al.*, 2015; Kempenaers *et al.*, 2008). Therefore, it is essential that such factors are taken into account in the interpretation of hormonal concentrations in birds.

2.4.2 Biometric data

The results of the current study showed that there were statistically significant differences in the bodyweights and cloacal gland areas in birds of all age groups investigated. While the cloacal gland areas of pre-pubertal, pubertal and adult birds in the current study measured 67.34 ± 12.34, 203.93 ± 13.63 and 268.30 ± 10.96 mm^2 respectively, previous studies reported cloacal gland areas of 32.1 ± 09 in pre-pubertal birds, which were 4-5 weeks old (Follett and Maung, 1978), 368.64 ± 64 in 6 week old pubertal birds (Khoobbakht *et al.*, 2018) and between 232.26 ± 1.21 and 480.82 ± 5.06 mm^2 in adult (more than 12 weeks of age) heavy bodyweight birds (Biswas *et al.*, 2010). Although the reported cloacal gland areas do not fall within the same ranges as those of the current study, the cloacal gland areas of the birds in the present investigation differed significantly with age. The cloacal gland area serves as an external indicator of testosterone production and testicular activity (Coil and Wetherbee, 1959; McFarland *et al.*, 1968; Siopes and Wilson, 1975). Thus, cloacal

gland area is an important endpoint in toxicological studies (Halldin, 2005). Pearson's correlation coefficients showed positive and statistically significant correlations between plasma testosterone concentrations and the biometric parameters of the quails studied. These results suggest that plasma testosterone levels positively affect the body weight, as well as cloacal gland area. These findings are consistent with those reported by Biswas *et al*. (2007) on the cloacal glands of quails.

2.4.3 Haematoxylin and eosin-stained sections

The present study has demonstrated the histological structure of the cloacal gland in pre-pubertal, pubertal and adult birds during a period of decreasing daylength. In pre-pubertal birds, the cloacal gland was divided into tubular glandular profiles separated by wide areas of dense irregular connective tissue. Each glandular unit in pubertal and adult birds corresponded to the simple tubular profiles that were observed in immature birds.

The glandular units of the cloacal gland in pubertal and adult quails were lined by a secretory, simple columnar epithelium which projected into the lumina of the glandular units as primary and secondary folds. These findings are in agreement with previous reports on the histological structure of the cloacal gland in sexually mature male Japanese quails (Coil and Wetherbee, 1959; McFarland *et al.*, 1968; Klemm *et al.*, 1973).

In the current study degenerating glandular units were observed in the cloacal glands of pubertal and adult quails. This finding is not surprising as the birds were sampled during a period of decreasing daylength. It is known that the level of testicular activity in the Japanese quail is determined by daylength (Nicholls *et al*.,

1973; Artoni *et al*., 1997). Long daylengths stimulate testicular growth, while short daylengths lead to the regression of the testes (Nicholls *et al*., 1973). Due to the fact that the cloacal gland is an androgen-dependent gland, any change in testicular activity affects its morphology and physiology (Siopes and Wilson, 1975; Massa *et al.*, 1980; Satterlee and Marin, 2004; Biswas *et al.*, 2007). Thus, the cloacal gland has been shown to undergo regression when quails reared under conditions of long daylengths are subjected to short daylengths (Sachs, 1967).

2.4.4 Morphometry of secretory epithelial cells

Statistically significant differences in epithelial cell heights were observed between pre-pubertal and pubertal birds, as well as between pre-pubertal and adult birds. No significant differences were observed between pubertal and adult birds. These results indicate a similarity in the heights of epithelial cells in the cloacal glands of pubertal and adult birds. In this study, the heights of the cloacal gland epithelial cells in pubertal and adult birds were 24.68 ± 0.45 µm and 24.54 ± 0.32 µm, respectively. These measurements correspond favourably with the epithelial cell height values reported by Klemm *et al.* (1973). The similarities in epithelial cell heights observed in pubertal and adult birds could be an indication that the cloacal gland epithelial cells reach their maximum heights in the pubertal stages.

Pearson's correlation test was used to determine the correlation between epithelial cell heights and testosterone concentrations in each age group. The analysis revealed a weak positive correlation (r=0.42), that was not statistically significant. These results suggest that testosterone levels do not affect the heights of epithelial cells in the cloacal gland. These findings are contradictory to observations reported by Sachs (1967). Sachs (1967) reported a regression in cloacal gland epithelial cells with a decrease in testosterone concentration caused by a change in photoperiod.

2.4.5 Periodic acid Schiff and alcian blue histochemistry

A positive reaction with periodic acid Schiff (PAS) and alcian blue stains was observed in the simple columnar secretory cells of the cloacal gland in pre-pubertal, pubertal and adult birds. Positive alcian blue staining indicated the presence of acidic mucopolysaccharides, while a positive PAS reaction signified the occurrence of neutral mucopolysaccharides. These findings were consistent with those reported by McFarland and colleagues (1968) on the presence of acidic and neutral mucopolysaccharides in the secretory cells of the quail cloacal gland.

In pre-pubertal, pubertal and adult birds, the cells lining the glandular units remained PAS positive after cloacal gland tissue sections were treated with diastase prior to staining with PAS. These results suggested that the cloacal gland secretion was not composed primarily of glycogen. The findings of the current study are in agreement with those of Coil and Wetherbee (1959), as well as Klemm *et al.* (1973).

2.4.6 TUNEL staining and morphometry

The cloacal glands of pre-pubertal birds displayed negative TUNEL staining, indicating the absence or low incidence of apoptotic cells. Several apoptotic cells were observed in pubertal birds, while numerous apoptotic cells were present in the cloacal glands of adult birds. As shown in this study, the levels of testosterone in the pre-pubertal birds was negligible compared to the levels in pubertal and adult birds. This finding suggests that the integrity of the cloacal gland in pre-pubertal birds is not significantly influenced by testosterone. Therefore, at this stage of development a decrease in daylength and presumably a decrease in circulating testosterone levels does not result in the regression of the cloacal gland. The presence of apoptotic cells in the pubertal and adult cloacal glands was probably due to the fact that the glands were sampled during periods of decreasing daylengths. During decreasing

daylengths the activity of the testes declines resulting in a reduction in circulating testosterone levels (Sachs, 1967). Due to the fact that the cloacal gland is an androgen-dependent organ, a decrease in testosterone levels results in the regression of the cloacal gland.

2.4.7 Androgen receptor immunohistochemistry and statistics

The current study showed the distribution of the androgen receptor in the cloacal glands of pre-pubertal, pubertal and adult birds. In pre-pubertal, pubertal and adult birds, androgen receptors were located in the secretory cells that lined the glandular units of the cloacal glands. These findings are in agreement with previous reports on the immunolocalization of the androgen receptor in the cloacal glands of 20 and 80 day old male Japanese quails which had been subjected to a photoperiod of 14L: 10D (Kaku *et al.*, 1993). These results indicate that epithelial secretory cells are the main targets for testosterone in the cloacal gland. In the current study fibroblasts within the connective tissue compartment of the cloacal gland exhibited varying intensities of androgen receptor immunoreactivity. Androgen receptor immunostaining has previously been demonstrated in fibroblasts of the prostate gland in the rat (Takeda *et al.*, 1990). Cano *et al.* (2007) suggested that the presence of androgen receptors in fibroblasts of the prostate gland was essential for the normal differentiation of this organ.

In the current study, smooth muscle and endothelial cells of blood vessels exhibited positive immunostaining for the androgen receptor. Liu *et al.* (2003) reported that vascular endothelial and smooth muscle cells contain functional androgen receptors. The observation of androgen receptors in the smooth muscle and endothelial cells of blood vessels are consistent with the role of androgens in angiogenesis (Abu *et al.*, 1997).

Pre-pubertal birds showed weak to moderate immunoreactivity in the nuclei of the secretory cells, while the cell cytoplasm displayed weak immunoreactivity. In pubertal birds, moderate immunoreactivity for the androgen receptor was observed in the nuclei of the secretory cells, while the cell cytoplasm displayed weak immunostaining. In adult birds, nuclei of the secretory cells showed strong immunostaining while the cytoplasm exhibited weak immunostaining. The presence of weak cytoplasmic androgen receptor immunostaining is consistent with observations made by Ungefroren *et al.* (1997) in a study on the human epididymis.

2.4.8 Transmission electron microscopy

The current study investigated the ultrastructure of the cells that constitute the lining of the glandular units of cloacal glands in pre-pubertal, pubertal and adult birds. Due to the fact that there is limited literature on the ultrastructure of the cloacal gland, the results of the current study will be related to those of similar, androgen-dependent structures, notably the prostate and Harderian glands.

Transmission electron microscopy revealed that the glandular units of pre-pubertal birds were lined by electron-dense secretory cells. However, in pubertal birds, the glandular units were lined by cells of low, intermediate and high electron density, while in adult birds the secretory cells were of low and intermediate electron density. In the current study, cloacal glands of pubertal and adult birds were found to contain different cell types (types 1-3). The presence of different cell types was reported in several studies on the prostate and the Harderian glands (Woodhouse and Rhodin, 1963; Aughey, 1973; Siwela and Tam, 1984; Wong *et al.*, 1985; Djeridane, 1992; McGadey *et al.*, 1992; Lóapez *et al.*, 1993). Although the presence of different cell

types was reported in these glands, the defining characteristics of the cells were dissimilar. In the prostate and Harderian glands, these characteristics ranged from the nature and size of the secretory vacuoles, nuclei size, microvilli distribution, to the presence of cytoplasmic polytubular bundles. However, in the current study the defining characteristic of the cell types was the cytoplasmic electron density. In the current study, the varying cell types observed in pubertal and adult birds were of different stages of development. Although a previous report on the ultrastructure of the secretory cells of the cloacal gland in male and female quails by Ochs (1979) did not reveal the presence of different types of secretory cells, the occurrence at varying secretory stages of secretory cells was reported.

In the current study, types 1 and 2 secretory cells of the adult cloacal glands exhibited 3 and 4 different stages of the secretory cycle, respectively. Stages 1 and 2 of type 1 and 2 cells in adult cloacal glands were indicative of the secretory product synthesis phases. The nuclei of these cells were euchromatic, indicating active transcription and synthesis of secretory product. The mitochondria were in close association with the RER profiles. This observation was consistent with the report of the presence of mitochondria that were encircled by RER profiles (Ochs, 1979). Giorgi *et al.* (2009) reported that the mitochondrial enclosure by the RER profiles are due to the shared regulatory factors that these organelles possess, as well as the mutually regulated functions that they have in healthy and apoptotic cells. In the current study, multiple Golgi complexes were only observed in stage 2 and not in stage 1 cells. However, Ochs (1979) reported the presence of Golgi complexes in stage 1 secretory cells. The stage 1 cells that Ochs (1979) reported did not correlate with those of the current study in that, the cells did not have tapered apices and exhibited short microvilli that were in contact with the lumina of the gland. In the

current study, cells in stages 1 and 2 displayed apices that did not reach the lumen of the glandular units. The fact that the apices of the secretory cells in these two stages did not reach the glandular lumen suggested that only the synthesis of the secretory product occurs and no secretory discharge ensues. Although Ochs (1979) reported the presence of a few mature secretory droplets and the protrusion into the glandular lumen of the apical regions of the secretory cells, there was no documentation of active secretion. These cells contained basally situated euchromatic nuclei, RER encircled elongate mitochondria, multiple Golgi complexes, as well as a few secretory droplets and condensing vacuoles. The apical border was lined by short microvilli that protruded into the glandular lumen. These cells could be related to the type 2 stage 2 cells found in the adult birds, except for the fact that these cells had tapered apices and did not extend into the glandular lumen. Furthermore, cells in the first stage of the secretory cycle in the Harderian gland also did not display any active secretion (Woodhouse and Rhodin, 1963). These cells displayed few secretory droplets in the apical and basal regions that were retained from a previous cycle, as well as swollen mitochondria resembling those of the cells in stage 3.

In type 2 cells that were in stage 2 of the secretory cycle, clear vacuoles that were different from the secretory vacuoles that usually contained a flocculent material of intermediate electron density, were observed in the infranuclear region. The differences observed in vacuoles of the secretory cells could be as a result of different mechanisms and structures involved in the formation of the vacuoles. These findings have a similarity to a report made by Wong *et al.* (1985) regarding the ultrastructure of epithelial cells in the prostate gland of the mouse. Wong and colleagues (1985) reported the presence of two types of secretory granules, G1 and

G2. Wong and colleagues (1985) postulated that one type of secretory granule was formed in the Golgi complex, while the other type was produced in the rough endoplasmic reticulum. In the current study, the secretory vacuoles observed among rough endoplasmic reticula in the infranuclear regions of the secretory cells, could indicate that the rough endoplasmic reticula do produce secretory vacuoles.

Stages 3 and 4 of type 1 and 2 cells in adult cloacal glands demonstrated active secretory activity. These stages were consistent with stages 2 and 3 of the secretory cycle described in the secretory cells of the cloacal gland of male and female quails, as well as in the rat Harderian gland (Woodhouse and Rhodin, 1963; Ochs, 1979). The apices of cells in these stages of the secretory process extended to the luminal surface and displayed pits which were an indication of a recent release of secretory product. McGadey *et al.* (1992) reported the presence of similar pits, which served as sites of lipid vacuole secretion in the secretory cells of the Harderian gland in the hamster. In the current investigation cytoplasmic protrusions at various stages of detachment were observed in the cloacal glands of pubertal and adult birds. The presence of such protrusions suggested that the secretory cells exhibited a form of apocrine release. These findings are in agreement with previous reports regarding the mode of secretion of the Harderian gland in the Albino mouse (Cohn, 1955). Johnston *et al.* (1985) further reported the occurrence of an apocrine mode of secretion in the Harderian gland secretory cells of the mouse. In contrast, due to insufficient evidence to support the notion of an apocrine secretory process in the Harderian gland of the hamster, McGadey *et al.* (1992) suggested that a merocrine mechanism existed in the gland.

Leukocytes and plasma cells were observed among basal cells of the epithelial lining of the glandular units. The presence of leukocytes and plasma cells within the lining

of the glandular units could be an inflammatory response triggered by the apoptotic processes occurring within the secretory cells. Leukocytes are cellular components of the blood that defend the body against infection and diseases by ingesting foreign materials and cellular debris (Augustyn, 2018), while plasma cells are short-lived cells that are derived from a type of leukocyte, the B cell, that produce antibodies (Augustyn, 2016). Although the process of apoptosis is said to be non-inflammatory, there have been reports that have refuted this concept (Rock and Kono, 2008).

In the current study, pyramidal, oval and elongated basal cells were observed in the epithelial lining of glandular units. The various basal cell types observed could be precursor cells of the different secretory cell types observed in pubertal and adult birds. However, El-Alfy *et al.* (2000) did not notice any stem cell characteristics in the basal cells of the human prostate. Furthermore, El-Alfy *et al.* (2000) reported that the cells displayed a moderate number of organelles, a relatively large Golgi apparatus and the accumulation of glycogen particles, all of which are indicators of an actively differentiating cell. El-Alfy *et al.* (2000) opined that the basal cells could be responsible for the regulation of the luminal cells. Due to the absence of extracellular space between basal cells, the molecular traffic from the stroma to the luminal cells could trigger basal cells to produce substances that function in regulating the activity of luminal cells.

3.0 Chapter 3

3.1 General discussion and conclusion

The aim of the current study was to establish a correlation between gross anatomical, histomorphological, and ultrastructural observations of the cloacal gland and plasma testosterone levels in pre-pubertal, pubertal and adult Japanese quails during a period of decreasing daylength. Although several authors have described the histological (Coil and Wetherbee, 1959; McFarland *et al.*, 1968; Klemm *et al.*, 1973) and ultrastructural (Ochs, 1979) morphology of the cloacal gland in sexually active male and female individuals, the current study appears to be the first to describe the histological and ultrastructural alterations occurring in the cloacal gland with maturity of the birds.

In pre-pubertal birds, cloacal glands were underdeveloped and appeared as lobes divided into narrow, tubular glandular units by wide areas of connective tissue. As the birds matured in the pubertal and adult stages, the wide areas of connective tissue separating the glandular units were reduced to thin connective tissue trabeculae. The glandular lobes were indiscernible and the glandular units were lined by columnar secretory cells that formed primary and secondary folds. PAS and alcian blue staining of the cloacal gland sections revealed that the secretory cells lining the glandular units produce acidic and neutral mucopolysaccharides. These findings were in agreement with those of McFarland *et al.* (1968) on the presence of acidic and neutral mucopolysaccharides in the secretory cells of the quail cloacal gland. The results obtained when the cloacal gland sections were treated with diastase before staining with PAS, indicated that the material within secretory cells was not predominantly glycogen. Coil and Wetherbee (1959), as well as Klemm *et*

al. (1973) made similar observations in studies on the cloacal gland of the Japanese quail.

TUNEL staining revealed the presence of apoptotic cells in pubertal and adult cloacal glands, with maximal numbers observed in adults. This finding is not surprising as the birds were sampled during a period of decreasing daylength, which in the Japanese quail is associated with decreased testicular activity and a reduction in testosterone levels.

Ultrastructural observations revealed that the cloacal glands contain different types of secretory cells with varying degrees of electron density and secretory activity. It is possible that each cell type is responsible for the production of particular components of the mucosubstances present in cloacal gland form. It was also noted that the secretory cells exhibited apocrine release.

The current study further described androgen receptor immunostaining of secretory cells of cloacal glands in relation to plasma testosterone concentrations observed in pre-pubertal, pubertal and adult birds. It was noted that as the birds matured androgen receptor immunostaining increased. This finding suggests that testosterone upregulates the expression of androgen receptors in the cloacal glands of Japanese quails.

References

ABDUL-RAHMAN, I., ROBINSON, J., OBESE, F., JEFFCOATE, I. & AWUMBILA, B. 2015. Effects of season on the reproductive organ and plasma testosterone concentrations in guinea cocks (*Numida meleagris*). *Poultry science,* 95**,** 636-644.

ABU, E., HORNER, A., KUSEC, V., TRIFFITT, J. & COMPSTON, J. 1997. The localization of androgen receptors in human bone. *The Journal of Clinical Endocrinology & Metabolism,* 82**,** 3493-3497.

ADKINS-REGAN, E. K. 1999. Foam produced by male Coturnix quail: What is its function? *The Auk,* 116**,** 184-193-184-193.

ADKINS, E. K. & ALDER, N. T. 1972. Hormonal control of behavior in the Japanese quail. *Journal of comparative and physiological psychology,* 81**,** 27.

ARTONI, S.M.B., ORSI, A.M., CARVALHO, T.L.L. & LOPES, R.A. 1997. The annual testicular cycle of the domestic quail (*Coturnix coturnix japonica*). *Anatomia Histologia Embryologia*. 26, 337-339.

AUGHEY, E. 1973. The ultrastructure of the prostrate gland in the cat. *Journal of reproduction and fertility,* 33**,** 351-352.

AUGUSTYN, A., BAVER, P., DAIGNAM, B., ELDRIDGE, A., GREGERSON, E., LEUBERING, J.E., MCKENNA, A., PETRUZZELLO, M., RAFFERTY, J.P., RAY, M., ROGERS, K., TIKKANEN, A., WALLENFELDT, J., ZEIDAN, A., ZELAZKO, A. 2016. *Plasma cell* [Online]. Available: https://www.britannica.com/science/plasma-cell [Accessed 19 November 2018].

AUGUSTYN, A., BAVER, P., DAIGNAM, B., ELDRIDGE, A., GREGERSON, E., LEUBERING, J.E., MCKENNA, A., PETRUZZELLO, M., RAFFERTY, J.P., RAY, M., ROGERS, K., TIKKANEN, A., WALLENFELDT, J., ZEIDAN, A., ZELAZKO, A. 2018. *White blood cells.* [Online]. Available: https://www.britannica.com/science/white-blood-cell [Accessed 19 November 2018].

BAKST, M. R. & CECIL, H. C. 1985. A microscopic examination of the male turkey proctodeal gland. *Journal of Morphology,* 186**,** 361-368.

BISWAS, A., MOHAN, J. & SASTRY, K. V. H. 2013. Effect of dietary supplementation of vitamin E on production peformance and some biological characteristics of cloacal foam in male Japanese quail. *Animal Reproduction Science,* 140**,** 92-96-92-96.

BISWAS, A., RANGANATHA, O. S. & MOHAN, J. 2010. The effect of different foam concentrations on sperm motility in Japanese quail. *Veterinary Medicine International***,** 1-4-1-4.

BISWAS, A., RANGANATHA, O. S., MOHAN, J. & SASTRY, K. V. H. 2007. Relationship of cloacal gland with testes, testosterone and fertility in different lines of male Japanese quail. *Animal Reproduction Science,* 97**,** 94-102-94-102.

CANO, P., GODOY, A., ESCAMILLA, R., DHIR, R. & ONATE, S. A. 2007. Stromal-epithelial cell interactions and androgen receptor-coregulator recruitment is altered in the tissue microenvironment of prostate cancer. *Cancer research,* 67**,** 511-519.

CHANG, C., KOKONTIS, J. & LIAO, S. 1988a. Molecular cloning of human and rat complementary DNA encoding androgen receptors. *Science,* 240**,** 324-326.

CHANG, C., KOKONTIS, J. & LIAO, S. 1988b. Structural analysis of complementary DNA and amino acid sequences of human and rat androgen receptors. *Proceedings of the National Academy of Sciences,* 85**,** 7211-7215.

CHELMONSKA, B., JERYSZ, A., LUKASZEWICZ, E. & KOWALCZYK, A. 2006. The effect of proctodeal gland foam diluent and dimetylacetamide addition on morphology and fertilizing ability of Japanese quail (*Coturnix japonica*) spermatozoa. *Journal of Poultry Science,* 43**,** 54-59-54-59.

CHENG, K. M., MCINTYRE, R. F. & HICKMAN, A. R. 1989a. Proctodeal gland foam enhances competitive fertilization in domestic Japanese quail. *The Auk,* 106**,** 286-291-286-291.

CHENG, K. M., HICKMAN, A. R. & NICHOLS, C. R. 1989b. Role of proctodeal gland foam of male Japanese quail in natural copulation. *The Auk,* 106**,** 279-285-279-285.

COHN, S. A. 1955. Histochemical observations on the Harderian gland of the albino mouse. *Journal of Histochemistry & Cytochemistry,* 3**,** 342-353.

COIL, W. H. & WETHERBEE, D. K. 1959. Observations on the cloacal gland of the Eurasian quail, Coturnix coturnix. *The Ohio Journal of Science,* 59**,** 268-270-268-270.

DAVEY, R. A. & GROSSMANN, M. 2016. Androgen receptor structure, function and biology: from bench to bedside. *The Clinical Biochemist Reviews,* 37**,** 3.

DE PERGOLA, G., XU, X., YANG, S., GIORGINO, R. & BJORNTORP, P. 1990. Up-regulation of androgen receptor binding in male rat fat pad adipose precursor cells exposed to testosterone: study in a whole cell assay system. *The Journal of steroid biochemistry and molecular biology,* 37**,** 553-558.

DJERIDANE, Y. 1992. The harderian gland of desert rodents: a histological and ultrastructural study. *Journal of anatomy,* 180**,** 465.

DOHLE, G., SMIT, M. & WEBER, R. 2003. Androgens and male fertility. *World journal of urology,* 21**,** 341-345.

EL-ALFY, M., PELLETIER, G., HERMO, L. S. & LABRIE, F. 2000. Unique features of the basal cells of human prostate epithelium. *Microscopy research and technique,* 51**,** 436-446.

EVANS, R. M. 1988. The steroid and thyroid hormone receptor superfamily. *Science,* 240**,** 889-895.

FAROOQ, U., CHO, S., RYBNIK-TRZASKOWSKA, P., SINGH, R. & MALECKI, I. 2015. Effect of proctodeal gland foam on sperm kinetics in Japanese quail (*Coturnix japonica*). *Theriogenology,* 83**,** 162-167.

FOLLETT, B. & MAUNG, S. 1978. Rate of testicular maturation, in relation to gonadotrophin and testosterone levels, in quail exposed to various artificial photoperiods and to natural daylengths. *Journal of Endocrinology,* 78**,** 267-280.

FUJIHARA, N. 1992. Accessory reproductive fluids and organs in male domestic birds. *World's Poultry Science Journal,* 48**,** 39-56.

GIORGI, C., DE STEFANI, D., BONONI, A., RIZZUTO, R. & PINTON, P. 2009. Structural and functional link between the mitochondrial network and the endoplasmic reticulum. *The international journal of biochemistry & cell biology,* 41**,** 1817-1827.

HALLDIN, K. 2005. Impact of endocrine disrupting chemicals on reproduction in Japanese quail. *Domestic animal* endocrinology, 29, 420-429.

HEINLEIN, C. A. & CHANG, C. 2002. Androgen receptor (AR) coregulators: an overview. *Endocrine reviews,* 23**,** 175-200.

HIORT, O. 2002. Androgens and puberty. *Best Practice & Research Clinical Endocrinology & Metabolism,* 16**,** 31-41.

HOWARD, L. 2004. "Galliformes" (On-line), Animal Diversity Web.

JENSTER, G., VAN DER KORPUT, H. A., VAN VROONHOVEN, C., VAN DER KWAST, T. H., TRAPMAN, J. & BRINKMANN, A. O. 1991. Domains of the human androgen receptor involved in steroid binding, transcriptional activation, and subcellular localization. *Molecular Endocrinology,* 5**,** 1396-1404.

JOHNSTON, H., MCGADEY, J., THOMPSON, G., MOORE, M., BREED, W. & PAYNE, A. 1985. The Harderian gland, its secretory duct and porphyrin content in the Plains mouse (*Pseudomys australis*). *Journal of anatomy,* 140**,** 337.

KAKU, A., CHANG, C., TAMURA, T., OKAMOTO, T. & YASHIMURA, Y. 1993. Immunolocalization of androgen receptor in the cloacal gland of male Japanese quail (*Coturnix coturnix japonica*). *Japanese Poultry Science,* 30**,** 413-418-413-418.

KAYANG, B. B., VIGNAL, A., INOUE-MURAYAMA, M., MIWA, M., MONVOISIN, J. L., ITO, S. & MINVIELLE, F. 2004. A first-generation microsatellite linkage map of the Japanese quail. *Animal Genetics,* 35**,** 195-200.

KELLER, E. T., ERSHLER, W. B. & CHANG, C. 1996. The androgen receptor: a mediator of diverse responses. *Front Biosci,* 1**,** d59-71.

KEMPENAERS, B., PETERS, A. & FOERSTER, K. 2008. Sources of individual variation in plasma testosterone levels. *Philosophical Transactions of the Royal Society of London B: Biological Sciences,* 363**,** 1711-1723.

KHOOBBAKHT, Z., MOHAMMADI, M., MEHR, M. R.-A., MOHAMMADGHASEMI, F. & SOHANI, M. M. 2018. Comparative effects of zinc oxide, zinc oxide nanoparticle and zinc-methionine on hatchability and reproductive variables in male Japanese quail. *Animal reproduction science,* 192**,** 84-90.

KLEMM, R. D., KNIGHT, C. E. & STEIN, C. 1973. Gross and microscopic morphology of the *glandula proctodealis* (foam gland) of *Coturnix c. japonica* (Aves). *Journal of Morphology,* 141**,** 171-184-171-184.

KOUATCHO, F. D., KENFACK, A., NGOULA, F. & TEGUIA, A. 2015. Sexual maturity prediction based on hormonal profiles, testes and semen characteristics in male Coturnix quail (Garsault, 1764) in the Western Highlands of Cameroon. *Int. J. Agr. and Agric. Res,* 7**,** 143-154.

LALLOUE, F. L. & AYER-LE LIEVRE, C. S. 2003. Experimental study of early olfactory neuron differentiation and nerve formation using quail-chick chimeras. *International Journal of Developmental Biology,* 49**,** 193-200.

LE DOUARIN, N. & KALCHEIM, C. 1999. *The neural crest*, Cambridge university press.

LEE, H.-J. & CHANG, C. 2003. Recent advances in androgen receptor action. *Cellular and Molecular Life Sciences CMLS,* 60**,** 1613-1622.

LIU, P. Y., DEATH, A. K. & HANDELSMAN, D. J. 2003. Androgens and cardiovascular disease. *Endocrine reviews,* 24**,** 313-340.

LÓAPEZ, J., TOLIVIA, J., ALVAREZ-URÍA, M., PAYNE, A., MCGADEY, J. & MOORE, M. 1993. An electron microscopic study of the Harderian gland of the Syrian hamster with particular reference to the processes of formation and discharge of the secretory vacuoles. *The Anatomical Record,* 235**,** 342-352.

LUBAHN, D. B., BROWN, T. R., SIMENTAL, J. A., HIGGS, H. N., MIGEON, C. J., WILSON, E. M. & FRENCH, F. S. 1989. Sequence of the intron/exon junctions of the coding region of the human androgen receptor gene and identification of a point mutation in a family with complete androgen insensitivity. *Proceedings of the National Academy of Sciences,* 86**,** 9534-9538.

MASSA, R., DAVIES, D. & BOTTONI, L. 1980. Cloacal gland of the Japanese quail: androgen dependence and metabolism of testosterone. *Journal of Endocrinology,* 84**,** 223-230.

MCFARLAND, L., WARNER, R., WILSON, W. & MATHER, F. 1968. The cloacal gland complex of the Japanese quail. *Experientia,* 24**,** 941-943.

MCGADEY, J., JOHNSTON, H. & PAYNE, A. 1992. The hamster harderian gland: a combined scanning and transmission electron microscopic investigation. *Journal of anatomy,* 180**,** 127.

NICHOLLS, T.J., SCANES, C.G. & FOLLETT, B.K. 1973. Plasma and pituitary luteinizing hormone in Japanese quail during photoperiodically induced gonadal growth and regression. *General and comparative endocrinology*, 21, 84-98.

OCHS, T. J. 1979. Ultrastructure of the secretory cells of the proctodeal gland in male and female Coturnix coturnix japonica (Aves). Master of Science, Kansas State University.

OTTINGER, M. A. & BRINKLEY, H. J. 1979. Testosterone and sex related physical characteristics during the maturation of the male Japanese quail (Coturnix coturnix japonica). *Biology of reproduction,* 20**,** 905-909.

OTTINGER, M. A., ABDELNABI, M., LI, Q., CHEN, K., THOMPSON, N., HARADA, N., VIGLIETTI-PANZICA, C. & PANZICA, G. C. 2004. The Japanese quail: a model for studying reproductive aging of hypothalamic systems. *Experimental gerontology,* 39**,** 1679-1693.

OTTINGER, M., QUINN JR, M., LAVOIE, E., ABDELNABI, M., THOMPSON, N., HAZELTON, J., WU, J., BEAVERS, J. & JABER, M. 2005. Consequences of endocrine disrupting chemicals on reproductive endocrine function in birds: establishing reliable end points of exposure. *Domestic animal endocrinology,* 29**,** 411-419.

QUARMBY, V. E., YARBROUGH, W. G., LUBAHN, D. B., FRENCH, F. S. & WILSON, E. M. 1990. Autologous down-regulation of androgen receptor messenger ribonucleic acid. *Molecular endocrinology,* 4**,** 22-28.

QUINN, M. J. 2012. Avian behavioral toxicity methods for use with the Japanese Quail Coturnix japonica as a model species. *Avian Ecology and Behavior,* 21**,** 41-50-41-50.

RIGAUDIERE, N., PELARDY, G., ROBERT, A. & DELOST, P. 1976. Changes in the concentrations of testosterone and androstenedione in the plasma and testis of the guinea-pig from birth to death. *Journal of reproduction and fertility,* 48**,** 291-300.

ROCK, K. L. & KONO, H. 2008. The inflammatory response to cell death. *Annu. Rev. pathmechdis. Mech. Dis.,* 3**,** 99-126.

RUIZEVELD DE WINTER, J., TRAPMAN, J., VERMEY, M., MULDER, E., ZEGERS, N. D. & VAN DER KWAST, T. H. 1991. Androgen receptor expression in human tissues: an immunohistochemical study. *Journal of Histochemistry & Cytochemistry,* 39**,** 927-936.

SACHS, B. D. 1967. Photoperiodic control of the cloacal gland of the Japanese quail. *Science,* 157**,** 201-203.

SATTERLEE, D. G. & MARIN, R. H. 2004. Photoperiod-induced changes in cloacal gland physiology and testes weight in male Japanese quail selected for divergent adrenocortical responsiveness. *Poultry science,* 83**,** 1003-1010.

SEIWERT, C. M. & ADKINS-REGAN, E. 1998. The foam production system of the male Japanese quail: characterization of structure and function. *Brain, behavior and evolution,* 52**,** 61-80.

SHAN, L.-X., RODRIGUEZ, M. C. & JÄNNE, O. A. 1990. Regulation of androgen receptor protein and mRNA concentrations by androgens in rat ventral prostate and seminal vesicles and in human hepatoma cells. *Molecular Endocrinology,* 4**,** 1636-1646.

SINGH, R. P., SASTRY, K. V. H., PANDEY, N. K., SINGH, K. B., MALECKI, I. A., FAROOQ, V., MOHAN, J., SAXENA, V. K. & MOUDGAL, R. P. 2012. The role of the male cloacal gland in the reproductive success in Japanese quail (*Coturnix japonica*). *Reproduction, Fertility and Development,* 24**,** 405-409-405-409.

SINGH, R. P., SASTRY, K. V. H., SHIT, N., PANDEY, N. K., SINGH, K. B., MOHAN, J. & MOUDGAL, R. P. 2011. Cloacal gland foam enhances motility and disaggregation of spermatozoa in Japanese quail (*Coturnix japonica*). *Theriogenology,* 75**,** 563-569-563-569.

SIOPES, T. D. & WILSON, W. O. 1975. The cloacal gland—an external indicator of testicular development in coturnix. *Poultry Science,* 54**,** 1225-1229.

SIWELA, A. A. & TAM, W. 1984. Ultrastructural changes in the prostate gland of a seasonally breeding mammal, the grey squirrel (Sciurus carolinensis Gmelin). *Journal of anatomy,* 138**,** 153.

TAKEDA, H., CHODAK, G., MUTCHNIK, S., NAKAMOTO, T. & CHANG, C. 1990. Immunohistochemical localization of androgen receptors with mono-and polyclonal antibodies to androgen receptor. *Journal of Endocrinology,* 126**,** 17-NP.

TAKEDA, H., NAKAMOTO, T., KOKONTIS, J., CHODAK, G. W. & CHANG, C. 1991. Autoregulation of androgen receptor expression in rodent prostate: immunohistochemical and in situ hybridization analysis. *Biochemical and biophysical research communications,* 177**,** 488-496.

UNGEFROREN, H., IVELL, R. & ERGÜN, S. 1997. Region-specific expression of the androgen receptor in the human epididymis. *Molecular human reproduction,* 3**,** 933-940.

VALI, N. 2008. The Japanese quail: A review. *International Journal of Poultry Science,* 7**,** 925-931.

WOLF, D. A., HERZINGER, T., HERMEKING, H., BLASCHKE, D. & HÖRZ, W. 1993. Transcriptional and posttranscriptional regulation of human androgen receptor expression by androgen. *Molecular Endocrinology,* 7**,** 924-936.

WONG, Y., BREED, W. & CHOW, P. 1985. Ultrastructure of the epithelial cells of the ventral prostate from the hopping mouse *Notomys alexis*. *Cells Tissues Organs,* 121**,** 163-169.

WOODHOUSE, M. & RHODIN, J. 1963. The ultrastructure of the Harderian gland of the mouse with particular reference to the formation of its secretory product. *Journal of ultrastructure research,* 9**,** 76-98.